Dissertation

submitted to the

Combined Faculties for the Natural Sciences and for Mathematics

of the Ruperto-Carola University of Heidelberg, Germany

for the degree of

Doctor of Natural Sciences

presented by

Diplombiologin Katharina Ehrhardt

born in Karlsruhe

Date of oral examination: _____

Redox-active 3-benzyl-menadiones as

new antimalarial agents:

Studies on structure-activity relationships, antiparasitic

potency and mechanism of action

Table of Contents

List of Abbreviations

Abbreviations of protein names

h	(prefix)	human
Pf	(prefix)	*Plasmodium falciparum*
y		yeast
6PGD		6-phosphogluconate dehydrogenase
6PGL		6-phosphogluconolactonase
AOP		antioxidant protein
CYP450		cytochrome P450 enzyme
DHODH		dihydroorotate dehydrogenase
G6PD		glucose-6-phosphate dehydrogenase
GLP		glutaredoxin-like proteins
GluPho		glucose-6-phosphate dehydrogenase 6-phosphogluconolactonase
GR		glutathione reductase
Grx		glutaredoxin
GS		glutathione synthetase
GST		glutathione S-transferase
hGrx1		human glutaredoxin-1
hGrx1-roGFP2		human glutaredoxin-1 linked to redox-sensitive green fluorescent protein 2
KAHRP		knob-associated histidine-rich protein
LipDH		dihydrolipoamide dehydrogenase
*Pf*EMP1		*P. falciparum* erythrocyte membrane protein 1
Plrx		plasmoredoxin
Prx		peroxiredoxin
roGFP2		redox-sensitive green fluorescent protein 2
SOD		superoxide dismutase
Tlp		thioredoxin-like protein
Trx		thioredoxin
TrxR		thioredoxin reductase
γGCS		γ- glutamyl-cysteine synthetase

Abbreviations

ARMD	accelerated resistance to multiple drugs
BSO	Buthionine sulfoximine
ca	circa
CO_2	carbon dioxide
CQr	chloroquine resistant
CQs	chloroquine sensitive
ddH_2O	double distilled water
DFO	desferrioxamine B
DMSO	dimethyl sulfoxide
DMSO	dimethyl sulphoxide
DNA	desoxyribonucleic acid
EDTA	ethylenediaminotetraacetate
FAD	flavin adenine dinucleotide
Fe	iron
FIC_{50}	fractional 50% inhibitory concentration
GSH	glutathione or γ-L-glutamyl-L-cysteinylglycine
GSSG	glutathione disulfide
h (prefix)	human (or hour as unite)
H_2O	hydrogen peroxide
Hb	hemoglobin
HCl	hydrogen chloride
HDAC	histone deacetylase
HEPES	N-(2-Hydroxylethyl)piperacin-N´-(2-ethylsulphonacid)
i.e.	that is, id est
IC_{50}	50% inhibitory concentration
IgG	immunoglobulin G
iRBC	infected red blood cells
malERA	Malaria Research Agenda initiative
MDR	multi-drug resistance
mETC	mitochondrial electron transport chain
MMV	Medicines for Malaria Venture

MNHN	Museum National d'Histoire Naturelle, Paris, France
N_2	nitrogen gas
$NADP^+$	nicotinamide adenine dinucleotide phosphate
NADPH	reduced nicotinamide adenine dinucleotide phosphate
NIH	National Institute of Health
niRBC	non-infected red blood cells
O_2	oxygen
$O_2^{-\bullet}$	superoxide anions
$OH^{-\bullet}$	hydroxyl radicals
P.	*Plasmodium*
p.i.	post invasion
PCT	parasite clearance time
Pf (prefix)	*Plasmodium falciparum*
PPP	pentose phosphate pathway
PRR	parasite reduction ratio
RBC	red blood cells
RPMI	Rosewell Park Memorial Institute
rs	Spearman nonparametric correlation coefficient
RT	room temperature
SD	standard deviation
TCP	target candidate profile
WHO	World Health Organization

Units of measurement

×	times
∑	sum
°C	degree Celsius
μ	micro
μl	microliter
μM	micromolar
Ci	curie
g	gram
h	hours (or human as prefix for protein names)
k	kilo
l	liter
m	milli
M	Molar
min	minutes
ml	milliliter
mM	millimolar
mm	millimeter
n	nano
nm	nanometer
pH	potential hydrogenii
rpm	revolutions per minute
sec	seconds
v/v	volume to volume
w/v	weight to volume

List of Figures and Tables

Figures

Tables

X

Appendix

Summary

Malaria is still one of the most important infectious diseases worldwide, responsible for more than 600 000 cases of death per year, most of them in young children. The infection is caused by apicomplexan parasites of the genus *Plasmodium* (amongst them *P. falciparum*) and transmitted by *Anopheles* mosquitoes. The emergence and spread of parasite resistance to previously effective drugs are a major threat to the control and elimination of the infection and raises an important need of new drug development strategies. Previously, the laboratory of medicinal chemistry (Dr. E. Davioud-Charvet) presented the chemical design of a series of very promising antimalarial agents, 3-[substituted-benzyl]-menadiones (abbreviated as benzylMD), with potent *in vitro* and *in vivo* activities. The 3-[4-(trifluoromethyl)benzyl]-menadione **1c** was selected as the lead compound for further studies. Ongoing studies on the mode of action evidenced that these agents disturb the redox balance of the parasitized erythrocyte by acting as redox-cyclers - a strategy that is broadly recognized for the development of new antimalarial agents.

The presented work on the *in vitro* activity of benzylMD **1c** represents an essential part of the lead optimization stage of the benzylMD drug development process. It could be shown that benzylMD **1c** is a potent inhibitor of *P. falciparum* blood-stage parasites, which was unaffected by the most common resistance mechanisms to clinically used antimalarials. Lead **1c** inhibited parasite development of all intra-erythrocytic stages with a preferential activity against early ring stages. The drug's potent activity against all parasite stages is similarly reflected in its fast speed of action (i.e. killing speed), which is comparable to artemisinin, one of the fastest compounds described so far. *In vitro* resistance selection studies revealed a low intrinsic potential to induce stable drug resistance. In parallel, the *in vitro* antimalarial activity of several benzylMD derivatives was investigated to gain a better understanding about the structure-activity relationships. The second part of this work focused on the mode of action of benzylMD **1c**. Most importantly, it could be shown that the lead benzylMD **1c** is not an inhibitor of the mitochondrial electron transport chain, in contrast to the structurally related antimalarial atovaquone. Furthermore, *in vitro* drug interaction studies were chosen as a tool to explore key features of benzylMD **1c**'s mode of action in a whole cell assay. Those studies provided insights into the roles of the glutathione reductase, NADPH, iron complexation and intracellular glutathione levels in drug activity. Overall, the findings of this work demonstrate the promising *in vitro* potency of lead benzylMD **1c** and highly support the further development of benzylMD series as antimalarial drug candidates.

Résumé

Le paludisme reste une des maladies infectieuses les plus importantes à travers le monde causant plus de 600 000 cas de décès par an, pour la plupart chez les jeunes enfants. L'infection est causée par des parasites apicomplexes du genre *Plasmodium* (dont *P. falciparum*) et transmise par les moustiques *Anophèles*. L'émergence et la propagation de la résistance des parasites aux médicaments usuels, de faible coût et autrefois efficaces, est une menace majeure pour contrôler et éliminer l'infection. Elle souligne un important besoin de nouvelles stratégies de développement de médicaments. Dans le passé, le laboratoire de chimie médicinale (Dr E. Davioud-Charvet) a conçu une série de 3-benzyl-ménadiones substituées (benzylMD) comme agents antipaludiques prometteurs avec une forte activité *in vitro* et *in vivo*. La 3-[4-(trifluorométhyl)-benzyl]-ménadione **1c** a été choisie comme tête de série pour des études complémentaires. Les études en cours sur le mode d'action ont mis en évidence que cette benzylMD déstabilise l'équilibre redox des érythrocytes infectés en agissant comme agent catalytique redox (redox-cycler), une stratégie qui est actuellement reconnue pour le développement de nouveaux agents antipaludiques. Les travaux présentés dans cette thèse sur l'activité *in vitro* de la benzylMD **1c** font partie de la phase principale d'optimisation du développement des benzylMDs. La benzylMD **1c** est démontrée comme un puissant inhibiteur des stades sanguins du parasite *P. falciparum*. La tête de série **1c** inhibe le développement du parasite à tous les stades intra-érythrocytaires, avec une activité préférentielle sur les stades précoces du cycle. La forte activité du composé contre tous les stades parasitaires est également reflétée par sa vitesse d'action, qui est comparable à celle de l'artémisinine, l'un des composés les plus rapides décrit jusqu'ici. Les études de sélection de résistance *in vitro* ont révélé un potentiel intrinsèque faible pour induire une résistance stable à la benzylMD **1c**. En parallèle, l'activité antipaludique *in vitro* de nouveaux dérivés benzylMDs a été étudiée pour acquérir une meilleure compréhension des relations structure-activité. De plus, la benzylMD **1c** n'est pas un inhibiteur de la chaîne de transport d'électrons mitochondriale, contrairement à l'atovaquone, un antipaludique structuralement apparenté. En outre, des études *in vitro* sur les interactions médicamenteuses ont été choisies comme outil pour explorer les principales caractéristiques du mode d'action de la benzylMD **1c** dans un essai cellulaire. Ces études ont fourni des indications sur le rôle de la glutathion réductase, du NADPH, de la complexation au fer ou du taux de glutathion intracellulaire dans l'activité de cet agent. Dans l'ensemble, les résultats de ce travail démontrent l'activité *in vitro* très prometteuse de la benzylMD **1c** et soutiennent l'amélioration de la série benzylMD comme nouveaux candidats-médicaments antipaludiques.

Zusammenfassung

Malaria ist auch heute noch eine der wichtigsten Infektionskrankheiten weltweit, welche mehr als 600 000 Todesfälle pro Jahr verursacht, die meisten von ihnen bei jungen Kindern. Die Infektion wird durch Parasiten der Gattung *Plasmodium* (darunter *P. falciparum*) verursacht und von Anopheles-Mücken übertragen. Die Entstehung und Ausbreitung von Resistenzen der Parasiten gegen bisher wirksame Medikamente stellt eine große Bedrohung für die Kontrolle und Eliminierung der Infektion dar und begründet die dringende Notwendigkeit neue Wirkstoffe zu entwickeln. Kürzlich stellte das Labor für medizinische Chemie (Dr. E. Davioud-Charvet) eine vielversprechende Wirkstoffserie mit ausgeprägten *in vitro* und *in vivo* Aktivitäten vor, die 3-[substituierte-benzyl]-Menadione (abgekürzt als benzylMD). Das 3-[4-(Trifluoromethyl)benzyl]-Menadion **1c** wurde als Leitsubstanz für weitere Studien ausgewählt. Laufende Untersuchungen belegen, dass benzylMD-Derivate das Redox-Gleichgewicht der infizierten Erythrozyten stören, indem sie als sogenannte Redox-Cycler agieren. Diese metabolische Wirkungsweise ist vielversprechend für die Entwicklung neuer Malariamedikamente

Die vorliegende Arbeit über die *in vitro* Aktivität der Leitsubstanz benzylMD **1c** stellt einen Teil der Evaluierungsphase im Laufe der Arzneimittelentwicklung dar. Es konnte gezeigt werden, dass benzylMD **1c** ein wirksamer Inhibitor der Blutstadien des Parasiten *P. falciparum* ist, welcher zudem nicht negativ von den häufigsten Resistenzmechanismen der Parasiten beeinflusst wurde. Leitsubstanz **1c** hemmte die Entwicklung aller intra-erythrozytären Parasitenstadien und war besonders aktiv gegen frühe Ringstadien. Die hohe Aktivität des Wirkstoffes wurde ebenso durch seine Wirkungsgeschwindigkeit widergespiegelt, welche im Bereich von Artemisinin liegt, einer der schnellsten bisher beschriebenen Verbindungen. *In vitro* Resistenzstudien erwiesen ein geringes Eigenpotenzial der Leitverbindung eine stabile Medikamentenresistenz der Parasiten zu induzieren. Parallel zu diesen Studien wurde die *in vitro* Aktivität von benzylMD-Derivaten gemessen, um ein besseres Verständnis über die Struktur-Aktivitäts-Beziehungen zu gewinnen. Der zweite Teil der Arbeit konzentrierte sich auf die Wirkungsweise von benzylMD **1c**. Vor allem konnte gezeigt werden, dass benzylMD **1c** im Gegensatz zu dem strukturell verwandten Medikament Atovaquon nicht als Inhibitor der mitochondrialen Elektrontransportkette fungiert. Darüber hinaus wurden im Rahmen von Medikamenten-Interaktionsstudien Einblicke in die Rollen der Glutathionreduktase, des NADPH-Spiegels, der Komplexbildung mit Eisen oder des intrazelluläre Glutathion-Spiegels für die Wirkstoffaktivität gewonnen. Insgesamt zeigen die Ergebnisse dieser Arbeit die vielversprechende *in vitro* Wirksamkeit der Leitsubstanz benzylMD **1c** und unterstützen daher die weitere Entwicklung der benzylMD-Serie als Arzneimittel-kandidaten gegen Malariaparasiten

1 INTRODUCTION

1.1 Malaria

Even today malaria is one of the most important infectious diseases worldwide. The infection is caused by protozoan parasites of the genus *Plasmodium* and transmitted by female *Anopheles* mosquitoes. In the past, malaria was widespread throughout many regions of the world but was successfully eliminated from Europe, North America and Russia (White et al, 2014). Nowadays, malaria is mostly prevalent in tropical regions of sub-Saharan Africa, Asia, South and Central America with an estimated population of 3.4 billion people at risk of infection in 2013 (Figure 1)(WHO, 2013). For the year 2012, the World Health Organization (WHO) estimated 207 million cases of malaria worldwide (80% in Africa) causing 627 000 cases of death (90% in Africa), most of them in children under the age of 5 (77%) (WHO, 2013). Malaria disproportionally affects the world's poorest communities and poses on significant toll on the health and economic development of these populations.
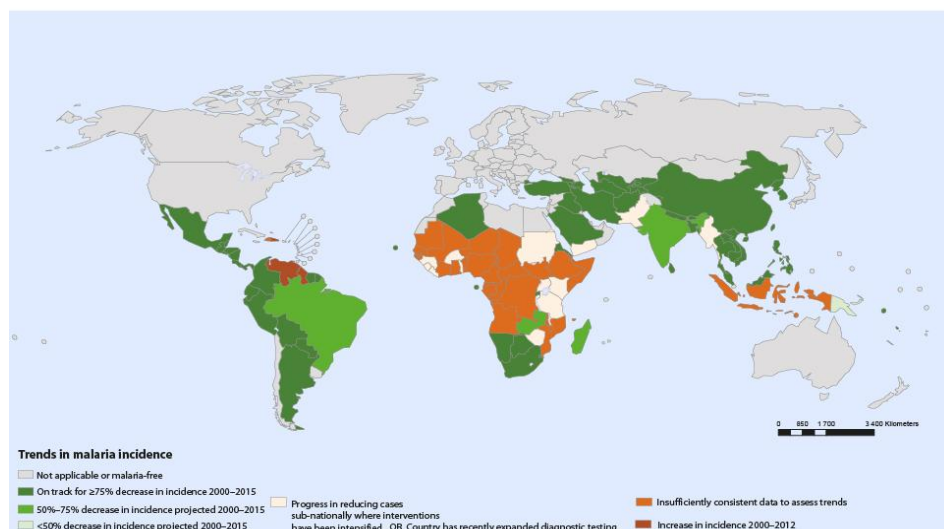
Figure 1 Trends in reported malaria incidence 2000 - 2012 (WHO, 2012)

1.1.1 Clinical manifestations

Malaria is a general term for infections with protozoan *Plasmodium* parasites (i.e. *P. falciparum*, *P. vivax*, *P. ovale*, *P. malariae or P. knowlesi*). The clinical picture of the disease is generally very similar though infections vary in their global distribution, length of prepatency, severity of symptoms and mortality rate (Tuteja, 2007; White et al, 2014). The development of clinical symptoms is highly dependent on age and immune status of the patient and ranges from asymptomatic infections to life-threatening cases. Individuals living in endemic regions with yearlong transmission of malaria (i.e. stable transmission) generally acquire a partial immunity to the clinical disease and to its severe manifestations during childhood (WHO, 2010). Young children (> 5 years) and pregnant women are particularly vulnerable to severe forms of malaria. The most severe forms and highest numbers of death are attributed to infections with *P. falciparum* (Malaria tropica) (WHO, 2013).

Malaria is an acute febrile illness with rather unspecific symptoms, such as headaches, fatigue, muscle aches, nausea and vomiting (Grobusch & Kremsner, 2005). Primary symptoms are often mild and not necessarily attributed to malaria. A typical malaria fever episode is characterized by an initial "cold stage" (sensation of cold, shivering), a "hot stage" of fever over few hours (increased body temperature, flushes, fever, vomiting, headaches) that is followed by a sharp decrease of body temperature accompanied by excessive sweating (Grobusch & Kremsner, 2005). Fever episodes stem from a simultaneous rupture of infected erythrocytes and consequential activation of the immune system (Oakley et al, 2011). Upon synchronization of the parasitic life cycle in the host, fever occurs periodically: every 3rd day for infections with *P. vivax* and *P. ovale* (Malaria tertiana) and *P. falciparum* (Malaria tropica), every 4th day for infections with *P. malariae* (Malaria quartana) and every 24 hours for infections with *P. knowlesi*. *Falciparum* malaria is often marked by irregular or persistent fever episodes (Oakley et al, 2011). In non-immune or untreated patients, high parasitemia causes clinical complications, including anemia, metabolic dysfunctions (acidosis, hypoglycemia) and organ impairment (renal injury, pulmonary edema) (Grobusch & Kremsner, 2005). The intensive sequestration of *P. falciparum*-infected erythrocytes to endothelia of small blood vessels causes microvascular obstruction, oxygen deprivation and provokes local inflammation of the capillaries, which may lead to severe symptoms and life-threatening forms of the disease,

such as multi-organ failure or neuronal complications (i.e. cerebral malaria) (White et al, 2014). A *P. falciparum* infection during pregnancy might cause intense accumulation of infected erythrocytes in the placental microcirculation (i.e. placental malaria) and is associated to congenital malaria, low birth weight and premature delivery (White et al, 2014). The other *Plasmodium* species only rarely cause life-threatening complications (Grobusch & Kremsner, 2005; White et al, 2014).

1.1.2 Natural protections against severe forms of malaria

Several genetic mutations of human erythrocytes are known for protecting carriers from the severe, life-threatening forms of malaria. Glucose-6-phosphate dehydrogenase (G6PD) deficiency and hemoglobinopathies, for instance thalassemia and sickle cell disease, are important examples of such genetic polymorphisms. The similar geographic distribution of these genetic traits and past or present malaria infections support the so-called malaria protection hypothesis, which claims that co-evolution of humans and *P. falciparum* shaped the human genome in these regions (Cappellini & Fiorelli, 2008; Cyrklaff et al, 2012)

The most widespread genetic defect of human erythrocytes is G6PD deficiency, which also represents the most common human enzyme defect (reviewed in Cappellini & Fiorelli, 2008). G6PD is the first enzyme of the pentose phosphate pathway and the main producer of NADPH (nicotinamide adenine dinucleotide phosphate) in erythrocytes. Affected individuals are generally asymptomatic but more susceptible to oxidative insults in forms of oxidant drugs, chemicals or food components that may induce acute hemolytic anemia. Hemoglobinopathies result from unpaired globin chains in α- or β-thalassemia or from structurally altered β-globin in sickle-cell hemoglobin (HbS), hemoglobin C (HbC) or hemoglobin E (HbE) (reviewed in Cyrklaff et al, 2012; Taylor et al, 2013). Heterozygous carriers are generally asymptomatic but may suffer from mild anemia.

The molecular mechanism(s) that protects affected individuals from the severe symptoms of malaria are complex and still not fully understood. Interestingly, in all cases, erythrocytes were shown to be more susceptible to oxidative stress, marked by a higher tendency of hemoglobin to oxidize and denature, caused either by structurally unstable mutant hemoglobin or decreased antioxidant capacity of the host cell (Ayi et al, 2004; Reeder, 2010; Cyrklaff et al, 2012). In support of this hypothesis, enhanced binding of

3

hemichrome [1] (i.e. denatured hemoglobin) to the erythrocyte membrane and enhanced phagocytosis of infected cells were observed for G6PD-deficient erythrocytes, heterozygous sickle cells (HbAS) and heterozygous thalassaemic cells (β-thalassemia and HbH) (see also section 1.2.2.3) (Cappadoro et al, 1998; Ayi et al, 2004). Furthermore, denatured and oxidized hemoglobin species were identified as candidates for preventing host actin re-organization in *P. falciparum*-infected homozygous HbCC and heterozygous HbSC erythrocytes (Cyrklaff et al, 2011). Remodeling of the host actin cytoskeleton was shown to be important to establish the parasite's protein trafficking system and their inhibition might contribute to the protection against severe malaria infections (Cyrklaff et al, 2011; Cyrklaff et al, 2012).

1.2   Causative agent of malaria - *Plasmodium* parasites

The malaria causing protozoan parasite *Plasmodium* belongs to the phylum Apicomplexa (Lucius & Loos-Frank, 2008). Apicomplexa are obligate endoparasites that cause serious diseases in humans and animals (livestock, wild animals). Their name derived from the apical complex, a characteristic structure essential for host cell invasion that comprises the conoid, rhoptries, micronemes and dense granules. Most apicomplexan parasites harbor a unique organelle of bacterial origin that emerged from secondary endosymbiosis, the so-called apicoplast (reviewed in detail in Lim & McFadden, 2010). The apicoplast retained a small genome and several metabolic functions and is therefore a potential target for chemotherapy, especially antibiotics (Botte et al, 2012).

The genus *Plasmodium* comprises nearly 200 species that parasitize mammals, rodents, birds and reptiles (Lucius & Loos-Frank, 2008). Five species infect humans, *P. falciparum*, *P. vivax*, *P. ovale, P. malariae* and *P. knowlesi.* The latter one is of non-human primate origin but causes human infections in many regions of Southeast Asia. From a clinical perspective, *P. falciparum* and *P. vivax* are the most important species: *P. falciparum* causes the highest numbers of infections and most deaths and is widely endemic in Africa; *P. vivax* is widely spread over regions that are unaffected by *P. falciparum* since it develops in the mosquito vector at lower temperatures and survives transmission-free periods in the host by dormant liver stages (hypnozoites) (WHO, 2013).

---

[1] For a definition of hemichrome, please refer to Table A1 in the Appendix

1.2.1 Life cycle of *Plasmodium falciparum*

The life cycle of the five human pathogenic *Plasmodium* species is exemplified by the life cycle of *P. falciparum*, but important species-specific differences are mentioned (summarized from Tuteja, 2007; Lucius & Loos-Frank, 2008; White et al, 2014).

The life cycle of *P. falciparum* involves asexual replication in the human host and sexual reproduction in the invertebrate host, a female *Anopheles* mosquito that further acts as vector. Only few *Anopheles* species are efficient vectors for *Plasmodium* parasites, important ones in Africa are the *A. gambiae* and *A. funestus* complexes.

Female *Anopheles* mosquitoes ingest sexually differentiated gametocytes (female macrogametocytes, male microgametocytes) during a blood meal on an infected individual. Inside the mosquito midgut, the gametocytes mature into gametes, fertilization occurs and the diploid zygote (ookinete) settles between the midgut epithelium and the basal lamina. The ookinete develops into an oocyst, inside which sporogony takes place, producing thousands of haploid sporozoites. After maturation, the oocyst ruptures and motile sporozoites migrate into the salivary glands of the mosquito to be further transmitted.

Infective sporozoites are transmitted to humans by a bite of a female *Anopheles* mosquito. They are released into the skin, where they actively migrate to enter the circulatory system in order to be transported to the liver. Sporozoites invade hepatocytes and follow a first asexual replication cycle (exoerythrocytic schizogony). The liver stage is a phase of intensive multiplication, though clinically silent, and represents the bottle neck of the infection. Different to *P. falciparum*, *P. vivax* and *P. ovale* additionally form dormant liver stages (hypnozoites) that can reactivate the parasite's life cycle and cause relapse of the disease still months after the primary infection (Wells et al, 2010). These dormant forms permit the parasite to survive periods without regular transmission by the mosquito vector.

The hepatocytic schizogony releases thousands of merozoites into the blood stream, which rapidly infect erythrocytes and initiate the intraerythrocytic development (blood stage). Merozoite invasion of erythrocytes is a complex process that is yet not entirely understood but is an attractive target for drug or vaccine development (Boyle et al, 2013). In erythrocytes, the parasite develops inside a parasitophorous vacuole and follows another asexual replication cycle (intraerythrocytic schizogony) that is characterized by three morphological distinct stages, namely ring, trophozoite and schizont. Each mature schizont

contains up to 20 merozoites, which are released upon rupture of the host cell and rapidly invade new erythrocytes. The duration of schizogony is 48 hours for *P. falciparum, P. vivax* and *P. ovale*, 72 hours for *P. malariae* and 24 hours for *P. knowlesi*. The simultaneous rupture of infected erythrocytes and release of cell debris, hemozoin and parasite antigens into the circulation activates the immune system and induces the typical malaria symptom, fever (Oakley et al, 2011). A small proportion of intraerythrocytic stages differentiate to sexual stages, gametocytes, which are crucial for transmission to the mosquito vector.
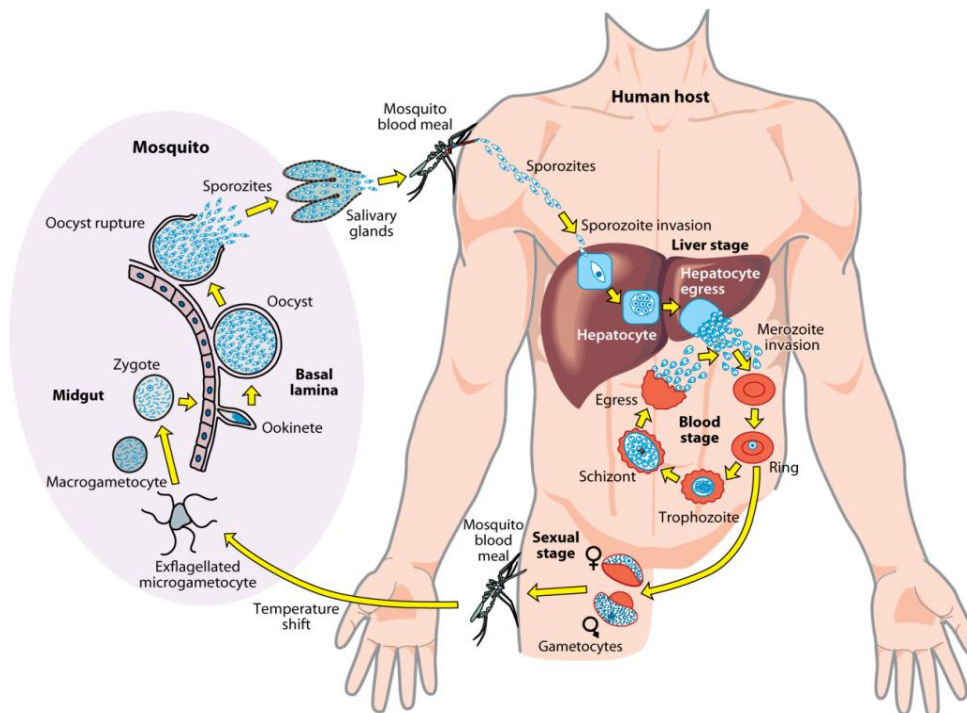
Figure 2 The life cycle of *Plasmodium falciparum* (Boddey & Cowman, 2013)

1.2.2 Intraerythrocytic development of *Plasmodium falciparum*

The intraerythrocytic development is characterized by three morphological distinct stages, namely ring (0-24 hours), trophozoite (24-36 hours) and schizont (36-48 hours), the so-called blood-stage parasites (Figure 3)(Maier et al, 2009).
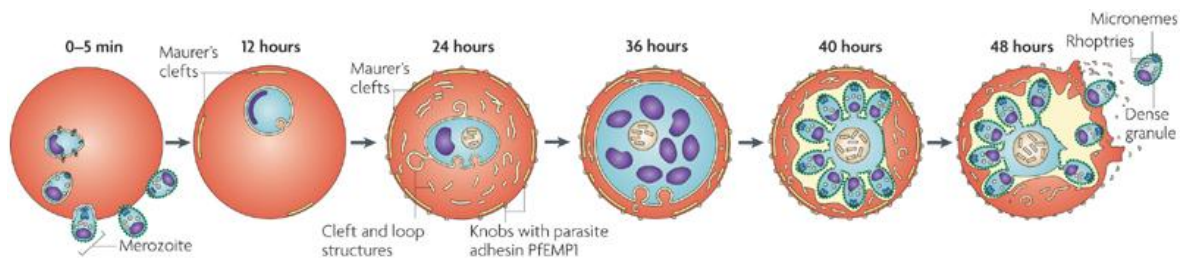
Figure 3 Development of *Plasmodium falciparum* in human erythrocytes (Maier et al, 2009)

Parasite development is marked by a high metabolic activity by means of glycolysis and proteolysis of hemoglobin (Tuteja, 2007). The digestion of hemoglobin is described in more detail in the next section. The survival of the parasite depends on a profound reorganization of its host cell that is accompanied by expression and transport of parasite proteins beyond the parasitophorous vacuole, into the cytosol and to the membrane of erythrocytes (reviewed in Boddey & Cowman, 2013). Mature erythrocytes have lost their ability to synthesize proteins and the parasite must therefore establish an extraparasitic protein trafficking network in the host cell cytosol. Important examples of parasite induced remodeling include new permeability pathway, J-dots, Maurer's clefts and knobs at the erythrocyte membrane. New permeability pathways enable the import of nutrients and exchange of waste products. Knob structures under the erythrocyte membrane contain knob-associated histidine-rich protein (KAHRP) and the *P. falciparum* erythrocyte membrane protein 1 (PfEMP1), which are responsible for cytoadhesion of infected erythrocytes to endothelia of small blood vessels. Cytoadhesion is a mechanism of immune evasion and moreover contributes to virulence and pathogenesis of malaria.

1.2.2.1 Hemoglobin digestion

Hemoglobin of the host erythrocyte is a necessary source of amino acids for the parasite's protein synthesis. *Plasmodium* digests the host's hemoglobin not only for nutritional purposes, as original suggested, but also in order to provide sufficient space for its growth and additionally in order to maintain the host cell's integrity and to prevent it from lysis (Krugliak et al, 2002; Lew et al, 2004).

In order to protect the parasitic cytosol from redox-active byproducts of hemoglobin degradation (i.e. free heme [2], iron and reactive oxygen species), this process occurs inside a specialized lysosome-like compartment, the digestive vacuole, under acidic conditions (pH 5.0 - 5.4) (Klonis et al, 2007; Coronado et al, 2014). In these conditions, oxyhemoglobin [2] (Fe^{2+}) is rapidly oxidized to methemoglobin [2] (Fe^{3+}), a reaction that produces superoxide anions ($O_2^{-\bullet}$). Superoxide anions dismutate spontaneously to hydrogen peroxide (H_2O_2) and oxygen (O_2) under the acidic conditions of the digestive vacuole (Reeder, 2010). In the cytosol of the parasite, dismutation of superoxide anions is catalyzed by superoxide dismutases (SODs) (Becuwe et al, 1996; Sienkiewicz et al, 2004).

Proteolysis of hemoglobin (i.e. methemoglobin) involves several well-characterized enzymes, for instance aspartic (plasmepsins I and II) and cysteine (falcipain) proteases (Goldberg et al, 1991; vander Jagt et al, 1992; Gluzman et al, 1994; Hogg et al, 2006). Further enzymes involved in hemoglobin digestion but also hemozoin [2] formation, as well as a recently identified protein complex, are in the focus of intense research (Jani et al, 2008; Chugh et al, 2013). Proteolytic degradation of hemoglobin releases its prosthetic group, heme [2] (or: Fe^{3+}-protoporphyrin-IX) in form of α-hematin [2] (i.e. hydroxylated heme), which is highly reactive and must be detoxified. Free heme is toxic to the parasite as it has been shown to inhibit enzymes, destabilize membranes by lipid peroxidation, cause osmotic changes and partake in Fenton reactions accompanied by the production of reactive oxygen species (Zhang et al, 1999) and (discussed in detail in Becker et al, 2004). *Plasmodium* parasites detoxify α-hematin by crystallization of it to hemozoin, the malaria pigment. The mechanism of hemozoin formation is not yet elucidated and is still under research. Different mechanisms have been proposed, such as a spontaneous autocatalytic process, an enzymatic process (e.g. histidine-rich proteins) and the involvement of lipids. The current theories about the mechanism of hemozoin formation are discussed in recent

---

[2] The definitions of hemoglobin species and heme-containing molecules are given in the Appendix, Table A1

reviews (Egan, 2008; Coronado et al, 2014). Their further understanding is of particular interest for the identification of new drug targets. In addition, there is increasing evidence that hemozoin is involved in the pathophysiology of malaria, for instance by regulating phagocyte activity and immune responses (reviewed in Coronado et al, 2014).

1.2.2.2 Oxidative stress in *Plasmodium falciparum*-infected erythrocytes

The intraerythrocytic-parasite stages have to cope with high fluxes of reactive oxygen species from endogenous but also exogenous sources, for example immune reactions (Becker et al, 2004). Reactive oxygen species are detoxified by the parasite's first line defense (e.g. SOD, peroxiredoxins, see below) and further components of glutathione or thioredoxin-based redox systems. The glutathione and thioredoxin-based redox systems of *P. falciparum* are not only essential for the anti-oxidant defense but also to maintain a stable intracellular (redox) homeostasis. The redox systems of *P. falciparum* are described in more detail in section 1.2.3.

Digestion of hemoglobin is the major endogenous source of oxidative stress for the parasite (see also section 1.2.2.1). This process is accompanied by the production of superoxide anions, hydrogen peroxide and the release of free redox-active heme. Another source of superoxide anions is the parasite's mitochondrial electron transport chain. Superoxide anions are detoxified by dismutation to molecular oxygen and hydrogen peroxide. This reaction is catalyzed by ubiquitous metallo-proteins, superoxide dismutases (SODs), but can also occur spontaneously under acidic pH as in the parasite's digestive vacuole (Reeder, 2010). Two iron-dependant SODs of *P. falciparum* were characterized so far, cytosolic *Pf*SOD 1 and mitochondrial *Pf*SOD 2, which might also be targeted to the apicoplast (Becuwe et al, 1996; Sienkiewicz et al, 2004). Hydrogen peroxide is readily participating in further redox reactions (e.g. Fenton reactions), thereby generating reactive hydroxyl radicals ($OH^\bullet$), which can induce lipid peroxidation and DNA oxidation (Figure 4) (Jortzik & Becker, 2012). *Plasmodium* parasites rely mainly on peroxiredoxins for detoxification of hydrogen peroxides since they lack catalase or a classical glutathione peroxidase (further described in section 1.2.3).
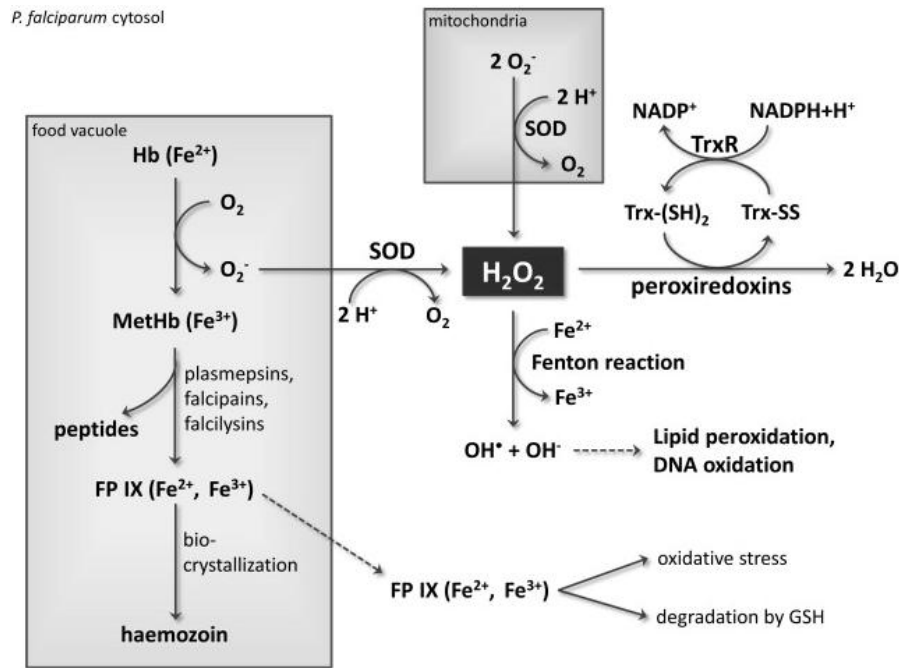
Figure 4 Sources of oxidative stress in *Plasmodium falciparum* (Jortzik & Becker, 2012)

Major sources of oxidative stress (e.g. O_2^-, OH^-, H_2O_2) are the parasite's food vacuole (Hb digestion) and mitochondria (mitochondrial electron transport chain). Means of detoxification are mitochondrial and cytosolic SOD and cytosolic thioredoxin (Trx)-dependent peroxiredoxins. See text for more details. Abbreviations: FPIX, ferriprotoporphyrin IX; H_2O_2, hydrogen peroxide; Hb, Hemoglobin; O_2^-, superoxide anion; OH^-, hydroxyl radicals; SOD, superoxide dismutase; Trx, thioredoxin; TrxR, thioredoxin reductase.

1.2.2.3 Phagocytosis of *Plasmodium falciparum*-infected erythrocytes

The removal of aged or damaged erythrocytes from the circulation - a short outlook

Under physiological conditions, hemoglobin is present in its ferrous oxidation state (Fe^{2+}), which allows binding and transport of oxygen (for an extensive review about redox activity of hemoglobin, please refer to Reeder (2010)). Though, by auto-oxidation or in reaction with peroxide, the heme group can be oxidized to its ferric (Fe^{3+}) oxidation state. Methemoglobin (Fe^{3+}) is physiologically inactive and its formation is tightly controlled by an extensive antioxidant system (e.g. NADH–cytochrome b5–methemoglobin reductase, glutathione system) (Kanias & Acker, 2010; Reeder, 2010). During erythrocyte senescence, under pathological conditions or oxidative damage, hemoglobin oxidizes as marked by increased formation of methemoglobin and denaturation to hemichromes (Kanias & Acker, 2010; Reeder, 2010). Hemichromes were demonstrated to be a key determinant for the clearance of senescent or damaged erythrocytes from the blood stream. In more detail, hemichromes bind to the cytoplasmic tail of band 3 molecules that

subsequently cross-link to form aggregates. Anion transporter band 3 is the major integral protein spanning the erythrocyte membrane. Those band 3 clusters represent the age-specific antigen on senescent erythrocytes for binding of autologous band 3-specific IgG antibodies, which initiate phagocytosis (Low et al, 1985).

Of note, enhanced rates of erythrocyte phagocytosis were observed in patients suffering from hemoglobinopathies or G6PD-deficiency. This is reported to stem from unstable hemoglobin variants that are more prone to denature (e.g. sickle cells) or from high levels of oxidative stress generated in G6PD-deficient cells (Cappadoro et al, 1998; Ayi et al, 2004).

Phagocytosis of *Plasmodium falciparum*-infected erythrocytes

The development of *P. falciparum* promotes important alterations in the host erythrocyte membrane, as marked by hemichromes binding and aggregation of band 3 molecules (Giribaldi et al, 2001; Turrini et al, 2003). Similar to senescent erythrocytes, those alterations were shown to attract the binding of autologous band 3-specific IgG antibodies, deposition of further opsonins (e.g. complement factor C3) and consequently phagocytosis *in vitro* (Turrini et al, 1992; Giribaldi et al, 2001; Turrini et al, 2003). The driving force behind those modifications is considered to be the oxidative stress in erythrocytes induced by the parasite and related denaturation of hemoglobin (Giribaldi et al, 2001 and further references cited herein). Supporting this hypothesis is the reported increase of erythrocyte membrane alterations and enhanced phagocytosis during parasite maturation. These events further correlate with the increase of oxidative stress exerted by the parasite to the host cell (Giribaldi et al, 2001).

Enhanced phagocytosis of early parasite stages (i.e. ring stages) was observed in mutant erythrocytes, such as G6PD-deficient, heterozygous sickle cells (HbAS) and heterozygous thalassaemic (β-thalassemia and HbH) (Cappadoro et al, 1998; Ayi et al, 2004). Those cells are naturally more susceptible to oxidative insult and additional *P. falciparum* infection might cause an overload of oxidative stress already in early parasite stages. Consequently, enhanced immunological clearance of ring-stage infected erythrocytes by phagocytosis has been suggested as a common mechanism, but not the only one, for protection against severe forms of malaria (Ayi et al, 2004 and further references cited herein).

1.2.3   The redox system of *Plasmodium falciparum*

P. falciparum possesses two closely interacting redox systems, based on either glutathione or thioredoxin, which fulfill important functions in the anti-oxidant defense and redox-regulatory mechanisms (reviewed in Jortzik & Becker, 2012; Mohring et al, 2014). The majority of the redox system acts in the parasitic cytosol but single components could be further localized to subcellular compartments, as the mitochondrion, apicoplast, endoplasmic reticulum and also to the parasitophorous vacuole (Kehr et al, 2010). A stable redox homeostasis of the entire host-parasite unit is considered to be important and is evidenced by the protection of G6PD-deficient individuals against severe malaria. The interactions between the redox systems of the parasite and its host cell are complex but yet not fully understood (Patzewitz et al, 2012).

The glutathione system of *P. falciparum* consists of glutathione, NADPH-dependent glutathione reductase, enzymes of glutathione *de* novo synthesis pathway, glutathione S-transferase, glyoxalases, glutaredoxin and three glutaredoxin-like proteins (Figure 5) (reviewed in Jortzik & Becker, 2012; Mohring et al, 2014).

The parasite relies highly on the tripeptide glutathione (γ-L-glutamyl-L-cysteinyl-glycine) in order to maintain the reducing environment of the cytosol. Furthermore, glutathione plays important roles in the anti-oxidant defense and the detoxification of metabolic byproducts (e.g. free heme) and xenobiotics (e.g. antimalarial compounds). The intracellular glutathione pool of the parasite must be maintained in its reduced form (GSH), since oxidized glutathione disulfide (GSSG) is toxic to the cell. GSSG is formed from oxidation of two GSH in numerous reactions, for instance reduction of reactive oxygen species and reactive nitrogen species, free radicals, dehydroascorbate or protein disulfides (Becker et al, 2003). GSSG might participate in uncontrolled *S*-glutathionylation of proteins and thereby disturb their regular functions. Protein *S*-glutathionylation is a common form of posttranslational modification of protein thiol groups and represents a redox-mediated regulatory mechanism of cellular functions (Kehr et al, 2011).

High concentrations of reduced GSH (i.e. high GSH:GSSG ratio) are maintained by GSSG efflux to the host cell and regulation of GSH regeneration or *de novo* biosynthesis (Patzewitz et al, 2012). In contrast to other *Plasmodium* species, *P. falciparum* is unable to import GSH from its host cell (Patzewitz et al, 2012). *De novo* synthesis of GSH is

sustained by two cytosolic enzymes, namely γ-glutamyl-cysteine synthetase (γGCS) and glutathione synthetase (GS) (reviewed in Jortzik & Becker, 2012). GSH synthesis is likely to be essential in *P. falciparum* blood-stage parasites (Patzewitz et al, 2012). The flavoenzyme glutathione reductase (GR) is mainly responsible for regeneration of reduced GSH by reduction of GSSG in a FAD (flavin adenine dinucleotide) and NADPH-dependant reaction (reviewed in Jortzik & Becker, 2012). The parasitic enzyme *Pf*GR differs slightly from the human GR enzyme in several structural features and was discussed as a potential drug target in the past. Though, recent studies raised questions whether the *Pf*GR might be indispensable for *P. falciparum* survival and identified further GSSG reducing proteins (e.g. Trx, Plrx), which might provide a backup system for regeneration of GSH in the parasite (discussed in Jortzik & Becker, 2012). Up to know, no clear conclusion could be drawn about the requirement of *Pf*GR for the development of *P. falciparum* blood-stage parasites (Buchholz et al, 2010; Patzewitz et al, 2012).
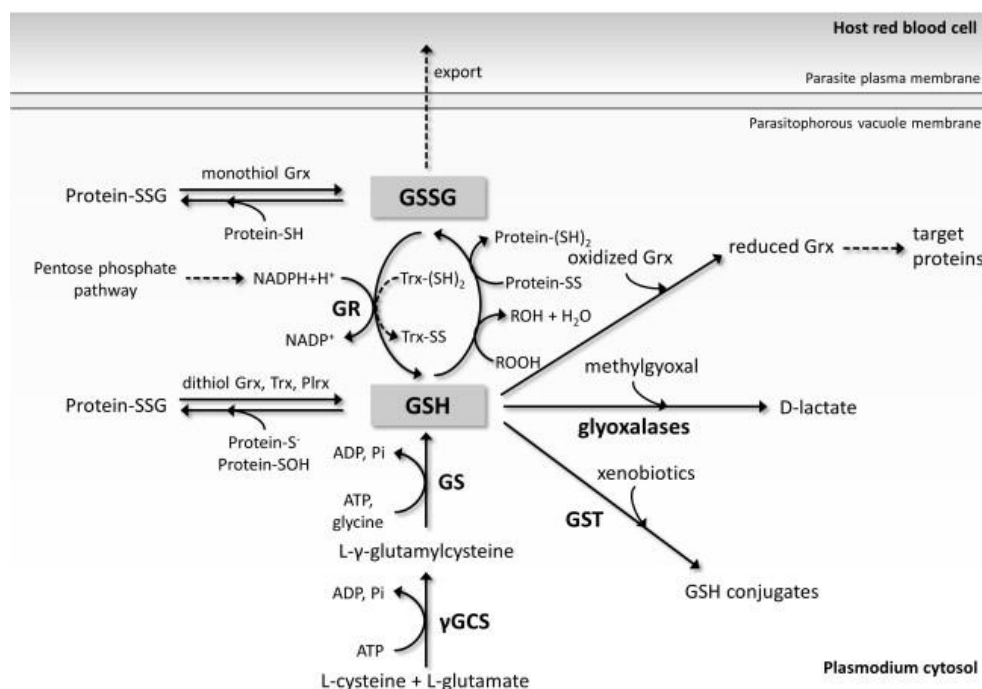
Figure 5 The glutathione system in *Plasmodium falciparum* (Jortzik & Becker, 2012)

This scheme depicts the various functions of oxidized glutathione (GSH), reactions leading to formation of reduced glutathione disulfide (GSSG) and pathways of glutathione regeneration or *de novo* biosynthesis. See text for more details. Abbreviations: GR, glutathione reductase; Grx, glutaredoxin; GSH, glutathione; GSSG, glutathione disulfide; GST, glutathione S-transferase; protein-SSG, protein *S*-glutathionylation; Trx, thioredoxin.

GSH serves as a coenzyme or reductant of several *P. falciparum* enzymes, which maintain the redox homeostasis and intracellular functions, such as glutathione S-transferase (GST), glyoxalases, glutaredoxin (Grx) and glutaredoxin-like proteins (GLP) (Mohring et al, 2014). Glutathione S-transferase detoxifies electrophilic xenobiotics by forming GSH-conjugates that are readily eliminated from the cell. The glyoxalase system detoxifies methylglyoxal, a toxic byproduct of glycolysis. Glutaredoxins are thiol-disulfide oxidoreductases that depend on a non-enzymatic reduction by GSH to further catalyze reduction of disulfide bridges in proteins (e.g. ribonucleotide reductase, plasmoredoxin). The physiological function of parasitic glutaredoxin-like proteins is yet unsolved but was proposed to be the deglutathionylation of proteins, which represents a mechanism of redox-related regulation of protein activity.

In addition, GSH is considered to contribute to the degradation of free or bound heme by destruction of its tetrapyrrole ring via Fenton reaction products (e.g. hydroxyl radicals) (Atamna & Ginsburg, 1995). This mechanism is considered to contribute to parasite resistance against chloroquine (Ginsburg & Golenser, 2003; Patzewitz et al, 2013).

The thioredoxin system of *P. falciparum* consists of three classical thioredoxins, two thioredoxin-like proteins, NADPH-dependent thioredoxin reductase, plasmoredoxin and five peroxiredoxins (Figure 6) (reviewed in Jortzik & Becker, 2012; Mohring et al, 2014).

Thioredoxins are small redox active dithiol proteins with multiple functions in the antioxidant defense and as cellular redox messenger by regulating protein activities (e.g. protein *S*-glutathionylation). *P. falciparum* expresses three classical thioredoxins (i.e. *Pf*Trx 1-3) and two additional thioredoxin-like proteins (i.e. *Pf*Tlp 1 and 2), that share sequence similarities with thioredoxins but are not substrates of the thioredoxin reductase. Cytosolic *Pf*Trx1 contributes to the antioxidant defense by directly reducing oxidants (e.g. hydrogen peroxide, *tert*-butylhydroperoxide, cumene hydroperoxide and S-nitroso-glutathione) and by reducing GSSG and the dithiol protein plasmoredoxin (Plrx). Plasmoredoxin is a unique member of *Plasmodium*'s thioredoxin family that shares similar functions with other members. Furthermore, *Pf*Trx1 possibly reduces dehydroascorbate, lipoamide and lipoic acid and may thereby sustaining their antioxidant capacities.

In addition, thioredoxins serves as reducing equivalents (i.e. electron donor) for peroxiredoxins (Prx) that build the first-line defense against reactive oxygen and reactive nitrogen species. The peroxiredoxin protein family are ubiquitous peroxidases with additional function in the regulation of H_2O_2-mediated signal transduction. *P. falciparum* expresses five peroxiredoxins (i.e. Prx1a, Prx1b, Prx1m, Prx6, Prx5 or antioxidant protein (AOP) and nuclear peroxiredoxin nPrx), which differ in their subcellular localization (e.g. cytosol, mitochondria, apicoplast or nucleus) and substrate specificities (e.g. hydrogen peroxide, *tert*-butylhydroperoxide, cumene hydroperoxide and peroxynitrite). *Plasmodium* parasites do not encode catalase or a classical glutathione peroxidase and are therefore highly dependent on peroxiredoxins for the detoxification of peroxides. In support of the latter ones, the parasite imports the human peroxiredoxin 2 (hPrx2) in functional form into its cytosol (Koncarevic et al, 2009). The reduced forms of the classical thioredoxins (*Pf*Trx 1-3) are maintained by a NADPH-dependent disulfide oxidoreductase, namely thioredoxin reductase (*Pf*TrxR). Both isoforms of the thioredoxin reductase can further transfer electrons to other substrates than thioredoxins, such as low molecular weight compounds.
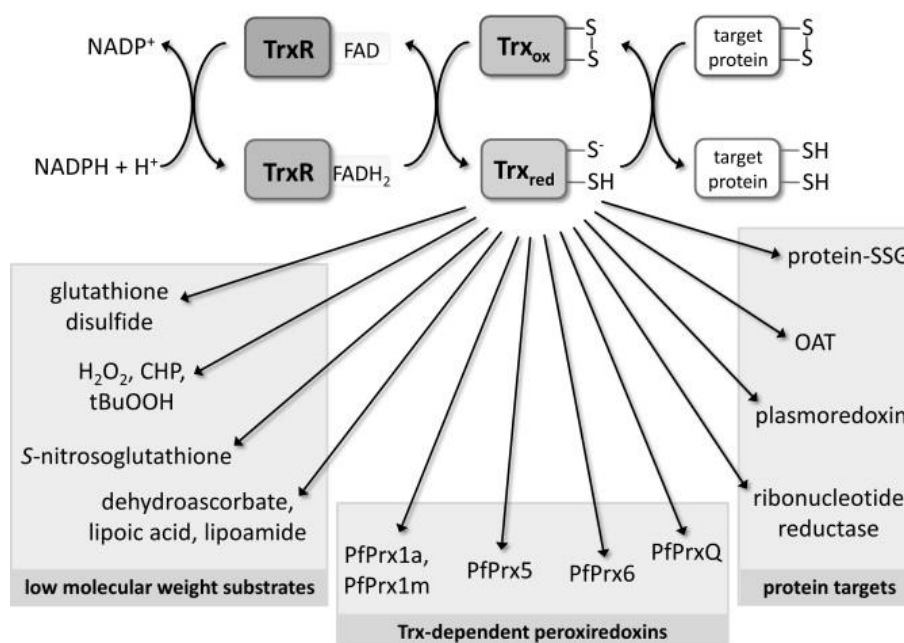
Figure 6 The thioredoxin system in *Plasmodium falciparum* (Jortzik & Becker, 2012)

This scheme illustrates reactions yielding reduced thioredoxin (Trx) and the various intracellular substrates of Trx reduction. See text for more details. Abbreviations: tBuOOH, *tert*-butylhydro-peroxide; CHP, cumene hydroperoxide; H_2O_2, hydrogen peroxide; Hb, Hemoglobin; O_2^-, superoxide anion; OH^-, hydroxyl radicals; protein-SSG, protein *S*-glutathionylation; Prx, peroxiredoxins; SOD, superoxide dismutase; Trx, thioredoxin; TrxR, thioredoxin reductase.

NADPH is the essential electron donor for GR and TrxR and is therefore an important reducing equivalent of the parasite's redox system. In *P. falciparum* and its hosting erythrocyte, NADPH is mainly generated in the pentose phosphate pathway (PPP) with the G6PD as key enzyme (Figure 7) (reviewed in Preuss et al, 2012b). Alternative sources for NADPH production in *P. falciparum* were previously suggested, for instance glutamate dehydrogenase and isocitrate dehydrogenase, but are not regarded to provide important amounts of NADPH.
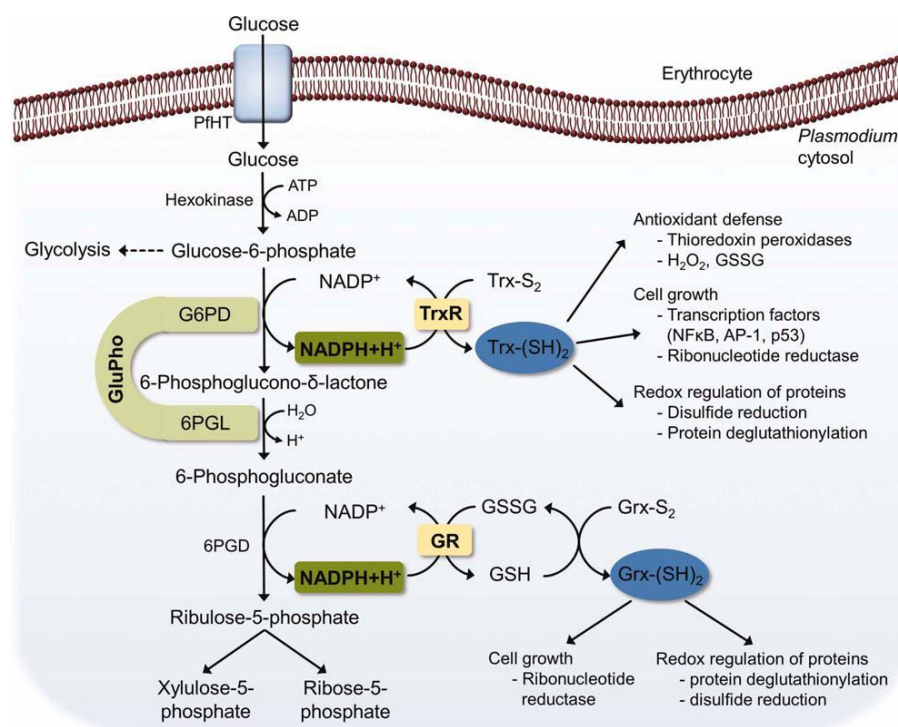
Figure 7 The pentose phosphate pathway of *Plasmodium falciparum* (Preuss et al, 2012b)

The parasite's pentose phosphate pathway produces NADPH for the glutathione and thioredoxin systems. Please refer to the text for more details. GSH, glutathione; GSSG, glutathione disulfide; GR, glutathione reductase; Grx, glutaredoxin; Trx, thioredoxin; TrxR, thioredoxin reductase; 6PGD, 6-phosphogluconate dehydrogenase; G6PD, glucose-6-phosphate dehydrogenase; GluPho, glucose-6-phosphate dehydrogenase 6-phosphogluconolactonase.

Different to its host cell, the parasite expresses a bifunctional enzyme, designated *Pf*GluPho, that combines G6PD and the second enzyme of the PPP, 6-phosphogluconolactonase (6PGL) (GluPho stands for glucose-6-phosphate dehydrogenase 6-phosphogluconolactonase) (Jortzik et al, 2011). *Pf*GluPho is regarded to account for the majority of NADPH production of the parasite (Preuss et al, 2012b) and appears to be essential for its survival (personal communication Prof. K. Becker). The parasitic enzyme

differs substantially in structure and kinetic mechanism from the human homologues G6PD and 6PGL and is therefore a suitable drug target (Jortzik et al, 2011; Preuss et al, 2012a). NADPH is formed by reduction of $NADP^+$ in two reactions catalyzed by the *Pf*GluPho and another enzyme of the PPP, 6-phosphogluconate dehydrogenase (6PGD) (Preuss et al, 2012b). The first reaction that produces NADPH converts glucose-6-phosphate into 6-phosphoglucono-d-lactone, which is further transformed by the *Pf*GluPho into 6-phosphogluconate. The second reaction converts 6-phosphogluconate into ribulose-5-phosphate and thereby produces NADPH.

1.3 Malaria prevention, treatment and control

The WHO recommends a multifaceted strategy to control and eliminate malaria by combining preventive measures, diagnostic testing, effective treatment and strong malaria surveillance (WHO, 2010; WHO, 2013). Preventive measures include vector control (i.e. insecticide treated nets, indoor residual spraying and larval control) and preventive chemotherapy for the most vulnerable patient groups (i.e. young children, pregnant women). Malaria diagnosis based on clinical symptoms should be confirmed by light microscopy or rapid diagnostic tests to avoid over-treatment.

The main goal of symptomatic treatment is obviously to cure patients (i.e. rapid, complete cure of infections), thereby preventing chronic infections and progression of uncomplicated malaria to severe forms. From a public health perspective, effective treatment is furthermore important to limit parasite transmission by reducing the parasite reservoir of infected individuals and to prevent the emergence and spread of drug-resistant parasites (WHO, 2010; WHO, 2013).

A crucial tool for control and important for elimination and eradication of malaria would be an effective vaccine. Despite enormous efforts of the scientific community, there is no licensed malaria vaccine to date (WHO, 2013). The most advanced vaccine candidate is RTS,S/AS01 that targets the *P. falciparum* circumsporozoite (CS) protein (Goldstein & Shapiro, 1997). Although this candidate already proved to be less efficient than expected in current clinical trials (Phase 3), the WHO will further guide the implementation of this vaccine after completion of the clinical studies (WHO, 2013). Several other vaccine candidates following different strategies are currently in early clinical trials (Phase 1, 2) and their development is expected to take another 5-10 years from now (reviewed in WHO, 2013; Arama & Troye-Blomberg, 2014).

Due to the lack of an effective vaccine, chemotherapy represents the solely frontline strategy for the control and future elimination of malaria. The emergence and spread of parasite resistance to currently effective drugs is a major obstacle to the control of the infection and highlights the need of new drug development strategies.

1.3.1 Emergence of drug resistance and the rational for combination therapy

The WHO defines drug resistance as "*the ability of a parasite strain to survive and / or multiply despite the proper administration and absorption of an antimalarial drug in the dose normally recommended*" (WHO, 2010). Emergence of drug resistance is considered as a two-step process: first, the genetic event raising mutants and secondly, the preferential transmission of resistant mutants in the presence of the drug (White & Pongtavornpinyo, 2003; Petersen et al, 2011). The probability of the first event depends on multiple factors, such as the frequency of genetic mutation, the fitness cost of resistant parasites, the number of drug-exposed parasites but also the selection pressure in terms of drug concentration. Transmission of drug-resistant mutants is mainly determined by the intensity of transmission and the fitness cost related to resistance. Resistant parasites must be able to produce fertile gametocytes and to complete their development in the mosquito in competition with sensitive parasites.

The resistance mechanisms described so far originate from mutations in genes or amplifications of gene copy numbers. Affected genes are either encoding the drug target (e.g. cytochrome bc1 complex, targeted by atovaquone) or transporters that affect the intracellular drug concentrations (e.g. *PF*CRT, *Pf*MDR1, conferring resistance to chloroquine and others) (White & Pongtavornpinyo, 2003). Identified drug resistance genes and mechanisms of drug resistance are discussed in details in the review of Petersen and colleagues (2011). Drug resistance has been reported for all currently used antimalarials, including the latest cases of artemisinin resistance in Southeast Asia (WHO, 2010). The emergence and spread of drug resistance is a major threat not only for sufficient patient's treatment but also for the control and elimination of malaria.

Currently, the only efficient tool to prevent or delay resistance development is the use of antimalarial combination therapy (White & Olliaro, 1996; WHO, 2010). The combined use of two or more drugs with independent mechanisms of action ensures that a resistant parasite arising *de novo* during treatment will be killed by the other compound of the drug combination.

1.3.2 The need of novel antimalarial medicines

In the perspective of a future emphasis on malaria elimination and eradication, the scientific malaria community (e.g. represented by the Malaria Research Agenda initiative (malERA)), together with the WHO, has defined a research agenda for the development of the next generation of antimalarial medicines (for instance Alonso et al, 2011; mal, 2011; Burrows et al, 2013). The ideal medicine for malaria elimination has been described as so-called Single Exposure Radical Cure and Prophylaxis (SERCaP), an agent that combines elimination of all parasite stages in the patient (i.e. radical cure), including gametocytes and hypnozoites, as well as prevention of reinfection for a defined time period (i.e. chemoprophylaxis). Up to now, no antimalarial drug or drug combination fulfills this ambitious ideal.

The need of new antimalarial medicines for control and elimination of the infection can be classified as follows (summarized from mal, 2011; Anthony et al, 2012; Burrows et al, 2013).

- New combination partners for first-line treatment:
  One fast clearing agent to reduce the initial parasite load and a long-living partner for clearance of remaining parasites that are both active against multiple drug-resistant parasites. An example is the artemisinin-based combination therapy, which is endangered by parasite resistance.

- Transmission-blocking agents:
  Compounds that kill or prevent the development of gametocytes or the development of parasite stages in the mosquito vector. Examples for gametocytocidal agents are artemisinin and primaquine, with the latter one being omitted in most African countries due to the risk of hemolysis in G6PD-deficient patients (WHO, 2010).

- Prevention of malaria relapse caused by hypnozoites:
  Agents that kill dormant liver stages (hypnozoite) of *P. vivax* and *P. ovale* and thereby prevent related relapse of the disease. An example is primaquine (see before).

- Chemoprophylaxis:

    Protection from clinical manifestation can be achieved by compounds targeting sporozoites, liver stages or early blood stages. A prerequisite is a very good safety-profile and a long half-life suitable for monthly administration. Current examples are atovaquone-proguanil combination and mefloquine.

The key criteria for these medicines were established by the Medicines for Malaria Venture (MMV) in form of so-called target candidate profiles (TCPs) (Burrows et al, 2013). TCPs are providing detailed description about the characteristics of an ideal candidate molecule, for instance the required *in vitro* efficacy, pharmacokinetic and pharmacological properties.

1.3.3 Antimalarial drugs targeting the parasite's redox system

A functional redox system is essential for the survival of *Plasmodium* parasites and especially intraerythrocytic parasite stages are particularly susceptible to oxidative stress (Becker et al, 2004). Disturbing the vulnerable redox homeostasis of the parasite-host unit has become a broadly recognized strategy for the development of new antimalarial drugs (Krauth-Siegel et al, 2005; Davioud-Charvet & Lanfranchi, 2011; Pal & Bandyopadhyay, 2012; Belorgey et al, 2013; Nepveu & Turrini, 2013). Destabilization of the redox equilibrium can be achieved in different ways: by agents that (i) directly or (ii) indirectly generate reactive oxygen species, (iii) by inhibition of vital components of the redox system, or (iv) by subversive substrates or redox-cyclers (Davioud-Charvet & Lanfranchi, 2011; Pal & Bandyopadhyay, 2012; Nepveu & Turrini, 2013). Selected examples of drugs targeting the parasite's redox system are further discussed in the following section but this list is not exhaustive. For more comprehensive and detailed description of redox-active antimalarial compounds, please refer to reviews of Krauth-Siegel and colleagues (2005), Davioud-Charvet and Lanfranchi (2011), Pal and Bandyopadhyay (2012), Nepveu and Turrini (2013), such as Belorgey and colleagues (2013).

(i) Pro-oxidative agents generating directly reactive oxygen species

Generation of reactive oxygen species by antimalarial drugs may ultimately cause an overload of oxidative stress in the parasite, cause important intracellular damage and inhibit further development. One important example is 4-aminoquinoline ferroquine (currently in clinical trials, Phase IIa in 2012) (Structure see Figure 8). Ferroquine acts as inhibitor of hemozoin formation likewise to its analogue chloroquine (Dubar et al, 2008). In addition, ferroquine contains a unique ferrocene core that allows reversible one-electron redox reactions under oxidizing conditions as present in the digestive vacuole (i.e. oxidation of ferrocene (Fe^{2+}) to ferricinium (Fe^{3+})) (Chavain et al, 2008). Owing to this reactions, ferroquine generates lethal hydroxyl radicals that contribute considerably to its antiparasitic activity (Chavain et al, 2008).
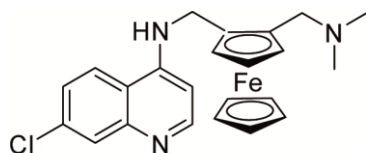
Figure 8 Structure of 4-aminoquinoline ferroquine
The characteristic ferrocene core containts two cyclo-pentadienyl rings with a central iron (Fe^{2+}) atom

Other pro-oxidative antimalarials are primaquine and dapsone, that both generate hydroxyl-metabolites, which participate in electron-transfer reactions in complex with O_2-bound hemoglobin species and thereby leading to formation of methemoglobin and reactive oxygen species. The elevation of methemoglobin levels in non-infected erythrocytes is an undesirable side effect of those drugs that causes hemolytic anemia in patients with G6PD deficiency. Therefore, both drugs are currently of minor clinical importance for the treatment of malaria (discussed in Belorgey et al, 2013).

(ii) Antimalarial agents generating reactive oxygen species indirectly

Quinolines and other clinically important antimalarials are acting as inhibitors of the vital hemozoin detoxification in the parasite's digestive vacuole. It could be shown that inhibition of hemozoin formation by those drugs resulted in release of pro-oxidant free

heme (Fe^{3+}) (Combrinck et al, 2013), which could consequently lead to generation of reactive oxygen species and oxidative stress. Though, these agents have no intrinsic redox potential and are unable to participate directly in electron-transfer reactions with hemoglobin species.

(iii) Enzymes of the antioxidant system as drug targets

Several proteins and enzymes involved in the redox systems of *P. falciparum* are validated drug targets, for instance *Pf*GR, *Pf*GST, *Pf*TrxR and *Pf*GluPho (Krauth-Siegel et al, 2005; Jortzik et al, 2011; Pal & Bandyopadhyay, 2012). Since the antioxidant systems of the parasite and its host cell are tightly connected, analogues host cell enzymes are also in the focus of inhibitor development (Krauth-Siegel et al, 2005). Respectively, a broad selection of enzyme inhibitors or suicide substrates was synthesized and demonstrated to inhibit development of blood-stage parasites. Please refer to reviews of Krauth-Siegel and colleagues (2005), Pal and Bandyopadhyay (2012) such as Belorgey and colleagues (2013) for a detailed description of these inhibitors and their antimalarial activities. So far, only one enzyme inhibitor, methylene blue, could enter clinical studies (Zoungrana et al, 2008).Some of those compounds were furthermore characterized as subversive substrates of *Pf*GR, hGR and *Pf*TrxR and are therefore proposed to act as redox-cyclers, such as methylene blue (Färber et al, 1998), aza-analogues of 1,4-naphthoquinones (Morin et al, 2008) and benzylMDs (Müller et al, 2011).

(iv) Antimalarial redox-cyclers

A particular group of redox-active drugs are subversive-substrates that act as redox-cyclers. The particular redox potential of those molecules allows them to take part in reversible one-electron or two-electron transfer reactions, for instance in a continuous reduction and oxidation cycle. Under physiological conditions, this would imply a NADPH-dependent transfer of electrons from disulfide reductases to intracellular key oxidant, for instance hemoglobin-associated or free heme species in infected erythrocytes, accompanied by formation of reactive oxygen species (previously discussed in detail for methylene blue and benzylMDs in Müller et al., 2011 and Ehrhardt et al., 2013).

Subversive substrates are also designated as turncoat inhibitors because they transform the antioxidant activity of disulfide reductases into a pro-oxidative activity, i.e. waste of the reductant NADPH and formation of reactive oxygen species (Morin et al, 2008).

The dye methylene blue is not only the first characterized redox-cycler but was once the first synthetic drug used for the treatment of malaria, discovered at the end of the 19th century by Guttman and Ehrlich (Guttmannn & Ehrlich, 1891)(Structure see Figure 9). The drug was replaced by more effective or rapidly acting drugs, such as chloroquine, but regained attention with the appearance and spread of parasite resistance to those drugs. Previous studies explored methylene blue's antimalarial activity and its mechanism of action in more detail and revealed its role as redox-cycler (reviewed in Schirmer et al, 2003; Davioud-Charvet & Lanfranchi, 2011; Schirmer et al, 2011; Blank et al, 2012). Methylene blue is a subversive substrate of various NADPH-dependent disulfide reductases (e.g. hGR and *Pf*GR, *Pf*TrxR and others) that catalyze activation of the drug to its reduced form, leucomethylene blue (Färber et al, 1998; Buchholz et al, 2008a; Buchholz et al, 2008b; Blank et al, 2012). After activation, the drug can reduce hematin-containing targets such as methemoglobin and free heme, resulting in inhibition of hemozoin formation in the parasite (Atamna et al, 1996; Blank et al, 2012). Likewise, methylene blue is clinically applied for the treatment of methemoglobinemia, which can also occur during severe forms of malaria (Schirmer et al, 2011). Of particular interest for drug application is methylene blue's activity against gametocytes that was explored *in vitro* and further confirmed in field studies (Akoachere et al, 2005; Coulibaly et al, 2009). Several methylene blue-based drug combinations are currently in clinical trials (Zoungrana et al, 2008).
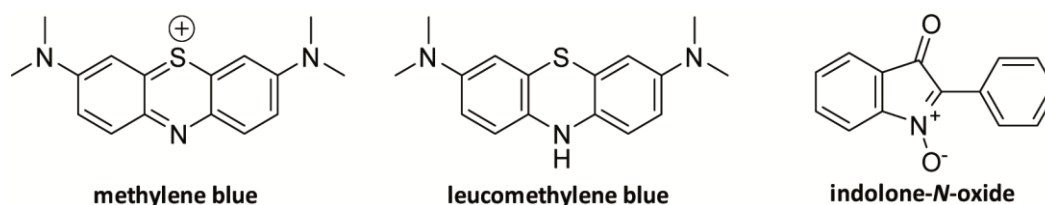
Figure 9 Structures of antimalarial redox-cyclers

A more recent example for antimalarial redox-cyclers is illustrated with indolone-*N*-oxide derivatives (INODs) (Nepveu et al, 2010; Tahar et al, 2011) (Structure see Figure 9). INODs contain a redox pharmacophore that enables reversible oxidation-reduction reactions, a prerequisite for their activity as redox-cyclers. Intracellular bioactivation of INODs was proposed to be thiol- and / or enzyme-dependent and leads to formation of a reduced metabolite, the dihydro-INOD, which could be isolated from uninfected and *P. falciparum*-infected erythrocytes (Ibrahim et al, 2011). The subsequent cascade of INODs redox reactions is not fully explored so far but the current understanding is discussed in a recent review from Nepveu and Turrini (2013). Ultimately, drug action was shown to cause a strong destabilization of the cell membrane in *P. falciparum*-infected erythrocytes, which might stem from a direct activation of redox signaling pathways INODs-generated radicals (Pantaleo et al, 2012; Nepveu & Turrini, 2013). It was considered that a stable erythrocyte membrane is vital for parasite maturation, a hypothesis that is supported by observations with erythrocytes that naturally present unstable membranes or mutations in critical structural proteins (discussed in Pantaleo et al, 2012).

Next to *P. falciparum*, other unicellular parasites (*Trypanosoma cruzi*, *Trypanosoma brucei*, *Leishmania donovani*, *Entamoeba histolytica* and *Trichomonas vaginalis*) and also multicellular helminthes (e.g. *Schistosoma mansoni*) are susceptible to oxidative stress and might therefore be similarly targeted by redox active drugs (reviewed in Krauth-Siegel et al, 2005; Pal & Bandyopadhyay, 2012).

1.4 Redox-active benzylmenadiones as novel antimalarial compounds

The natural protection of GR- and G6PD-deficiencies against severe forms of malaria was the inspiration for the development of new antimalarial compounds, which should act by disturbing the vulnerable redox homeostasis of the parasite-host unit. GR is a key enzyme in the antioxidant systems of *Plasmodium* parasites and its hosting erythrocytes and both enzymes are validated drug targets (Krauth-Siegel et al, 2005). The chemical class of 1,4-naphthoquinones is a major natural product class that includes several anti-infective agents. Their significant biological activities originate from their ability to act as electron(s)-acceptor in redox processes (Hillard et al, 2008). From menadione as a starting point, different types of GR inhibitors were designed, for instance uncompetitive inhibitors (Biot et al, 2004; Bauer et al, 2006), fluorine-based suicide inhibitors (Bauer et al, 2006) or refined analogues of those compounds that are proposed to act as Trojan horse drugs (i.e. dual prodrugs) (Davioud-Charvet et al, 2001; Friebolin et al, 2008).

Interestingly, the most potent antimalarial activity was observed for a group of benzylmenadiones (abbreviated benzylMD) that were proposed to act as prodrugs of subversive substrates of the GR (Müller et al, 2011). A subversive substrate is defined as an agent that "*changes the physiological functions of the enzyme to the opposite*" (Buchholz et al, 2008b). The enzymatic substrates, benzoylmenadions (abbreviated as benzoylMDs), are predicted to be formed intracellularly by oxidation at the benzylic chain (Müller et al, 2011). In order to act as subversive substrates, benzoylMDs are reduced by GR at the expense of NADPH (1 or 2 eletron(s)-transfer) (Figure 10). These reactions are occurring at the naphthoquinone core of the molecule. Under oxidizing conditions, oxidized benzoylMDs are regenerated, with the concomitant formation of reactive oxygen species, and can act again as substrate of the GR.
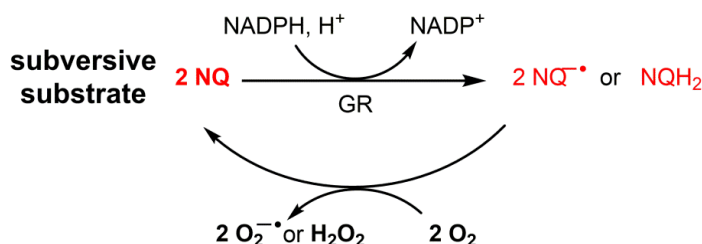
Figure 10 Reactions of subversive substrates of NADPH-dependent disulfide reductases (Müller et al, 2011)
GR, glutathione reductase; NQ, naphthoquinone core of the benzoylMD molecule.

The described redox reactions can be expected to continue until complete consumption of NADPH. Taking the formation of reactive oxygen species in account, benzylMDs reverse the antioxidative function of the GR into a pro-oxidative enzyme. The specific redox properties of benzoylMDs support the hypothesis that they act as continuous redox-cyclers and are therefore proposed to disturb the intracellular redox equilibrium of the infected erythrocyte (Müller et al, 2011; Johann et al, 2012) - a strategy that is broadly recognized for the development of new antimalarial agents (Pal & Bandyopadhyay, 2012; Belorgey et al, 2013; Nepveu & Turrini, 2013). Additionally, in respect to their pharmacokinetic properties, these benzylmenadiones are more drug-like and promise a better potential for lead optimization for drug development, than redox-cycler methylene blue.

Further work led to the selection of a series of 3-[substituted-benzyl]-menadiones (abbreviated as benzylMD) that are active against drug-sensitive and chloroquine-resistant *P. falciparum* strains in culture and additionally showed moderate antiparasitic activity in *P. berghei*-infected mice (*per os*) (Müller et al, 2011). Based on its promising antimalarial activity, low cytotoxicity such as ease and low cost of synthesis, the (3-[4-(trifluoro-methyl)benzyl]-menadione) **1c** (benzylMD **1c**, former also referred to as benzyl-naphthoquinone **1c**) was selected as the lead compound for further optimization studies (Structure see Figure 11). The synthesis of benzylMD **1c** is achieved in only one step from commercially available starting menadione and phenylacetic acid derivatives, in a silver-catalyzed radical decarboxylation reaction (Müller et al, 2011).
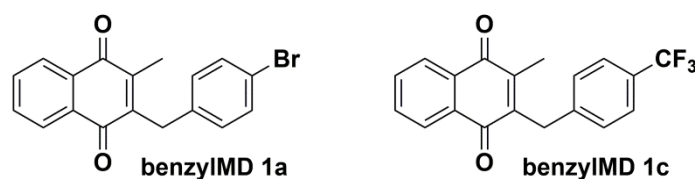
Figure 11 Structures of benzylMD 1a (first hit) and benzylMD 1c (lead compound)

In addition, selected benzylMD-derivatives were evaluated as potent compounds that inhibit the survival of helminths *Schistosoma mansoni* (Johann et al, 2012; Lanfranchi et al, 2012b).

1.4.1 Postulated mechanism of action of benzylMD redox-cyclers

Based on a multidisciplinary approach, the lead benzylMD and its redox-active metabolites are postulated to (i) disturb the redox homeostasis of the parasite by cycling hemoglobin-bound iron between three different oxidation states (+II, +III and +IV, influencing both spin state and axial ligation), (ii) enhance important NADPH-consuming processes that disrupt the antioxidant defense of infected erythrocytes, (iii) and lead to denaturation of hemoglobin, marked by binding of hemichromes to membranes of ring-infected erythrocytes which are known to enhance phagocytosis (Bielitza et al, submitted, 2014.).

The generation and recycling of benzylMD **1c**'s metabolites is proposed to occur in a continuous cascade of redox reactions, more precisely, by electron-transfer reactions in interaction with different intracellular components, such as NADPH-dependent disulfide reductases, iron or hemoglobin species (further detailed in the next section). Several predicted benzylMD-derived metabolites were synthesized (Müller et al, 2011; Cesar-Rodo et al, in preparation) and characterized in detail on their electrochemical, physicochemical and biochemical properties (Müller et al, 2011; Johann et al, 2012; Bielitza et al, submitted, 2014.). Of particular interest was thereby to evaluate their capacities to act as GR substrate, to interact with ferric targets (e.g. Fe^{3+} species, heme or methemoglobin) and to function as redox-cyclers. The structures of selected metabolites (i.e. benzoylMD **2c**, reduced benzoylMD **3c**, or benzoxanthone **4c**) are depicted in Figure 12. Their electrochemical, physico- and biochemical properties and their antimalarial activities are presented in the Appendix (Table A2) (Müller et al, 2011; Johann et al, 2012; Bielitza et al, submitted, 2014.). The reduced metabolite benzoylMD **3c** is not stable in open air and was therefore replaced by stabilized analogues **3c*** (fluoro analogue) and **3c-MOM** (methoxymethyl monoether of **3c**) for further *in vitro* studies (Bielitza et al, submitted, 2014.).
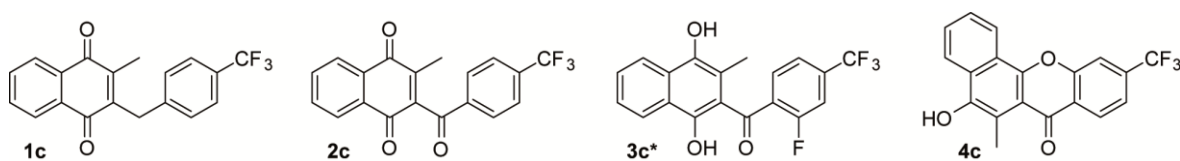
Figure 12 Structures of postulated benzylMD 1c-derived metabolites

Formation of redox-active benzylMD metabolites

The initial benzylMD **1c** is considered to be a prodrug that is activated intracellularly by oxidation at the benzylic position (e.g. catalyzed by free or bound heme), generating the first metabolite, benzoylmenadione **2c** (abbreviated as benzoylMD, step①, Figure 13). In comparison to benzylMD **1c**, metabolite benzoylMD **2c** possesses a markedly more oxidant character, which significantly enhances its efficiency to accept electrons and therefore to act as substrate of NADPH-dependent disulfide reductases, as demonstrated with the GR. Previous studies evidenced that benzoylMD **2c** and analogues are efficient substrates of both, the human and the *P. falciparum* GRs in infected erythrocytes. Of note, in all biochemical studies carried out with benzylMD **1c** and predicted metabolites, the metabolite benzoylMD **2c** was shown to be the key player in NADPH-dependent GR-mediated redox-cycling and drug-induced hemoglobin catabolism.

BenzoylMD **2c** is consequently proposed to be reduced by GR (1 or 2 electron(s)-transfer) revealing the reduced benzoylMD **3c** (step②, Figure 13). Metabolite benzoylMD **3c** was demonstrated to target relevant intracellular ferric iron Fe^{3+} species and to participate in electron exchange reactions. Numerous sources of iron (ferrous iron Fe^{2+}, ferric iron Fe^{3+}, labile iron pool) are present within the parasitized erythrocyte (oxyhemoglobin, methemoglobin, heme, hemozoin, hemichrome, labile iron pool) and play an important role in redox reactions (reviewed in Scholl et al, 2005). First, benzoylMD **3c** was characterized as effective chelator of ferric iron (Fe^{3+}), in contrast to benzoylMD **2c**, which was not effective in binding to Fe^{3+} species. Chelation of ferric iron (Fe^{3+}) was proposed to assist in drug transport between different compartments of the infected erythrocyte (siderophore-like transport) and might cycle benzoylMD-species into the parasite's acidic vesicles or digestive vacuole. Secondly, benzoylMD **3c** was proposed to transfer electrons to key oxidants that are abundant inside *P. falciparum*-infected erythrocytes, such as the hemoglobin-catabolites methemoglobin and hematin. Recent biochemical studies evidenced the proposed reduction of methemoglobin under quasi-physiological conditions, using the stabilized benzoylMD **3c*** (step③, Figure 13). In line with the proposed redox-cycling, reductions of methemoglobin and hematin were also fulfilled by oxidized benzoylMD **2c** in the presence of GR and NADPH, which continuously regenerates the reduced benzoylMD **3c** *in vitro* (designated as methemoglobin reduction assay). This UV-Vis spectrophotometric assay was set up with the NADPH-based GR system and synthetic

methemoglobin and evidences methemoglobin reduction by a shift in the soret absorbance spectrum. The conditions of this assay are described in detail in (Johann et al, 2012). Once again benzylMD **1c** was unable to directly reduce hemoglobin catabolites, irrespective of the presence of the GR / NADPH system.

Reduction of hemoglobin catabolites is considered toxic for the parasite since they inhibit two essential processes of the parasite's hemoglobin digestion. In detail, oxyhemoglobin (Fe^{2+}) is a poor substrate of the hemoglobinase falcipain-2 (Hogg et al, 2006) and reduced heme (Fe^{2+}-protoporphyrin-IX) was demonstrated to inhibit the crystallization of β-hematin (i.e. synthetic hemozoin equivalent) *in vitro* (Monti et al, 1999). The generation of damaging Fe^{2+}-species is additionally proposed to contribute to the production of harmful reactive oxygen species owing to Fenton chemistry.

Re-oxidation of reduced benzoylMD **3c** will regenerate metabolite benzoylMD **2c**, which could then initiate another cycle of redox-reactions by acting as substrate of GR or another disulfide reductase. (steps ③ and ②, Figure 13) In theory, this redox-cycling can be expected to continue until depletion of the intracellular NADPH stock.

In addition to this continuous redox-cycling, the formation of another metabolite was envisioned to occur by oxidative phenolic coupling reaction of the reduced benzoylMD **3c** radical that could generate the benz[*c*]-xanthen-7-one derivative **4c** (shortened as benzoxanthone **4c**) (Figure 13, step④). The generation of this metabolite represents a death end of benzylMD **1c**'s redox-cycling but the benzoxanthone **4c** itself showed a moderate antimalarial activity. Others xanthone derivatives were characterized as antimalarial agents that are postulated to act by inhibiting hemozoin formation (reviewed in Riscoe et al, 2005; Johann et al, 2012). Consistent with those studies, the benzoxanthone **4c** was recently proved to be the most efficient inhibitor of β-hematin formation under quasi-physiological conditions among all benzylMD **1c**-derived metabolites. In addition, the benzoxanthone was shown to reduce methemoglobin to oxyhemoglobin, although to a lower extent than benzoylMDs.
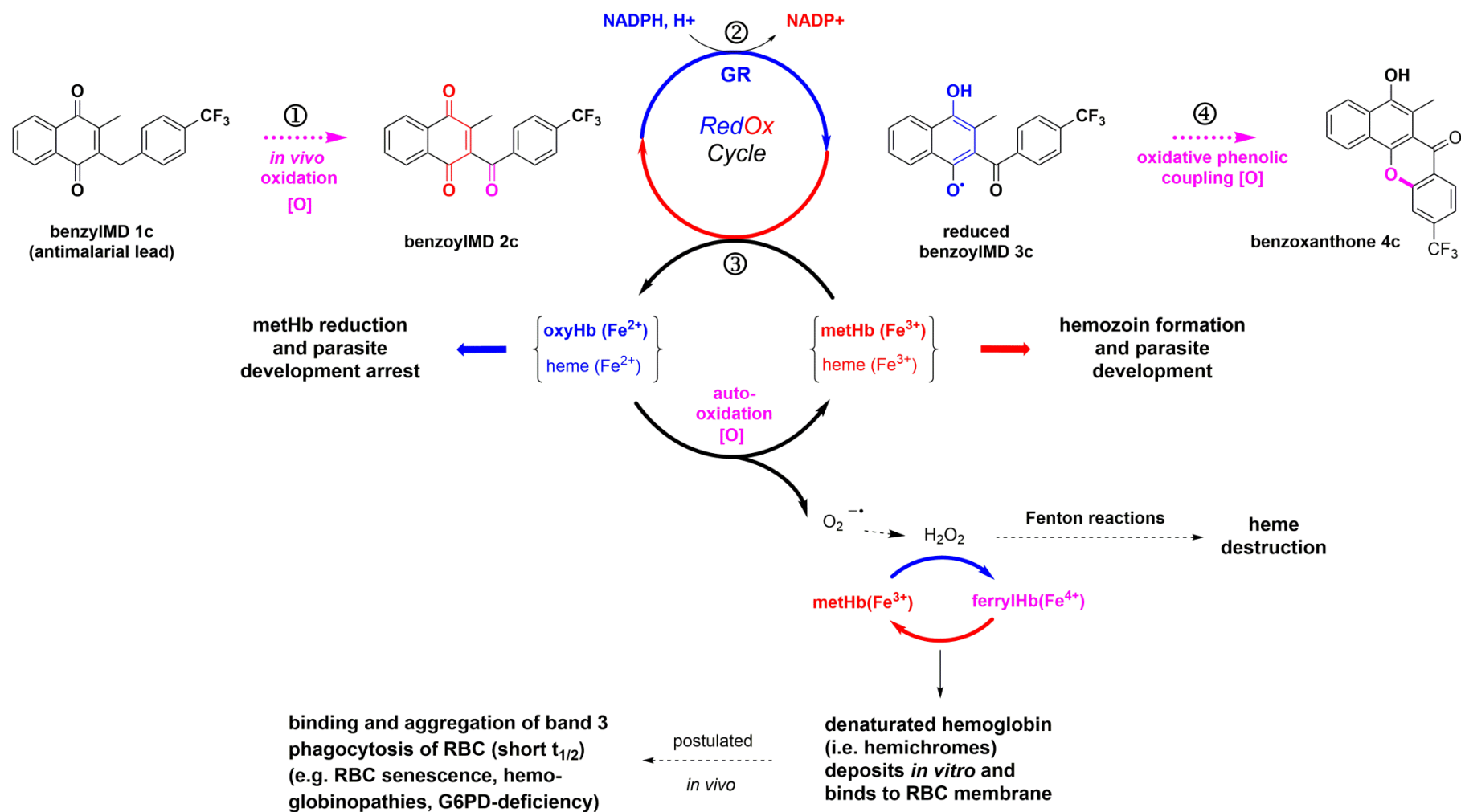
Figure 13 Cascade of redox reactions accounting for bioactivation of benzylMD 1c, formation of redox-active metabolites, formation of hemoglobin catabolites and antimalarial activity (modified after Bielitza et al, submitted, 2014.)

BenzylMD action is ultimately leading to generation of reactive oxygen species, denaturation of hemoglobin *in vitro* and binding of hemichromes to membranes of ring-infected erythrocytes in culture

As mentioned before, the proposed key feature of benzylMD **1c**'s mechanism of action is the continuous NADPH-consuming redox cycling of naphthoquinones based on the interplay of drug metabolites with hemoglobin catabolites and free- or bound-iron species. These GR-catalyzed reactions are accompanied with the release of reactive oxygen species and are expected to disturb the redox homeostasis in infected erythrocytes.

A prolonged methemoglobin reduction assay (benzoylMD **2c** in the presence of the NADPH-based GR system and methemoglobin as described before) evidenced oxidation of hemoglobin catabolites and reactive oxygen species (e.g. H_2O_2, $O_2^{-\bullet}$) in the presence of benzoylMD **2c**, marked by the formation of ferrylhemoglobin [3] (Fe^{4+}) and ultimately denaturation of hemoglobin to hemichrome, as evidenced by the formation of a greenish precipitate in the cuvette (Bielitza et al, submitted, 2014.). Evidence of ferrylhemoglobin formation in the 7h-long methemoglobin reduction assay was reached by using a derivatization reaction, i.e. the formation of the sulfhemoglobin (maximal absorbance at 620 nm) following sodium sulfide addition to the reaction mixture. Indirect evidence of hemichrome formation at the end of the prolonged methemoglobin reduction assay was provided by conversion of hemichrome (Fe^{3+}) to hemochrome (Fe^{2+}) following dithionite addition to the cuvette. Hemochrome spectrum has a specific spectrum characterized by maximal absorbances at 530 and 558 nm (Bielitza et al, submitted, 2014.).

Drug-induced hemoglobin denaturation is not solely mediated by direct interaction of benzylMD-metabolites with hemoglobin but also implies destruction of the heme structure via Fenton reactions triggered by reactive oxygen species. In such a way, after benzoylMD **3c**-catalyzed reduction of methemoglobin to oxyhemoglobin, the latter one re-oxidizes spontaneously to methemoglobin (Reeder, 2010). This reaction is accompanied by the formation of superoxide radical anions ($O_2^{-\bullet}$), which dismutate spontaneously to hydrogen peroxide (H_2O_2) and oxygen (O_2). Hydrogen peroxide is a reactive two-electron acceptor that further reduces ferrous or ferric iron to its ferryl (Fe^{4+}) oxidation state (Reeder, 2010). Ferryl iron is reactive and unstable and readily returns to the ferric (Fe^{3+}) oxidation state. Ferrylhemoglobin can further induce uncontrolled oxidation of

---

[3] For a definition of ferrylhemoglobin, please refer to Table A1 in the Appendix

macromolecules, such as lipids, DNA or proteins, including its own cross-linking. For instance, ferrylhemoglobin was reported to disturb actin dynamics during the parasite-induced remodeling of the host's cytoskeleton (Cyrklaff et al, 2011). In the process of uncontrolled reactions, the heme moiety may be irreversible damaged by a covalent binding to the protein or may be released from the protein structure, ultimately leading to denaturation of hemoglobin and formation of hemichrome (Kanias & Acker, 2010; Reeder, 2010). Hemichromes are irreversible and insoluble denaturation products of hemoglobin and are marked by significant alterations in the tertiary structure of the protein.

It is important to note, that NADPH was the limiting factor for the degradation of hemoglobin species   and consequent formation of ferrylhemoglobin in the methemoglobin reduction assay. This observation adds further support to the hypothesis, that benzylMD should highly consume intracellular NADPH and thereby contribute to the disbalance of redox homeostasis.

In support of these *in vitro* observations, benzylMD-induced hemoglobin denaturation was furthermore proven to take place in *P. falciparum*-infected erythrocytes, as evidenced by membrane-bound hemichromes. Significantly increased amounts of hemichromes were observed in ring-stage infected cells treated with benzylMD **1c** compared to untreated control cells, thereby providing a first proof of principle for the postulated mechanism of action. As discussed before in section 1.2.2.3, membrane binding of hemichromes was identified as a key determinant for phagocytosis of *P. falciparum*-infected erythrocytes (Turrini et al, 1992; Giribaldi et al, 2001; Turrini et al, 2003; Ayi et al, 2004). Given the high amount of membrane-bound hemichromes after benzylMD **1c** treatment, one would expect that phagocytosis of benzylMD-treated infected erythrocytes might importantly contribute to parasite clearance *in vivo*. It is of particular interest to further investigate this possibility in adequate *in vitro* and *in vivo* studies. However, it is important to consider that hemoglobin denaturation and resulting hemichrome formation is not necessarily the mechanism by which parasites are killed upon benzylMD **1c** treatment.

BenzylMD action is ultimately leading to perturbation of cytosolic GSH-dependent redox potential of trophozoite-infected erythrocytes in culture

As stated before, the interplay of drug metabolites with hemoglobin catabolites in a continuous redox cycling is accompanied by the release of reactive oxygen species and is therefore expected to disturb the redox homeostasis in infected erythrocytes. The redox homeostasis in infected erythrocytes largely depends on the glutathione systems of both, host and parasite, with reduced thiol GSH as a major component of those systems. Genetically encoded redox-sensitive green fluorescent protein linked to human glutaredoxin-1 (hGrx1-roGFP2) is a real-time biosensor of the glutathione-dependent redox potential of living *P. falciparum* blood-stage parasites (developed by Kasozi et al, 2013). Upon treatment with benzylMD **1c**, microscopical analysis of the cytosolic expression of hGrx1-roGFP2 in trophozoites detected a change of the GSH:GSSG equilibrium towards GSSG, indicative of a shift towards a more oxidizing redox potential in the cytosol (Bielitza et al, submitted, 2014.). This finding is a first evidence for the perturbation of intracellular redox homeostasis upon treatment with benzylMD **1c** and provides important support for the proposed mechanism of action.

1.5   Aim of the Study

Previously, the Laboratory of Medicinal Chemistry (Dr. E. Davioud-Charvet) presented the chemical design of a series of very promising antimalarial agents, 3-[substituted-benzyl]-menadiones (abbreviated as benzylMD), with potent *in vitro* and *in vivo* activities (Müller et al, 2011). Based on its antimalarial activity, low cytotoxicity as well as ease and low cost of synthesis, the benzylMD **1c** was selected as the lead compound for further biological evaluation and chemical optimization studies. Ongoing work on the mode of action shows that benzylMDs disturb the redox balance of the parasitized erythrocyte by acting as redox-cyclers (Müller et al, 2011; Johann et al, 2012; Belorgey et al, 2013; Ehrhardt et al, 2013), a strategy that is broadly recognized for the development of new antimalarial agents (Blank et al, 2012; Belorgey et al, 2013; Nepveu & Turrini, 2013). Drug development for malaria treatment is a rather complex process that is not only challenged by the changing parasite landscape (i.e. emergence of drug resistance) but is also guided by strategies to control and eliminate malaria that are developed by the WHO and leading experts of the scientific community (e.g. represented by MMV or malERA initiative) (mal, 2011; Burrows et al, 2013).

The aim of this doctoral project was to contribute to the evaluation and further development of the benzylMD series as antimalarial compounds. This work comprised:

(I) a detailed characterisation of the *in vitro* activity profile of the lead compound **1c** against cultured *P. falciparum* blood-stage parasites (i.e. lead evaluation studies)

(II) studies for further understanding of the mechanism of action of these redox-cyclers

(III) a screening of benzylMD derivatives for their *in vitro* antimalarial activity against cultured *P. falciparum* blood-stage parasites to guide further structural optimization of the lead compound by medicinal chemistry (i.e. lead optimization studies)

2 MATERIALS AND METHODS

2.1 Materials

2.1.1 Equipment

Analytical scales	Sartorius, Göttingen Germany
Autoclave	Tuttnauer Systec 2540, Wettenberg Germany
Cell counter	Beckman Coulter GmbH, Germany
Centrifuges:	
Biofuge fresco	Heraeus Instruments, Hanau Germany
Microcentrifuge MC13	Amicon Bioseparatia/ Millipore, Germany
Megafuge 2.0R	Heraeus Instruments, Hanau Germany
Megafuge 1.0R	Heraeus Instruments, Hanau Germany
Fluorescence plate reader (FluoStar optima)	BMG Labtech GmbH, Ortenberg Germany
Freezer (-80 °C)	UF85-300S Heraeus GmbH, Hanau
Freezers (-20 °C)	Liebherr, Biberach Germany
Fridges (+4 °C)	Liebherr, Biberach Germany
Gas burner (gasprofi 1)	micro WLD-TEC, Germany
Heat block (Digi-block)	JR Laboratory devices INC, USA
Incubator for *P. falciparum* cultures	Heraeus Instruments, Germany
Liquid nitrogen tank	Air Liquide, Ludwigshafen
Microscope: optical light microscope	Zeiss, Jena Germany; Leica, Wetzlar Germany
pH-meter (pH 537)	WTW, Weilheim Germany

Pipettes and pipette fillers:

Single channel pipettes (Research, 0-10 µl, 20-200 µl, 200-1000 µl)	Eppendorf, Germany
Multichannel pipette (Xplorer, 15-300 µl)	Eppendorf, Germany
Electric pipette filler (Pipetus® standard)	Hirschmann Labortechnik, Eberstadt Germany

Plate shaker (BioShake IQ)	Analytica Jena, Germany
Sterile work bench (Herasafe)	Heraeus Instruments, Hanau Germany
Stop watch	Roth, Karlsruhe Germany
Vortex (Genie 2)	Roth, Karlsruhe Germany
Water bath (Julabo 7A)	Julabo, Seelbach Germany

2.1.2 Disposables

96-well plates, v-bottom	Corning Costar
96-well plates: black, clear	Greiner Bio-One, Kremsmünster Germany
Aluminium foil	Roth, Karlsruhe Germany
Cell culture plates	Greiner Bio-One, Kremsmünster Germany
Centrifugation tubes	Greiner Bio-one, Kremsmünster Germany
Cryovials	Nalgene®, Wiesbaden Germany
Culture flasks for cell culture	Greiner Bio-One, Kremsmünster Germany
Eppendorf tubes (dark or clear)	Sarstedt, Nümbrecht Germany Germany
Falcon tubes (15 ml; 50 ml)	Corning incorporation, Bodenheim Germany
Gloves	Hartmann, Heidenheim Germany
Immersion oil	Zeiss, Jena Germany
Kimwipes lite 200	Kimberly Clark
Object slides	Marienfeld, Lauda-Königshofen Germany
Parafilm	American International CanTM, USA
Petri dishes for cell culture	Greiner Bio-one, Frickenhausen

(10 cm, 25 cm diameter)

Pipette tips (0,2-20μl)	Kisker, Steinfurt Germany
Pipette tips (20-200μl, 200-1000μl)	Corning incorporation, Bodenheim Germany; Eppendorf Germany; Biohit, Rosbach, Germany;
Plastic pipettes (1 ml; 2 ml; 5 ml; 10 ml, 25 ml)	Corning incorporation, Bodenheim Germany
Sterile filters (0,2 μm)	Millipore GmbH, Ashburn
Sterile filtration devices	Corning incorporation, Bodenheim

2.1.3 Chemicals

Chemicals were ordered from the following companies: Amersham Pharmacia Biotech Europe GmbH, Boehringer JT Baker, Fluka, Gibco Invitrogen, Carl Roth GmbH, Sigma-Aldrich, Serva, Grüssing, Merck, VWR International, Fresenius Medical Care and Ferax Berlin.

2.1.4 Buffers, media, solution

Albumax II   5% (w/v) Albumax II
in RPMI 25 mM HEPES L-Glutamine (Gibco),
filter sterilize

Cell culture media

Non-transfectants   10% human serum
0.2 μg/ml Gentamycin
0.2 mM Hypoxanthine
in RPMI 25 mM HEPES L-Glutamine (Gibco)

Transfectants   5% human serum
5% Albumax II
0.2 μg/ml Gentamycin
0.2 mM Hypoxanthine
in RPMI 25 mM HEPES L-Glutamine

Freezing Solution	6.2 M glycerol
	0.14 M Na-lactate
	0.5 mM KCL
	add ddH$_2$O, adjust to pH 7.2 with
	0.5 M NAHCO3, pH 9, filter sterilize
Lysis buffer for IC$_{50}$ determination	20mM Tris base (2.423g) in 1l water
	adjust pH to 7.4 with concentrated HCl
	5mM EDTA (10ml 0.5M EDTA)
	0.008% w/v saponin (80mg saponin)
	0.08% w/v Triton X-100 (0.8ml)
	mix, vacuum filter, store at RT
Sorbitol Solution	5% (w/v) D-sorbitol in ddH2O
	filter sterilize
Thawing solution I	12% NaCl autoclave
Thawing solution II	1.6% NaCl autoclave
Thawing solution III	0.9% NaCl / 0.2% glucose
	filter sterilize

2.1.5 Inhibitors

The lead benzylMD **1c** was prepared as previously described (Müller et al, 2011). The synthesis of other benzylMD derivatives will be described in future publications (Cesar-Rodo et al, in preparation; Urgin et al, in preparation).

The compounds allopurinol, amodiaquine (dihydrochloride, dihydrate), artemisinin, atovaquone, chloroquine (diphosphate salt), cycloguanil (HCl), 5-fluoroorotic acid hydrate (5-fluoroorotate), E64, fosmidomycin (sodium salt hydrate), methylene blue (trihydrate), proguanil (HCl) and pyrimethamine were purchased from Sigma-Aldrich. Quinine (HCl) was purchased from Serva (Heidelberg, Germany). Dihydroartemisinin was purchased from Euromedex (Souffelweyersheim, France). Cytochalasin D and ferroquine was a gift from Freddy Frischknecht (University Hospital Heidelberg, Germany) and Jacques Brocart (Lille University, France), respectively. Plasmion was purchased from Fresenius Kabi, France.

In general, stock solutions of compounds were prepared in DMSO, with the following exceptions. Methylene blue, chloroquine and fosmidomycin were prepared in pure water; quinine was dissolved in 70% ethanol and proguanil in 50% ethanol. All stock solutions were stored in aliquots at -20 °C. A fresh aliquot was used for each experiment in order to avoid drug degradation by repeated freezing and thawing.

For some experiments it was necessary to use an identical drug solution over several days (e.g. stage specificity or killing speed experiment). In these cases, drug dilutions in culture medium (working solutions) were distributed into several eppendorf tubes in the volume required for one part of the experiment and stored at -20 °C or -80 °C. Aliquots were thawed immediately prior use and remaining drug solution was discarded. Any other storage of drug solution in aqueous solutions such as culture medium was strictly avoided.

2.1.6 *P. falciparum* strains

Two familiar *P. falciparum* laboratory strains were used for this study, the chloroquine-sensitive (CQs) 3D7 strain and the chloroquine-resistant (CQr) Dd2 strain. Their chemosusceptibility to common antimalarials is given in the Appendix (Table A3).

Transfectant *P. falciparum* strains 3D7attB and 3D7attB-yDHODH were kindly provided by Hangjun Ke and Akhil B. Vaidya (Department of Microbiology and Immunology, Drexel University College of Medicine, Philadelphia, U.S.A) (Ke et al, 2011).

2.1.7 Computer software

EndNote X6	Thomson Reuters, CA, USA
FIJI/Image J version 1.47c	available at http://fiji.sc/Downloads, (Schindelin et al, 2012)
MS Powerpoint 2010	Microsoft Corporation, CA USA
MS Word 2010	Microsoft Corporation, CA USA
MS Excel 2010	Microsoft Corporation, CA USA
SigmaPlot 12.5	Systat Software Inc., IL, USA
GraphPad Prism 6	GraphPad Software Inc., USA
Illustrator CS4	Adobe Systems Software Ireland Ltd.
ChemBio Draw Ultra 13.0	PerkinElmer Informatics

2.2 Methods

Experiments presented in this work were performed in two different Laboratories, at the Department of Parasitology, Heidelberg, Germany and the Museum National d'Histoire Naturelle, Paris, France (further designated as MNHN Paris). Cultures were maintained under the respective standard culture conditions of both laboratories and are described in detail in the following paragraphs. If not stated differently, the experiments are described as conducted at the Department of Parasitology, Heidelberg, Germany

The drug concentrations chosen for several experiments were based on multiples of the drug's IC_{50} values. Though, it is known that IC_{50} values of a given drug may differ between laboratories, depending on the respective assay and culture conditions. In order to exclude any experimental fluctuations, IC_{50} concentrations were determined prior to each experiment in the identical conditions of the experiment itself (e.g. parasitemia, hematocrit) and in the routine culture condition of the respective laboratory as described below.

2.2.1 Cell culture of *Plasmodium falciparum* parasites

2.2.1.1 Culture conditions

Intraerythrocytic stages of *P. falciparum* were cultured according to standard protocols (Trager & Jensen, 1976). Cultures were maintained in an incubator with a fixed atmosphere of 5% O_2, 3% CO_2, 92% N_2 and 95% humidity at 37 °C. Routine cultures were established at a hematocrit of 3% - 4% in final volumes of 14 ml or 35 ml in a 10 cm or 25 cm diameter petri dish, respectively. The parasitemia varied between 0.5% - 5% according to need. The detailed composition of culture media is stated in section 2.1.4, Strains 3D7 and Dd2 were cultured in non-transfectant medium, containing 10% human serum. Strains 3D7attB and 3D7attB-yDHODH were cultured in transfectant medium, in which half of human serum was replaced by Albumax.

At the MNHN Paris, routine cultures were established at a hematocrit of 1 - 2% in final volumes of 25 ml – 50 ml in culture flasks as previously described in detail (Fromentin et al, 2013). A prepared gas mix, containing 3% CO_2, 6% O_2, 91% N_2, was directly injected into culture flasks with closed lids and those were maintained in an incubator at 37 °C.

42

Short time incubation of culture plates (e.g. growth-inhibition assay) were performed in a candle jar with an atmosphere of approximately 17% O_2, 3% CO_2 and 80% N_2 at 37 °C. Cultures were grown in complete medium consisting of RPMI 1640 (Life Technologies Inc.) supplemented with 11 mM glucose, 27.5 mM $NaHCO_3$, 100 UI/ml penicillin, 100 μg/ml streptomycin, and 8-10% heat-inactivated human serum.

Hematocrit and parasitemia were adjusted for individual experiments according to the respective protocol (see respective paragraph). Cultures were surveyed regularly (latest every 3rd day) on Giemsa-stained thin blood smears (see next paragraph). According to need, solely the medium was exchanged in order to avoid accumulation of toxic parasite metabolites or cultures were diluted with fresh erythrocytes in order to decrease parasitemia. The detailed composition of culture media is stated in section 2.1.4.

2.2.1.2 Morphological monitoring of parasites cultures and determination of parasitemia

Parasite cultures were examined on Giemsa-stained thin blood smears that allowed determining developmental stages, morphological alterations and parasitemia. Thin blood smears were prepared from a small volume (few microliters) of concentrated erythrocytes on microscope slides and subsequently air dried, fixed in 100% methanol for several seconds, and stained in Giemsa solution for 10 - 30 min. After staining, slides were washed under running tap water and air dried. Smears were analyzed on a light microscope under oil immersion using a 100× objective. Parasitemia is defined as the percentage of infected erythrocytes and is established by counting a total of 1000 cells.

2.2.1.3 Synchronization techniques

Different techniques are available to synchronize, enrich or purify different stages of the parasite's intraerythrocytic development (i.e. ring, trophozoites or schizonts).

Synchronization of cultures to the ring stage was performed using the sorbitol method (Lambros & Vanderberg, 1979). Sorbitol destroys trophozoite and schizont-stage parasites, which possess the tubovesicular network, by osmotic shock. Ring-stage parasites are still lacking this induced transport system and therefore survive sorbitol treatment. Briefly, pelleted infected erythrocytes (0.5 - 1.5 ml) were resuspended in prewarmed 5% sorbitol

solution (8 - 10 ml) and incubated for 5 min in a closed falcon tube at 37 °C (e.g. water bath or incubator). After incubation, cells were centrifuged (1900 rpm, 2 min, room temperature (RT)) and the supernatant sorbitol solution was removed. An additional washing step in culture medium is optional but may increase lysis of mature parasites. Cells were resuspended in culture medium, adjusted to the desired hematocrit and returned to culture.

Enrichment (and thereby synchronization) of mature schizonts was obtained using the plasmion method (Pasvol et al, 1978; Lelievre et al, 2005). Plasmion is a commercially available gelatin solution and the separation of schizont-infected erythrocytes from trophozoite or ring-infected erythrocytes and non-infected erythrocytes is based on their different sedimentation behavior in gelatin solutions. Briefly, infected erythrocytes were pelleted by centrifugation (1900 rpm, 2 min, RT) and the majority of culture medium was removed, except for ca 0.5 ml culture medium per 0.5ml cell pellet. The cells were resuspended in the remaining culture medium, mixed with 4 ml prewarmed plasmion and incubated for 20 min in a closed falcon tube at 37 °C (e.g. water bath or incubator). The falcon tube should be maintained in a stable upright position. During the incubation period, non-infected and trophozoite or ring-infected erythrocytes sediment whereas segmenters are retained in the plasmion phase. The supernatant, containing schizonts and segmenters, was transferred to a fresh falcon tube and washed twice with prewarmed culture medium. Cells were resuspended in culture medium, adjusted to the desired hematocrit and returned to culture. If needed, the pelleted infected and non-infected erythrocytes were separately washed and further maintained in culture.

2.2.1.4 Cryopreservation

P. falciparum ring-stage parasites are suitable for cryopreservation in a designated freezing solution (composition see section 2.1.4). For freezing, a culture rich in ring-stage parasites (3 - 5% parasitemia) was pelleted and the supernatant completely discarded. The remaining pellet was mixed with approximately 1/3 volume freezing solution (e.g. 500 µl cell pellet + 150 µl freezing solution) and incubated for 5 min at room temperature. Subsequently, another 4/3 volume of freezing solution was added (e.g. 600 µl) and the solution thoroughly mixed. The cell solution was transferred to specific cryovials (300 - 500 µl per

vial) and frozen at -80 °C. Short-term storage was maintained in a -80 °C freezer, while cryovials were transferred to liquid nitrogen tanks for long-term storage.

For thawing of parasite cultures, frozen cryovials were shortly warmed up in a 37 °C water bath until cell solution was passably liquid. Then, 200 µl of thawing solution I was added dropwise and the resulting solution transferred to a fresh 15 ml falcon tube. Slowly, 9 ml of thawing solution II were added dropwise under steady rotation of the falcon tube. The solution was centrifuged (1900 rpm, 2 min, RT) and the supernatant removed. In a last step, the cell pellet was slowly resuspended in 7 ml of thawing solution III, which was added dropwise. The solution was centrifuged (1900 rpm, 2 min, RT), the supernatant removed and the pellet resuspended in few milliliters culture medium. The cell solution was then transferred to a petri dish and fresh erythrocytes such as more culture medium were added.

2.2.1.5 Cloning of parasites by limiting dilution

Clonal parasite populations were obtained by a limiting dilution approach. Therefore, a parasite culture was highly diluted and distributed in 96-well plates with an initial inoculum of 0.6 parasites per well to assure that parasite cultures in each well originate from only one single parasite (i.e. individual clones).

A synchronised ring stage culture was adjusted to a fixed volume at 1.8% hematocrit. The total number of erythrocytes was determined using a cell counter. Parasitemia was counted on a freshly prepared blood smear and used to calculate the number of iRBC (infected red blood cell) per ml culture. The culture was diluted in serial steps to an initial number of 3 parasites per ml (i.e. 0.6 parasites per well) and 20 ml volume per plate. If required, benzylMD **1c** was added to the respective cultures. Parasite culture was distributed on a 96-well plate, 200 µl volume per well. Two plates were prepared per culture and condition. Weekly, culture medium (150 µl) was changed with the addition of fresh erythrocytes (at 0.4% hematocrit). After three weeks, cultures were tested for the living parasites by DNA detection with SYBRgreen (as described in section 2.2.2).

2.2.2 Growth inhibition assay and determination of IC$_{50}$ values

The antimalarial activity of an agent is generally assessed by measuring the growth (i.e. multiplication) inhibition of *P. falciparum* blood-stage parasites under drug treatment and is expressed as 50% inhibitory concentration (short IC$_{50}$ value). The IC$_{50}$ value indicates the concentration needed to inhibit the parasite's multiplication by 50% over a chosen time period. Growth inhibition assays were performed according to standard protocols based on detection of parasitic DNA by fluorescent SYBR$^{®}$ green staining (Smilkstein et al, 2004; Beez et al, 2011). Briefly, a synchronous culture of *P. falciparum* blood-stage parasites was incubated for 72 h in the presence of decreasing drug concentrations in a 96-well microtiter plate. The final conditions of the tests were 100 µl volume per well, 0.5% parasitemia and 1.5% final hematocrit (2% final hematocrit at the MNHN, Paris), 72 h incubation time at 37 °C. Cultures were synchronized using the sorbitol method as described earlier.

On the day of the assay, a culture of ring-stage parasites was established at 0.5% parasitemia and 3% hematocrit (4% hematocrit at the MNHN, Paris), ca 6 ml were needed for one 96-well plate. A solution of niRBC at 3% hematocrit was used as negative control (ca 1 ml per 96-well plate).

Drug solutions were prepared as working solutions (6×) in culture medium by diluting a freshly thawed stock solution (e.g. 5 - 6 mM in DMSO / water) to 6× starting concentration (i.e. highest drug concentration to be tested). Per drug, 50 µl of working solution is required to test the compound in duplicates. The starting concentration was chosen to allow the IC$_{50}$ concentration to fall around the midpoint of a threefold serial dilution. This concentration was calculated based on IC$_{50}$ values found in literature or was tested in preceding growth-inhibition assays. The range of drug concentrations should cover parasite viability from 0 - 100% with sufficient data points all over this range in order to assure correct IC$_{50}$ value calculation by SigmaPlot (or any other appropriate software). Starting concentrations for the benzylMD derivatives tested in this work ranged from 1 - 30 µM but are dependent on parasitemia and hematocrit.

Growth inhibition assays were performed on black 96-well plates according to the following plate scheme. The outer rows were omitted from use due to extensive evaporation and were filled with 100 µl culture medium. Firstly, 50 µl of culture medium

was filled in each well. For preparation of serial drug dilutions, 25 µl of drug working solution (6×) was added in the first well and thoroughly mixed. An 8-point 1:3 serial dilution was obtained by transferring 25 µl each from one row to the next row containing 50 µl of culture medium. The 25 µl drug solution from the final row was discarded. One column of wells was reserved for non-infected erythrocytes (negative control) and another one for infected erythrocytes (positive control). Subsequently, 50 µl of prepared parasite culture was added to each well, 50 µl niRBC solution were added to respective wells. Plates were covered with clear lids and incubated for 72 h in the usual incubator. At the MNHN Paris, drug incubation on 96-well plates was performed in a candle jar. After the incubation period, plates were wrapped in aluminum foil and frozen at -80 °C until use in order to obtain complete lysis of erythrocytes (for 2 h at least).

Plate scheme of growth-inhibition assay

1	RBC	iRBC	Drug 1	Drug 1	Drug 2	Drug 2	Drug 3	Drug 3	Drug 4	Drug 4	X
2	RBC	iRBC	Highest concentrations								X
3	RBC	iRBC									X
4	RBC	iRBC									X
5	RBC	iRBC			1:3 dilution						X
6	RBC	iRBC									X
7	RBC	iRBC									X
8	RBC	iRBC									X

Abbreviations: RBC= non-infected red blood cells, iRBC = infected red blood cells.

Parasite multiplication was assessed by fluorescent SYBR® green staining of parasitic DNA. Measured fluorescence intensity stems from SYBR® green binding to double-stranded DNA and is associated to DNA replication by multiplying parasites. However, it had to be considered that benzylMD-derivatives and putative metabolites are autofluorescent to a certain extent. This autofluorescence was indeed observed at the emission wavelength used for SYBR® green detection and could therefore be expected to increase the total fluorescence signal. An artificial increase of fluorescence intensity originating from autofluorescent compounds would be regarded as DNA content, therefore artificially increase IC_{50} value and the compound would seem less active. In order to circumvent this, the background fluorescence of the assay content (i.e. autofluorescence of compounds in lysed cell solution) was measured in a first step and deducted from the

fluorescence signals originating from SYBR® green staining. The reliability of this approach was validated using chloroquine (non-fluorescent compound), methylene blue (highly fluorescent compound) and benzylMD **1c** (weakly-fluorescent compound).

On the day of the measurement, the plates were thawed for at least 1 h at room temperature. For the first step, 80 µl lysis buffer were added per well, the plate was shaken briefly to mix the suspension and incubated for 20 min in the dark. Afterwards, fluorescence was measured in a fluorescence plate reader at 520 nm emission wave length after excitation at 485 nm using specific program settings (gain 1380, 10 flashes/well, top optic). These results, representing the background (i.e. self-induced) fluorescence of tested compounds, were saved and the plates carefully removed from the plate reader. For the second step, 1.5 µl SYBR® green were mixed into 2.5 ml lysis buffer (per 96-well plate) while avoiding exposure to bright light. Then, 20 µl of this solution was added per well, the plate was shaken briefly to mix the suspension and incubated for 40 min in the dark. After the incubation time, fluorescence was measured as in the first step and stored separately. For non-fluorescent compounds, one would mix 1.2 µl SYBR® green into 10 ml lysis buffer (per 96-well plate), distribute 100 µl per well, shake the plates briefly to mix the suspension and incubate the plate for 1 h in the dark.

At the MNHN Paris, parasite multiplication was assessed using the ^{3}H-hypoxanthine incorporation assay (Desjardins et al, 1979) as described recently (Fromentin et al, 2013). In brief, after 24 h incubation, 0.5 µCi ^{3}H-hypoxanthine was added per well and the plates were returned to the candle jar to complete the incubation period. After the incubation period, plates were wrapped in aluminum foil and frozen at -20 °C until analysis. Thawed plates were harvested on filters and filtered dried at room temperature. Dried filters were moistened in scintillation liquid mixture (OptiScint, Hisafe). Radioactivity was counted in a 1450 Microbeta counter (Wallac, PerkinElmer). Radioactive signals originate from ^{3}H-hypoxanthine uptake and incorporation into DNA by multiplying parasites

IC_{50} values were calculated as follows. First, the background fluorescence values (measured in step 1) were deducted from the SYBR® green fluorescence values (measured in step 2) for each individual well of the entire plate. The fluorescence intensity of non-infected erythrocytes represents the background fluorescence of the cell solution, thus the calculated mean fluorescence intensity of non-infected erythrocytes (6 wells at least) was deducted from all infected erythrocytes measurements. The fluorescence intensity of

untreated infected erythrocytes represents 100% parasite multiplication. Thus, the multiplication of treated infected erythrocytes was calculated based on the calculated mean fluorescence intensity of infected erythrocytes and expressed as percentage. These values, together with the respective drug concentrations, were plotted in form of a dose-response curve in SigmaPlot (x-axis = drug concentration (M), y-axis = parasite multiplication (%); curve fit function, sigmoidal non-linear regression). The IC_{50} values were calculated by SigmaPlot according to the Hill function (four parameters).

Growth inhibition assay and determination of IC_{50} values conducted at the Institut de Médecine Tropicale du Service de Santé des Armées, Marseille, France

Dr. Bruno Pradines[4] determined the *in vitro* antimalarial activity of lead benzylMD **1c** and control antimalarials against multiple drug resistant *P. falciparum* strains originating from different countries.

The following strains of *P. falciparum* (familiar laboratory strains or strains obtained from isolates after growth in culture for an extended period of time) were used in this study: Dd2 (SE Asia), 3D7 (Africa), D6 (Sierra Leone), **IMT** 8425 (Senegal), IMT Vol (Djibouti), **IMT** L1 (Niger), PA (Uganda), **IMT** Bres (Brazil), FCR3 (the Gambia), W2 (Indochina), FCM29 (Cameroon), **IMT** K2 and **IMT** K14 (Cambodia). Strains **"IMT"** were isolated at the Institut de Recherche Biomédicale des Armées, Marseille. All strains are clonal and clonality was verified using PCR genotyping of polymorphic genetic markers, *msp1*, *msp2* and microsatellite loci (Bogreau et al, 2006; Henry et al, 2006). The chemosusceptibility profiles of these *P. falciparum* strains to common antimalarials in use and multidrug resistance (MDR) phenotypes of the strains are given in the Appendix (Table A3).

Atovaquone was obtained from GlaxoSmithKline (Evreux, France), all other agents were purchased from Sigma-Aldrich. Stock solutions were prepared in DMSO with the following exceptions: Quinine, dihydroartemisinin and atovaquone were dissolved first in methanol and then diluted in water.

Growth inhibition assays were performed as previously described in detail (Wenzel et al, 2010) using the ^{3}H-hypoxanthine incorporation assay (Desjardins et al, 1979). Briefly, synchronous parasitized red blood cells (final parasitemia, 0.5%; final hematocrit, 1.5%)

---

[4] Dr. Bruno Pradines, Unité de Recherche en Biologie et Epidémiologie Parasitaires, Institut de Recherche Biomédicale des Armées, Institut de Médecine Tropicale du Service de Santé des Armées, Marseille, France

were incubated for 48 h in the presence of different drug concentrations in 96-well plates. All strains were synchronized twice with sorbitol before use. Inhibitors were analyzed in twofold serial dilutions in duplicates and in 3 - 5 independent repetitions. Parasite multiplication was assessed by adding ^{3}H-hypoxanthine at time zero.

Identification of cross-resistance to clinical antimalarials

A possible *in vitro* cross-resistance of benzylMD **1c** with clinical antimalarials was assessed by a correlation analysis as previously described (Briolant et al, 2010; Pradines et al, 2010). This analysis was conducted in GraphPad Prism by pairwise correlation of the IC$_{50}$ values of benzylMD **1c** and others antimalarial compounds using the Spearman nonparametric correlation. This nonparametric test was selected as the IC$_{50}$ values for a given drug does not fit a normal distribution, as confirmed with the D'Agostino & Pearson omnibus and Shapiro-Wilk normality tests in GraphPad Prism. Results are presented as the coefficient of correlation (rs, Spearman nonparametric correlation coefficient) and the two-tailed P value. The correlation coefficient quantifies the direction and strength of correlation and ranges from -1 (i.e. strong negative correlation) over 0 (i.e. no correlation) to +1 (i.e. strong positive correlation).

2.2.3 *In vitro* stage specificity

Stage specificity of drug action was assessed by exposing highly synchronous parasites for only short incubation times to benzylMD **1c** or control antimalarial chloroquine and analysing subsequent parasite development. Briefly, highly synchronous *P. falciparum* 3D7 parasites were transiently incubated with drug concentrations representing $1 \times$IC$_{50}$, $5 \times$IC$_{50}$, $10 \times$IC$_{50}$ values for consecutive 8 hours periods (with the exception of a first, 4 hours period). Subsequently, cells were washed, resuspended in drug-free medium and maintained until reinvasion was completed. The parasite development under drug treatment was assessed by counting parasitemia after reinvasion on Giemsa-stained blood smears. The experiments were performed at the MNHN under the respective routine conditions as described before. Drug incubation on 96-well plates was performed in a candle jar. The IC$_{50}$ values of benzylMD **1c** and chloroquine were determined before and moreover in parallel to the experiment under the respective conditions (see below).

To obtain 4 independent highly synchronous cultures, parasites were synchronized on a 4h-time window by several successive plasmion and sorbitol treatments. Therefore mature schizonts (segmenters) were enriched using plasmion, as described before, and the culture was returned into the incubator to allow further development (i.e. reinvasion). With the first appearance of newly invaded ring-stage parasites (generally 4 - 5 hours later) the culture was synchronized again using sorbitol in order to destroy remaining trophozoite and schizont stages. This procedure was repeated over several life cycles in order to obtain a highly synchronous culture. Two days before the experiment, parasites were splitted into four culture flasks containing erythrocytes and plasma from different donors each and grown for 48 hours in normal culture conditions. On the day of the assay, another round of plasmion / sorbitol treatment was performed. Approximately 1 - 2 h after sorbitol treatment, the four independent highly synchronous cultures were adjusted to 0.5% parasitemia and 2% hematocrit, distributed in small culture flasks (10 ml per flask per culture) and maintained at regular culture conditions for complete duration of the experiment. The experiment was started with parasites aged 0-4 hours. At different times of parasite development (i.e. every 8 h with the exception of an initial 4 h time point), the required amount of parasite culture was taken from the initial culture flask and distributed on 96-well plates (see below). Parasite development in the initial culture flask was followed over time by microscopic examination of Diff-Quick-stained smears. BenzylMD **1c** and chloroquine effects on the whole parasite cycle were controlled by continuous incubation (48h) of the parasites with drugs.

Drug treatment was performed on black 96-well plates according to the plate scheme depicted below. Drug solutions for the complete experiment were prepared as 4× working solutions in a mix of the 4 different culture media by diluting a freshly thawed stock solution. Different concentrations were prepared as serial dilutions. Drug solution was aliquoted for each experimental step and stored at -20 °C. One plate was used per incubation period and was prepared directly before use. The outer rows were omitted from use due to extensive evaporation and were filled with 100 µl culture medium. First, 25 µl of drug working solutions (4×) or culture media (for untreated controls) were added in the respective wells. Subsequently, 75 µl of parasite solution from the initial stock culture was added to each well. Plates were covered with lids and incubated in a candle jar.

Plate scheme of stage specificity experiment

X	benzylMD 1c				X	chloroquine				X
X	**Culture 1**	**Culture 2**	**Culture 3**	**Culture 4**	X	**Culture 1**	**Culture 2**	**Culture 3**	**Culture 4**	X
X	untreated control	untreated control	untreated control	untreated control	X	untreated control	untreated control	untreated control	untreated control	X
X	$1\times IC_{50}$	$1\times IC_{50}$	$1\times IC_{50}$	$1\times IC_{50}$	X	$1\times IC_{50}$	$1\times IC_{50}$	$1\times IC_{50}$	$1\times IC_{50}$	X
X	$5\times IC_{50}$	$5\times IC_{50}$	$5\times IC_{50}$	$5\times IC_{50}$	X	$5\times IC_{50}$	$5\times IC_{50}$	$5\times IC_{50}$	$5\times IC_{50}$	X
X	$10\times IC_{50}$	$10\times IC_{50}$	$10\times IC_{50}$	$10\times IC_{50}$	X	$10\times IC_{50}$	$10\times IC_{50}$	$10\times IC_{50}$	$10\times IC_{50}$	X
X	X	X	X	X	X	X	X	X	X	X

After drug incubation, cells were washed twice with 2 volumes of culture medium by repeated centrifugation of the culture plates. The cells were resuspended in their respective culture medium and the plates returned into the candle jar. Parasites were allowed to complete their development until reinvasion.

The experiment was stopped at approximately 62h post invasion (p.i.) to assure that re-invasion was fully completed. Smears were made from all samples at time zero and time 62h p.i. Parasitemia was determined by optical counting of 2000 RBCs (red blood cells) per smear. Reinvasion rate in percent was established for each culture and incubation period, taken that the 100% value was the parasitemia from the corresponding untreated control culture.

Drug effect on early (ring) and late development stages (trophozoites and schizonts) was assessed similarly. Therefore, Rings (aged 0-4h) or trophozoites (aged 24-28h) were incubated for 22- 24 h in normal medium (control) or in medium with benzylMD **1c** or chloroquine at $1\times IC_{50}$, $5\times IC_{50}$, $10\times IC_{50}$ or $50\times IC_{50}$ final concentrations.

Inhibition of parasite egress and / or invasion:

Drug effect on parasite egress and / or invasion was assessed similarly to the stage specific drug activity described before. The experiment started when the culture showed appreciable enrichment in mature schizonts (segmenters). Parasitemia and hematocrit were adjusted to 1% and 1.5%, respectively. The initial number and proportion (in percentage) of schizonts and rings was established by optical counting on a Diff-Quick-stained thin smear. The culture was then splitted into five sub-cultures, transferred on 96-well plates and incubated with either 10 μM E64, 100 nM Cytochalasin D or with $5\times IC_{50}$ or $10\times IC_{50}$

concentrations of benzylMD **1c** (final concentrations) or normal culture medium for control. Treated parasites were incubated for 8 h in a candle jar of 37°C to allow egress and reinvasion to proceed. At the end of the incubation period, parasitemia and number and proportion (in percentage) of schizonts and rings in each culture were determined by optical examination of Diff-Quick-stained smears. At least 2,000 RBC were counted per smear.

2.2.4 *In vitro* speed of action or killing speed experiment

The *in vitro* speed of action (or killing speed) of benzylMD **1c**, artemisinin and atovaquone were assessed according to the original protocol established by Sanz and colleagues (2012). Treatment was performed with concentrations representing $5 \times IC_{50}$ value of each drug, which were established prior to the experiment under the respective conditions (0.5% parasitemia, 2% final hematocrit, 48 h incubation time). In principle, the experiment is based on determination of parasite viability in response to drug treatment by assessing re-growth of treated parasites over time.

Briefly, a culture of *P. falciparum* 3D7 blood-stage parasites (asynchronous culture with a predominant ring-stage population) was treated with $5 \times IC_{50}$ concentrations for a total duration of 6 days (144 h). Every 24 h, a defined sample of parasites was taken from the treated culture, washed with drug-free medium and transferred to a 96-well plate. On the 96-well plate, parasites were diluted in a 12-step, 1:3 series in order to obtain a limiting dilution (i.e. one single parasite per well). Parasites were cultured for a total duration of 28 days to allow viable parasites to grow to higher parasitemia, which can be detected by SYBR® green (alternatively by ^{3}H-hypoxanthine). On days 21 and 28, a part of the culture was analyzed for the detection of viable, growing parasites using SYBR® green. The number of the last dilution step containing growing parasites was used to recalculate the number of viable parasites present in the initial aliquot. Results are presented in graphical form as numbers of viable parasites over time of drug treatment. These results furthermore allow to determine a drug's lag phase (i.e. time needed to reach the maximal killing rate) and to calculate the parasite reduction ratio over one parasitic life cycle of 48 h (short PRR) and the parasite clearance time (i.e. time needed to kill 99.9% parasites, short PCT).

On the day of the assay, one asynchronous culture was established at 0.5% parasitemia and 2% hematocrit, which corresponds to 10^6 iRBC / ml, and distributed in small culture flasks (10 ml per flask per drug treatment). An aliquot of 1 ml of the initial culture was kept separately in order to establish the first serial dilution of untreated parasite (0 h). Drug solutions for the complete experiment were prepared as 100× working solutions in culture medium by diluting a freshly thawed stock solution, aliquoted for each day and stored at -20 °C. Culture medium and drug were renewed daily over the entire treatment period.

Drug treatment was started on day 0 by adding 100× working solution (10 µl / 1 ml) into prepared culture flasks that were subsequently maintained under usual conditions in the incubator. At different time points (8 h, 24 h, 48 h, 72 h, 96 h, 120 h, 144 h), 3 aliquots of treated parasites à 150 µl (i.e. $1.5×10^5$ iRBC) were taken from the treated culture. Before preparing the serial dilutions, treated parasites were thoroughly washed 3 times with fresh culture medium (> 1 ml) to wash out the drug. After the last washing step it was important to restore the original volumes and thereby the original hematocrit (i.e. number of cells / µl).

Serial dilutions (12 steps, 1:3 dilutions) of untreated or treated parasites were prepared in triplicates on 96-well plates (V-bottom). Therefore, a solution of non-infected red blood cells (niRBC) at 2% hematocrit was prepared (ca 4 ml per drug, per day). The plates were prepared as follows. The outer rows were omitted from use due to extensive evaporation and were filled with 150 µl culture medium. Wells 2-12 of the serial dilution (in triplicates) were filled with 100 µl of the prepared niRBC solution, leaving the first well empty for the treated parasite culture. These ones were then filled with the washed parasites (150 µl). A 1:3 serial dilution was obtained by transferring 50 µl each from one row to the next row containing 100 µl niRBC solution. One additional column of wells was filled with 100 µl niRBC solution as negative control for SYBR® green detection. At the end, another 50 µl of prewarmed culture medium was added to each well (final conditions: 150 µl volume, 1.33% hematocrit).

Plates were maintained under usual conditions in the incubator for a total duration of 28 days. Medium was replaced twice a week (100 µl), once a week with addition of fresh erythrocytes (100 µl niRBC solution of 0.66% hematocrit). For detection of viable parasites, the cultures were divided in halves on day 21. Therefore, a solution of non-infected erythrocytes (niRBC) at 2% hematocrit (ca 4 ml per dilution series in triplicates)

and black 96-well plates were prepared. A maximal volume of supernatant was removed from the cell pellet, the wells refilled with 100 µl niRBC solution and the cell solution thoroughly mixed. Then, 100 µl of the resuspended solution were transferred to the black 96-well plate, which was maintained in the incubator for another 3 days before analysis. The original wells were filled again with 100 µl niRBC solution and maintained in the incubator for another 7 days until day 28.

Detection of viable parasites was performed using SYBR® green according to the protocol described before, without measuring background fluorescence (section 2.2.2). Giemsa-stained blood smears of all wells were prepared to confirm results from SYBR® green detection.

Calculation of viable parasites, parasite reduction ratio and parasite clearance time

All parameters were calculated as described in the original protocol established by Sanz and colleagues (2012). The number of viable parasites was back-calculated by using the formula $X^{(n-1)}$. X stands for the dilution factor (i.e. 3) and n is the number of wells detected positive for viable parasites (in other words, the number of the last dilution step containing growing parasites). In the case that no parasites recovered in all wells (n=0), the number of viable parasites was estimated as zero. The numbers of viable parasites after drug treatment are presented in graphical form as "viable parasites +1" in logarithmic scale ($\log_{10}$). This presentation was adopted from the original protocol (Sanz et al, 2012) since only values greater than zero can be plotted on a logarithmic scale. A possible stagnation of parasite numbers during the first days (hours) of drug treatment is generally considered as lag phase (i.e. time needed to reach the maximal killing rate) and is characterized by a plateau of the curve. The parasite reduction ratio (PRR) was calculated as the decrease of viable parasite numbers over 48 h in the phase of maximal killing, meaning by excluding the period of lag phase. As an example, if a drug has a lag phase of 72 h, the PRR is calculated by dividing the number of viable parasites at 72 h by the number of viable parasites at 120 h. The parasite clearance time (i.e. time needed to kill 99.9% parasites, PCT) was determined using a linear regression of the time-response curve. The linear regression was calculated from time-point 0 h until the first time point at which parasites were cleared (parasite number =0) and included a possible lag phase.

2.2.5 *In vitro* parasite resistance development

Experiments on parasite resistance were performed with the *P. falciparum* Dd2 strain, owing to its ability to easily acquire resistance to drugs under *in vitro* conditions, commonly designated as *accelerated resistance to multiple drugs* (ARMD) phenotype (Rathod et al, 1997; Trotta et al, 2004; Castellini et al, 2011). The ARMD phenotype was linked to a defective DNA repair machinery, which could explain the acquisition of beneficial point mutations under drug pressure (Castellini et al, 2011).

2.2.5.1   Risk of *de novo* resistance development

The intrinsic potential of benzylMD **1c** to induce parasite resistance was assessed by continual exposure of blood-stage parasites to lethal drug concentrations, based on the method established by Rathod and colleagues (Rathod et al, 1997). By using different parasite inocula, this experiment allows to determine the minimum number of parasites necessary for the development of resistant mutants (so-called frequency of resistance selection). Therefore, a series of *P. falciparum* Dd2 blood-stage cultures with high parasite inocula (10^8, 10^7, 10^6, 10^5 iRBC) were maintained in the presence of $5 \times IC_{50}$ or $10 \times IC_{50}$ concentrations of benzylMD **1c** (corresponds to approx. $2 \times IC_{90}$ and $4 \times IC_{90}$ concentrations). According to the original protocol, control cultures were maintained in the presence of 100nM 5-fluoroorotate. The cultures were regularly checked for the emergence of resistant parasites on blood smears.

Two lethal benzylMD **1c** concentrations were chosen for drug treatment: 250 nM and 500 nM. Those concentrations were chosen according to the IC_{50} value that was determined directly before the experiment: IC_{50} value of 51 nM (Appendix, Table A5). Working solutions ($1\,000\times$) of benzylMD **1c** and 5-fluoroorotate were prepared in pure DMSO in the following concentrations: 0.5 mM and 0.25 mM for benzylMD **1c**, as well as 0.1 mM for 5-fluoroorotate. Small aliquots were stored at -20°C and thawed freshly before use.

Parasites were prepared as follows. Drug-pressure experiments were started with *P. falciparum* Dd2 ring-stages parasites. Several big parasite cultures (i.e. 40 ml volume, 1.5 ml erythrocytes) were allowed to grow to high parasite density (ca 5-8% parasitemia). Parasites were synchronised with the sorbitol method and washed once with culture

medium. Cells were resuspended in one big culture flask at 2% hematocrit. The parasites were allowed to rest for at least two hours in the incubator at 37°C. In the meantime, the total number of erythrocytes in the culture was determined using a cell counter. Parasitemia was counted on a freshly prepared blood smear and used to calculate the number of infected erythrocytes per 1 ml of culture.

A series of 10 ml cultures were inoculated with decreasing numbers of parasites: 10^8, 10^7, 10^6 and 10^5 infected erythrocytes (in total). Therefore a serial dilution of infected erythrocytes was prepared in a non-infected erythrocyte suspension of 2% hematocrit. For each condition, two independent cultures of synchronous ring-stage parasites were established from two individual stock cultures and maintained in parallel. Treatment was initiated by adding 1 µl drug working solution (1 000×) per 1 ml culture. Three control flasks with untreated parasite cultures were maintained to survey the quality of erythrocytes and culture medium.

Cultures were maintained as follows. Parasites were initially cultured in a volume of 10 ml and at 2% hematocrit. Culture medium was changed regularly: daily during the first week of the experiment, four times in the second week, twice a week from week 3-12 and also twice a week for the last 4 weeks. Parasites were challenged with drug with every medium change, besides after drug removal for the last 4 weeks of culturing. Therefore 1 µl drug working solution (1 000×) per 1 ml culture was added to the medium. A blood smear was prepared with every medium change to check for the emergence of resistant parasites and for the state of erythrocytes. Fresh erythrocytes were added regularly to the cultures regarding their appearance on the blood smear. To maintain a hematocrit between 2-4%, the culture volume was increased over the time to a final volume of 25 ml by the end of the experiment.

The original time scale of the experiment (8 weeks) was prolonged to an overall duration of 16 weeks. Over week 1-12, cultures were exposed continuously to the drug to allow the emergence of resistant mutants. By the end of week 12, treatment with benzylMD **1c** was stopped. The drug was removed by washing the cultures twice in fresh culture medium and cells were resuspended in fresh culture medium (2% hematocrit). The cultures were maintained for another 4 weeks to allow the proliferation of possibly retained tolerant parasites.

2.2.5.2   Selection of drug-adapted parasites

Drug-adapted or resistant parasites were selected under drug pressure with stepwise increasing concentrations of benzylMD **1c** according to the protocol established by Beez et al. (2011). Therefore, a culture of *P. falciparum* strain Dd2 with high parasite inoculum was maintained in the presence of sublethal concentrations of benzylMD **1c** until the reappearance of normally growing parasites. Subsequently, concentrations for drug pressure were increased according to the altered susceptibility of drug-selected parasites. BenzylMD **1c** concentrations for selection were chosen in the order of the IC_{90} concentration of the respective parasite population.

The sublethal benzylMD **1c** concentration of 125 nM, representing the IC_{90} value was chosen for drug treatment. This concentration was chosen according to the IC_{90} value that was determined directly before the experiment. For the second selection cycle, culture F3 was treated with 800 nM. Culture F2 was initially challenged with 500 nM benzylMD **1c** but the concentration was raised to 550 nM at the end of the first week. Working solutions (1 000×) of benzylMD **1c** were prepared in pure DMSO at concentrations of 0.125 mM (first selection cycle) and 0.5 mM or 0.8 mM (second selection cycle). Small aliquots were stored at -20°C and thawed freshly before use.

Parasites for each selection step were prepared as follows. Drug-pressure experiments were started with *P. falciparum* Dd2 ring-stages parasites (see below for detailed conditions of each selection step). To obtain a maximal parasite inoculum, several big parasite cultures (i.e. 40 ml volume, 1.5 ml erythrocytes) were allowed to grow to high parasite density (ca 10-14% parasitemia). These cultures were pooled and adjusted to the starting conditions: 200 ml total volume at 2% hematocrit. The parasites were allowed to rest for at least one hour until further use in the incubator at 37°C. In the meantime, the total number of erythrocytes in the culture was determined using a cell counter. Parasitemia was counted on a freshly prepared blood smear and used to calculate the total parasite inoculum. Drug pressure was started by adding 1 μl drug working solution (1 000×) per 1 ml culture. Subsequently, the initial culture was distributed in four culture flasks à 50 ml each.

Conditions of the first selection cycle: Initial culture was established with an inoculum of 3.6×10^9 iRBC. The parasitemia increased to high levels over the first three days. To avoid crashing of parasites, pooled iRBC were diluted with non-infected RBC (1:0.625). The

resulting culture was assessed to 250 ml volume, 2,6% hematocrit and distributed into 5 culture flasks. The 1st selection cycle was independently repeated with the same parasite inoculum (3.6×10^9 iRBC). The initial culture was challenged with 125 nM benzylMD **1c.** During the first week of drug treatment, parasites continued to multiply to high parasitemia. Therefore, drug concentration was increased to 150 nM and the cultures were divided into 6 culture flasks in total that were subsequently treated identically.

Conditions of the second selection cycle: Initial cultures were established with an inoculum of 1.1×10^9 iRBC for culture F2 and 1.0×10^9 iRBC for culture F3. This culture was subsequently divided into 4 culture flasks that were treated identically.

Cultures were maintained as follows. Parasites were initially cultured in a volume of 50 ml and at 2-2,6% hematocrit. Culture medium was changed regularly: 3-4 times during the first 3 weeks of the experiment and twice a week until appearance of growing parasites. Parasites were challenged with benzylMD **1c** with every medium change. Therefore 1 µl drug working solution (1 000×) per 1 ml culture was added to the medium. A blood smear was prepared with every medium change to check for the emergence of resistant parasites and for the state of erythrocytes. Fresh erythrocytes were added regularly to the cultures regarding their appearance on the blood smear.

Cultures with growing parasites were checked daily. Parasites were allowed to recover from drug pressure until they presented a normal multiplication rate and a regular life cycle. As soon as they grew nicely, the cultures were splitted into two parts: one part was kept further with treatment and the other one without treatment. The cells of the latter ones were washed twice with fresh medium. After two life cycles, these parasites were used for growth-inhibition assays to determine their susceptibility to benzylMD **1c** (i.e. IC$_{50}$ and IC$_{90}$ values). Additionally, parasites were prepared for cryopreservation.

Growth inhibition assays were conducted according to the standard protocol (refer to section 2.2.2). A culture of progenitor *P. falciparum* Dd2 parasites was used as control. BenzylMD **1c** was tested in 3 different starting concentrations: 10 µM, 5 µM and 3 µM for the cultures of the first selection cycle and the Dd2 control culture, as well as 20 µM, 10 µM and 5 µM for the cultures of the second selection cycle. Chloroquine was used as a control drug (5 µM starting concentration).

2.2.6 *In vitro* drug combination assays

In vitro drug-drug interactions between two agents of choice were investigated using the fixed-ratio isobologram method established by Fivelman and colleagues (2004). This approach is based on determining the IC_{50} values of each individual drug alone and the IC_{50} values of a mixture of both drugs at fixed concentration ratios. In principle, the shift of a drug's IC_{50} value determined in combination with a second agent compared to the IC_{50} value determined for this drug alone is indicative for the nature of drug-drug interaction. Arithmetical analysis requires several calculation steps to reveal the unit of measurement, the so-called mean sum of fractional 50% inhibitory concentration (mean $\sum FIC_{50}$). Arithmetical analysis was furthermore supported by graphical analysis of results in form of isobolograms.

The principle experimental set-up is similar to the growth-inhibition assay for determination of IC_{50} values, please refer to section 2.2.2. Briefly, an asynchronous culture of *P. falciparum* blood-stage parasites was incubated for 48 h in the presence of decreasing drug concentrations in a 96-well microtiter plate. The final conditions of the test were 100 µl volume per well, 1% parasitemia and 1.5% final hematocrit (2% final hematocrit at the MNHN, Paris) and 48 h incubation time at 37 °C.

On the day of the assay, an asynchronous parasite culture was established at 1% parasitemia and 3% final hematocrit (4% final hematocrit at the MNHN, Paris). Drugs were applied alone (A or B) and in combination at fixed concentration ratios (A:B) and analyzed in threefold serial dilutions. Drug mixtures were prepared from 2× working solutions of each drug in the following fixed concentration ratios (v/v): ratio A : B = 1:4, 2:3, 2.5:2.5, 3:2, 4:1 (ratios 1:4, 2:3, 3:2, 4:1 at the MNHN, Paris). Drug mixtures were prepared directly on the 96-well plates in a total volume of 100 µl (see below). IC_{50} values of drugs A and B alone were determined on the same plate to ensure accurate calculation of drug interactions.

Drug combination assays were performed on black 96-well plates according to the plate scheme depicted below. The outer rows were omitted from use due to extensive evaporation and were filled with 100 µl culture medium. Firstly, 50 µl of culture medium was filled in wells 2-12 of the serial dilution, leaving the first well empty for the drug solutions. For preparation of serial drug dilutions, a total of 100 µl of 2× drug working

solution (individual or as mix of drug A and B) was added in the first wells and thoroughly mixed. 25 µl of drug solution was discarded. An 8-point 1:3 serial dilution was obtained by transferring 25 µl each from one row to the next row containing 50 µl of culture medium. The 25 µl drug solution from the final row was discarded. One column of wells was reserved for non-infected erythrocytes (negative control) and another one for infected erythrocytes (positive control). Subsequently, 50 µl of prepared parasite culture was added to each well, 50 µl niRBC solution were added to respective wells. Plates were covered with clear lids and incubated for 72 h in the usual incubator. At the MNHN Paris, drug incubation on 96-well plates was performed in a candle jar. After the incubation period, plates were wrapped in aluminum foil and frozen at -80 °C until use in order to obtain complete lysis of erythrocytes (for 2 h at least).

Plate scheme of drug combination assay

1	RBC	iRBC	Drug A 5:0	Drug mix 4:1	Drug mix 3:2	Drug mix 2.5:2.5	Drug mix 2:3	Drug mix 1:4	Drug B 0:5	X
2	RBC	iRBC	Highest concentrations							X
3	RBC	iRBC								X
4	RBC	iRBC								X
5	RBC	iRBC		1:3 dilution						X
6	RBC	iRBC								X
7	RBC	iRBC								X
8	RBC	iRBC	X	X	X	X	X	X	X	X

Abbreviations: RBC= non-infected red blood cells, iRBC = infected red blood cells.

Parasite growth was assessed using the SYBR® green method or the ³H-hypoxanthine incorporation assay at the MNHN Paris as described in section 2.2.2. At the MNHN Paris, drug incubation on 96-well plates was performed in a candle jar. Calculation of IC_{50} values was performed as described before, please refer to section 2.2.2.

For arithmetical analysis, the FIC_{50} of each drug in a given combination was calculated according to the following definitions:

FIC_{50} (A) = IC_{50} of A in combination / IC_{50} of A alone

FIC_{50} (B) = IC_{50} of B in combination / IC_{50} of B alone.

The sum of FIC_{50} (A) and FIC_{50} (B) ($\sum FIC_{50}$) was established for each combination and then the mean value of the four $\sum FIC_{50}$s was calculated. A mean $\sum FIC_{50} \leq 0.7$ was

assumed to reflect a synergistic interaction and a mean $\sum FIC_{50} \geq 1.3$ an antagonistic interaction between the tested drugs. Any value in between (0.7 - 1.3) was considered as indifferent interaction. The inherent variability of the experimental set-up was estimated by combining two individual working solutions of lead compound **1c**.

Graphical analysis was performed on isobolograms, which were established by plotting pairs of FIC_{50} values of drug A and drug B for each combination. Figure 20 illustrates the characteristic isoboles for different drug-drug interactions, as they have been assessed during this project. A straight line indicated an indifferent interaction (in other words no interaction, formerly described as additive), a concave curve towards the origin of the axes represented synergy and a convex curve towards the opposite indicated antagonism.

An essential prerequisite of the fixed-ratio isobologram method is a precise calculation of the IC_{50} values of both drugs. For some experimental compounds (e.g. ascorbic acid, nicotinamide, 6-aminonicotinamide) it was not possible to determine their IC_{50} values due to poor growth inhibition activities and poor solubility of the compounds. Thus, the fixed-ratio isobologram method was not applicable for such agents. Though, to explore the *in vitro* interactions with these agents, the IC_{50} values of lead compound **1c** were determined in the presence of a fixed dose of the agent of choice that showed no inhibition of parasitic multiplication when applied alone. Therefore, the compound was added directly in the required concentration (i.e. $2\times$ final concentration) to the parasite culture before this was distributed on the 96-well plate. The IC_{50} values of lead compound **1c** in the absence of the second agent were determined on the same plate to ensure accurate interpretation of drug interactions. The IC_{50} values were determined as described before (section 2.2.2). For interpretation of results, the shift of the IC_{50} value of lead compound **1c** in the presence or absence of a second agent was calculated and expressed in percentage.

2.2.7 Morphological analysis of drug-treated parasites

Morphological analysis of drug-treated parasites was performed as previously described (Ehrhardt et al, 2013). Briefly, Pictures of Giemsa-stained blood smears of treated and untreated parasite cultures of strain 3D7attB-yDHODH were taken at different time points with an AxioCam ICc 3 at an Axioplan microscope using the software ZEN 2011 blue edition (Zeiss). Individual images were imported into Fiji/Image J, cropped, and stored as a

TIF file. The TIF file was imported into CorelDraw, labels were added, and the figure was saved without any gamma, contrast or color adjustments.

2.2.8 *In vitro* cytotoxicity against hepatic HepG2 cells determined using the Trypan Blue Exclusion Assay, Laboratoire SRSMC, Université de Lorraine, France

Ms. T. Tzanova [5] assessed the cytotoxicity of benzylMD **1c** and chloroquine against hepatic HepG2 cells using the Trypan Blue Exclusion Assay according to a standard protocol (Freshney, 1987). Briefly, a cell suspension containing the floating and adherent cells detached by trypsin is mixed with Trypan Blue Stain (0,04% final concentration). The dye is excluded from the live cells displaying intact membranes whereas the dead cells will have a blue cytoplasm. Viable and dead cell number were determined with a Malassez cell.

---

[5] Ms. T. Tzanova (Laboratory Dr. D. Bragel) Laboratoire SRSMC, Université de Lorraine, France.

3 RESULTS

3.1 *In vitro* antimalarial activity of benzylMD derivatives

The first evaluation of new antimalarial compounds is generally assessed by measuring the inhibition of multiplication or survival of cultured *P. falciparum* blood-stage parasites under drug treatment, designated as antimalarial activity. The unit of measurement used to express the effectiveness of a compound is the so-called half maximal inhibitory concentration (in short IC_{50} value), that indicates the concentration needed to inhibit the parasite's development by 50% over a chosen time period. Standard techniques all have in common to determine IC_{50} values and differ mostly in the method applied to measure parasite multiplication, amongst others by microscopy ("WHO micro-test", Rieckmann et al, 1978), or by incorporation of radio-labeled ^{3}H-hypoxanthine or fluorescent dyes, such as SYBR[®] green, into parasitic DNA (Desjardins et al, 1979; Smilkstein et al, 2004). The IC_{50} values presented in this work were determined using the protocol based on the detection of parasitic DNA with SYBR[®] green, unless stated otherwise.

3.1.1 *In vitro* antimalarial activity and cytotoxicity of lead benzylMD 1c

To determine its *in vitro* antimalarial activity, lead benzylMD **1c** was tested against two common *P. falciparum* laboratory strains, the chloroquine-sensitive (CQs) 3D7 strain and the chloroquine-resistant (CQr) Dd2 strain. Their chemosusceptibility to common antimalarials is given in the Appendix (Table A3). The following antimalarial agents were used as reference drugs: chloroquine, the most common 4-aminoquinoline; atovaquone, a 1,4-naphthoquinone structurally related to benzylMD **1c** and methylene blue, another antimalarial redox-cycler. Lead compound **1c** displayed a potent antimalarial activity against both strains in the low nanomolar concentration range with IC_{50} values of 46 nM to 60 nM (Table 1). A comparable low IC_{50} value for benzylMD **1c** was formerly

determined against the *P. falciparum* Dd2 strain by using the ^{3}H-hypoxanthine incorporation assay (Müller et al, 2011). Similar to benzylMD **1c**, chloroquine resistance of *P. falciparum* Dd2 strain had no influence on the activities of atovaquone and methylene blue, as reflected in their IC$_{50}$ values (Table 1). The IC$_{50}$ values for control antimalarials chloroquine, atovaquone and methylene blue corresponded well with values reported elsewhere (Vennerstrom et al, 1995; Baniecki et al, 2007; Wein et al, 2010).

Table 1 *In vitro* **activity against** *P. falciparum* **blood-stage parasites and cytotoxicity against mammalian cell lines of lead benzylMD 1c and control antimalarial agents**

| | *P. falciparum* strain [a] | | Human cell line [c] | Selectivity index |
| | IC$_{50}$ ± SD (nM) | | IC$_{50}$ ± SD (µM) | |
Agent	3D7 (CQs) [b]	Dd2 (CQr)	HepG2	IC$_{50}$ HepG2 / IC$_{50}$ *P. falciparum*
1c	46 ± 3.5	60 ± 11	10 ± 0.6	166 - 217
CQ	10 ± 0.6	116 ± 3.4	24 ± 2.2	207 - 2400
Ato	0.2 ± 0.05	0.2 ± 0.06	ND	ND
MB	3.1 ± 0.4	3.6 ± 0.9	ND	ND

[a] Activity against cultured *P. falciparum* parasites is presented as mean IC$_{50}$ values ± standard deviation (SD) determined from 3 independent experiments using the SYBR® green technique. [b] IC$_{50}$ values of all agents determined on *P. falciparum* 3D7 strain were previously published (Ehrhardt et al, 2013) and are presented in identical form in section 3.3.1. [c] Cytotoxicity of benzylMD 1c and CQ against human HepG2 cells, a hepatocellular carcinoma cell line, is presented as mean IC$_{50}$ values ± standard deviation (SD) determined from 4 independent experiments using the Trypan blue exclusion method. Cytotoxicity results were kindly provided by Ms. T. Tzanova and Dr. D. Bragel, Université de Lorraine, Laboratoire SRSMC, France. 1c, lead benzylMD 1c; Ato, atovaquone; CQ, chloroquine; CQs, chloroquine sensitive; CQr, chloroquine resistant; MB, methylene blue; ND, not determined.

The cytotoxicity of benzylMD **1c** against human cell lines was recently assessed on the human buccal carcinoma cell line cell (KB) and the human lung MRC-5 fibroblasts using the Alamar blue assay (Müller et al, 2011). In these tests, benzylMD **1c** displayed low cytotoxicity against both cell lines, with an IC$_{50}$ value of 80 µM for KB cells and an IC$_{50}$ value > 32 µM (i.e. the highest tested concentration) for MRC-5 cells. To further explore the cytotoxicity profile of benzylMD **1c** towards a human cell line of different origin, Ms. T. Tzanova and Dr. D. Bragel [6] tested benzylMD **1c** for cytotoxicity on a liver carcinoma cell line (HepG2) using the trypan blue exclusion method. The dye trypan blue penetrates the cell membranes of death cells, staining their cytoplasm blue, but is not

---

[6] Ms. T. Tzanova and Dr. D. Bragel, Laboratoire SRSMC, Université de Lorraine, France

absorbed by intact living cells (Freshney, 1987). After incubation of HepG2 for 48 hours, the IC_{50} values measured for benzylMD **1c** and the control agent chloroquine were 10 μM and 24 μM, respectively (Table 1). Given that benzylMD **1c** had an IC_{50} of ~50 nM against *P. falciparum*, the cytotoxicity data on HepG2 cells established an *in vitro* selectivity index (i.e. IC_{50} HepG2 / IC_{50} *P. falciparum*) of 166 -217 (Table 1).

The presented results on *in vitro* antimalarial activity and cytotoxicity of lead benzylMD **1c** are currently prepared for publication (Ehrhardt et al, in preparation).

3.1.2 *In vitro* antimalarial activity of lead benzylMD 1c against multiple drug-resistant *P. falciparum* strains originating from different countries

The emergence and spread of drug resistance is not only a drawback for most currently applied antimalarials, but also represents an important challenge for the development of new antimalarial compounds. It is therefore important to identify possible cross-resistance patterns with structurally related as well as unrelated antimalarial compounds (Ding et al, 2012). For this purpose, Dr. Bruno Pradines[7] investigated the activity of lead compound **1c** against drug resistant parasites. Therefore, he selected a panel of twelve *P. falciparum* strains of different geographical origins: 3D7 (Africa), D6 (Sierra Leone), 8425 (Senegal), Vol (Djibouti), L1 (Niger), PA (Uganda), Bres (Brazil), FCR3 (the Gambia), W2 (Indochina), FCM29 (Cameroon), K2 and K14 (Cambodia). Those strains can be regarded as representatives of common resistance mechanisms to clinically used antimalarial compounds, namely the resistances to quinolines, mefloquine, monodesethylamodiaquine and / or pyrimethamine. The chemosusceptibility profiles of these *P. falciparum* strains to common antimalarials in use and the multidrug resistance (MDR) phenotypes of these strains are given in the Appendix (Table A3). More information about these strains, such as genetic mutations of known resistance markers, can be obtained from a recent publication (Briolant et al, 2010). Important to note is that nine strains are resistant to chloroquine ($IC_{50} > 100$ nM) and seven strains have an intermediate susceptibility to quinine (500 nM $< IC_{50} > 800$ nM). The respective resistance cut-off values are presented in the Appendix (Table A3). In parallel to benzylMD **1c**, Dr. Bruno Pradines determined the IC_{50} values of chloroquine, quinine, monodesethylamodiaquine and mefloquine, as reference drugs.

---

[7] Dr. Bruno Pradines, Unité de Recherche en Biologie et Epidémiologie Parasitaires, Institut de Recherche Biomédicale des Armées, Institut de Médecine Tropicale du Service de Santé des Armées, Marseille, France

Figure 14 illustrates the *in vitro* activities (presented as IC_{50} values) of benzylMD **1c**, the 4-methanolquinoline quinine and 4-aminoquinoline chloroquine against the twelve *P. falciparum* strains. Remarkably, benzylMD **1c** exhibited a potent activity against all the strains, irrespective of their resistance to chloroquine or quinine or to any other antimalarial drug (e.g. mefloquine, monodesethylamodiaquine or pyrimethamine, see Appendix, Table A3). The IC_{50} values ranged from 41 nM (FCM29) to 215 nM (W2) for benzylMD **1c**, from 21 nM (3D7) to 829 nM (FCM29) for chloroquine and from 62 nM (D6) to 684 nM (Bres) for quinine (Figure 1). Interesting to note is that benzylMD **1c** showed the highest activity against FCM29, the most resistant strain to chloroquine. A table listing all IC_{50} and IC_{90} values of benzylMD **1c**, chloroquine and quinine is given in the Appendix (Table A4).
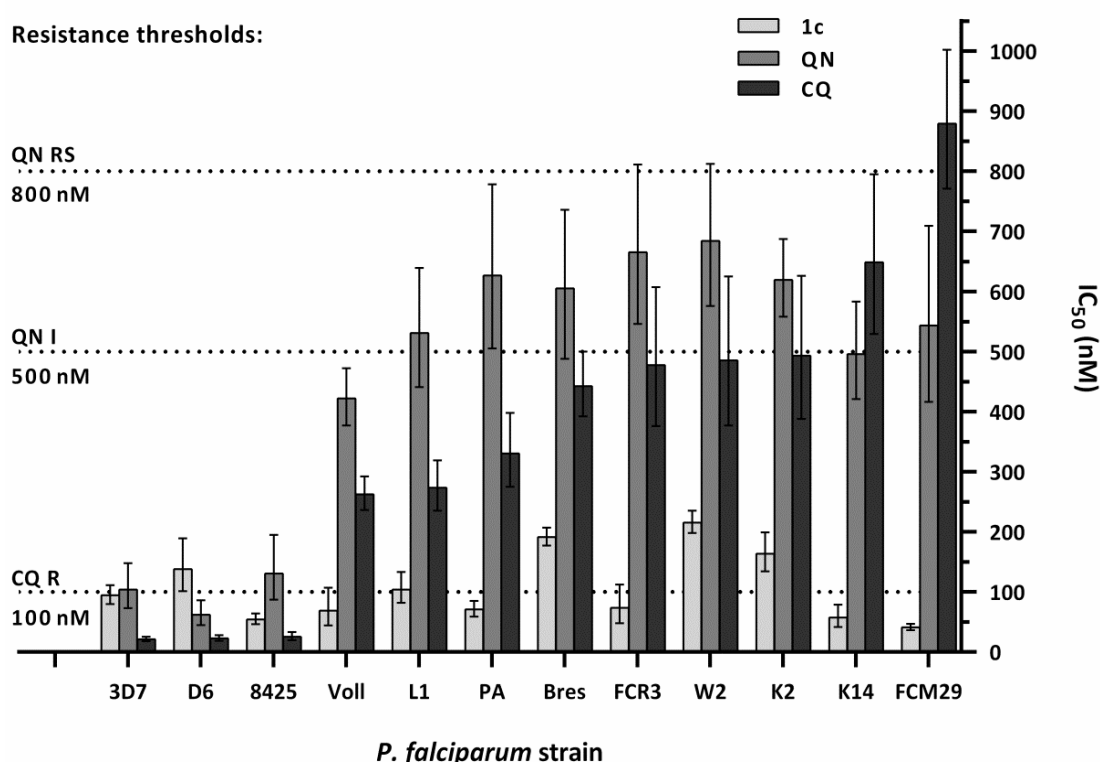
Figure 14 *In vitro* **antimalarial activity of benzylMD 1c, chloroquine and quinine against twelve drug-sensitive or drug-resistant** *P. falciparum* **strains originating from Asia, Africa or South America**

Antimalarial activity (presented as IC_{50} values) was determined on *P. falciparum* blood-stage parasites using the ^{3}H-hypoxanthine incorporation assay. The chemosusceptibility profiles and multi-drug resistance phenotypes of the strains are given in the Appendix (Table A3). Strains are ordered according to increasing degree of chloroquine resistance. Results are presented as mean IC_{50} values ± 95% confidence interval from 3 - 5 independent growth-inhibition assays. Collective IC_{50} and IC_{90} values of all agents are given in the Appendix (Table A4). Results were kindly provided by Dr. Bruno Pradines, Institut de Médecine Tropicale du Service de Santé des Armées, Marseille, France. 1c, benzylMD 1c; CQ, chloroquine; I, intermediate; R, resistant; RS, reduced susceptibility; QN, quinine.

To reveal a possible *in vitro* cross-resistance between benzylMD **1c** and clinical antimalarials, a correlation analysis of the *in vitro* drug responses of the twelve *P. falciparum* strains was performed. Four clinical antimalarial compounds were selected, namely chloroquine, quinine, monodesethylamodiaquine and mefloquine. A table listing all IC_{50} values of these antimalarial agents is given in the Appendix (Table A4). *In vitro* cross-resistance is indicated by a positive correlation between the IC_{50} values of two antimalarial agents and is estimated with the coefficient of correlation (rs, Spearman nonparametric correlation coefficient). The correlation coefficient quantifies the direction and strength of correlation and ranges from -1 (i.e. strong negative correlation) over 0 (i.e. no correlation) to +1 (i.e. strong positive correlation). The correlation analysis was conducted in GraphPad Prism by pairwise correlation of the IC_{50} values of benzylMD **1c** and four antimalarials as previously described (Briolant et al, 2010; Pradines et al, 2010).

Strikingly, no significant correlation could be determined between the *in vitro* responses of all *P. falciparum* strains to benzylMD **1c** and to antimalarials chloroquine, quinine, monodesethylamodiaquine or mefloquine (Table 2).

Table 2 Correlation of *in vitro* responses of twelve *P. falciparum* strains to lead benzylMD 1c and clinically used antimalarials

Correlation of *in vitro* response to drug pairs		rs	P value	Significance
BenzylMD **1c**	Chloroquine	-0,08392	0,8004	NS
BenzylMD **1c**	Quinine	0,3217	0,3085	NS
BenzylMD **1c**	MDAQ	-0,01399	0,9739	NS
BenzylMD **1c**	Mefloquine	0,08392	0,8004	NS
Chloroquine	Quinine	0,6503	0,0257	S
Chloroquine	MDAQ	0,9161	< 0,0001	S
Quinine	MDAQ	0,5455	0,0708	NS

Correlation of *in vitro* responses of *P. falciparum* strains to lead benzylMD 1c and clinical antimalarials was determined by pairwise correlation of mean IC_{50} values using the nonparametric Spearman correlation. Results are presented as coefficient of correlation (rs) and statistical p value. IC_{50} values for benzylMD 1c and antimalarial agents are given in the Appendix (Table A4). The IC_{50} values were kindly provided by Dr. Bruno Pradines, Institut de Médecine Tropicale du Service de Santé des Armées, Marseille, France. MDAQ, monodesethylamodiaquine; rs, Spearman nonparametric correlation coefficient; S, significant; NS, not significant.

In accordance with previous studies, a significant positive correlation was found for chloroquine and quinine (rs = 0.6503, p < 0.05), as well as chloroquine and monodesethylamodiaquine (rs = 0.9161, p < 0.0001) (Briolant et al, 2010; Pradines et al, 2010). In contrast, the reported positive correlation of *in vitro* responses to quinine and monodesethylamodiaquine was not confirmed in the current analysis. This might be explained by a higher number of *P. falciparum* strains analyzed in the previous studies.

In conclusion, benzylMD **1c** presented a high activity against multiple drug-sensitive and drug-resistant strains. The statistical correlation analysis revealed the lack of *in vitro* cross-resistance to a set of clinical antimalarials. Based on this analysis, the observed variation of benzylMD **1c**'s IC_{50} values (41 nM to 215 nM) might be attributable to natural phenotypic variations of the tested *P. falciparum* strains.

The presented results on *in vitro* activity of lead benzylMD **1c** against multiple drug-resistant *P. falciparum* strains and cross-resistance with four clinical antimalarials are currently prepared for publication (Ehrhardt et al, in preparation).

3.1.3 Structure-activity relationships of benzylMD derivatives

The first series of antimalarial benzylMD derivatives, represented by benzylMD **1a** and **1c**, were synthesized in only one step starting from menadione and phenylacetic acid derivatives, in a silver-catalyzed radical decarboxylation reaction (Müller et al, 2011). While numerous phenylacetic acid derivatives are commercially available, this is only the case for two menadione derivates, which highly limits the spectrum of functional groups on the menadione core at varying R1 groups (see Figure 15). To overcome this limitation, a versatile, regioselective and high yielding synthetic methodology was established that allows building of polysubstituted menadione cores for a fast synthesis of benzylMD derivatives. This new synthesis methodology is currently prepared for publication and will not be described in this work (Cesar-Rodo et al, in preparation; Urgin et al, in preparation). It is worth mentioning that the medicinal chemistry team in Strasbourg first aimed at establishing the synthetic methodologies, to prepare polysubstituted benzylMD derivatives and predicted benzylMD metabolites, before screening benzylMD derivatives for detailed structure-activity relationships.

The derivatization of the benzylMD core was performed based on the structures of the first hit (benzylMD **1a**) that harbours a bromide group and the lead compound benzylMD **1c** that contains a trifluoromethyl group. Figure 15 illustrates the structure of a non-substituted benzylMD core with numeration of positions for derivatization as well as the structures of benzylMD **1a** and **1c**.
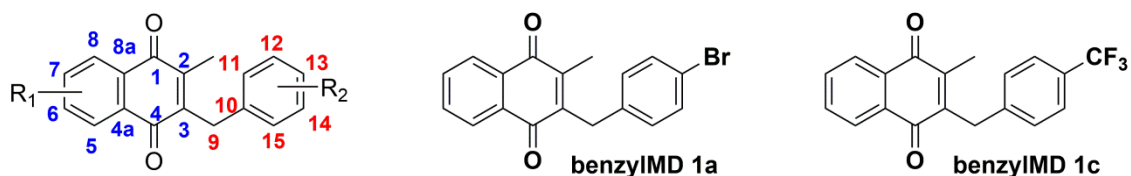
Figure 15 Structures of a non-substituted benzylMD, first hit benzylMD 1a and lead compound benzylMD 1c

A series of recently synthesized compounds was tested during this doctoral thesis on their *in vitro* antimalarial activity against cultured parasites of the *P. falciparum* Dd2 strain (expressed as IC_{50} values).

As a first attempt, a methyl group was introduced on positions 5, 6, 7 or 8 to identify tolerant positions for derivatization (see Figure 15). The IC_{50} values are presented in the Appendix (Table A8). To conclude, positions 6 and 7 are the most tolerant towards substitutions. Those derivatives (EC019, EC020, EC146, EC145) showed acceptable antimalarial activities with IC_{50} values below 1 µM. Introduction of a methyl group on other positions (5 or 8 or 6 and 7) rendered the compounds inactive, reflected in IC_{50} values in the micromolar range (2 µM to 4 µM).

The next set of derivatives was synthesized containing a fluorine atom or a diethyl-phosphate at positions 6 or 7. Substitution with a fluorine atom increases the lipophilicity of the compound and furthermore renders it more resistant to oxidation by cytochrome P450 (CYP450) enzymes in the human liver. The latter group increases compound solubility in aqueous mediums. The IC_{50} values of those compounds are presented in the Appendix (Table A9). Substitution with a fluorine atom at C6 or C7 showed no effect on the IC_{50} values, while 6- and 7-diethyl-phosphate-benzylMD **1c** analogues were slightly less active than the parent compound benzylMD **1c**.

The intention for the third set of compounds was to synthesize benzylMD **1a** and **1c** derivatives with increased metabolic stability in the human liver. This is attempted by derivatization of the phenyl ring of the benzyl chain, which hinders the attack of CYP450 enzymes. These modifications caused only little alterations of the *in vitro* antimalarial activities, the IC_{50} values are presented in the Appendix (Table A10). Drug metabolism studies with human liver microsomes are currently ongoing.

Group 4 of the benzylMD derivatives comprises structures substituted with methoxy groups at different positions. Precursor material containing methoxy groups are very cheap. Again, position 6 was found to be very tolerant for modification, while methoxylation of position 7 appeared to disturb the antimalarial activity of the final compounds. The IC_{50} values are presented in the Appendix (Table A11).

The objective for the next set of compounds was the introduction of a protonable N-dimethyl or N-diethyl group as found in the antimalarials chloroquine and methylene blue. According to their example, the compounds should be trapped inside the digestive vacuole and thereby hinder the shuttling and possibly redox cycling of benzylMD derivatives. To conclude, most of these compounds presented a moderate *in vitro* activity with IC_{50} values in the range of 300 nM to 500 nM. One might speculate that the antimalarial activity stems from inhibition of hematin formation in the digestive vacuole. The IC_{50} values are presented in the Appendix (Table A12).

The last group of compounds contains putative metabolites of benzylMD **1c** (EC195, EC199, EC277), their synthetic intermediates (EC172, EC197) and "blocked" metabolites (EC276, EC279, EC285). These compounds were primarily synthesized for an extensive study of intracellular drug metabolisms (in terms of metabolite formation by redox-cycling) by a mass spectrometry approach.

In conclusion, the presented data (IC_{50} values) on *in vitro* antimalarial activity of benzylMD derivatives will be used together with their chemical and electro-physicochemical properties to generate a virtual library and database for chemoinformatics. In addition, benzylMD derivatives with promising *in vitro* activities will be selected for further *in vivo* activity and pharmacokinetic studies. The results presented in this section are currently prepared for publication (Cesar-Rodo et al, in preparation; Urgin et al, in preparation).

3.2   Detailed characterization of benzylMD 1c's *in vitro* activity profile

Drug development for malaria treatment is a rather complex process that is not only challenged by the changing parasite landscape (i.e. emergence of drug resistance) but also has to adapt to strategies of malaria control and elimination, developed by the WHO and leading experts of the scientific community (e.g. represented by malEra or MMV) (for instance mal, 2011; Burrows et al, 2013). In the recent years, the scientific community has provided several robust *in vitro* methodologies and frameworks in order to standardize drug development in academic research (Ding et al, 2012; Sanz et al, 2012; Burrows et al, 2013). Worth mentioning is the research and development portfolio, published by MMV, that informs about essential experiments and data required at different stages of the drug-development process (MMV).

There are several features of a drug's activity profile that are important to be characterized during the early phase of drug development (i.e. lead evaluation stage). Speed of action and stage specificity will help to estimate clinical efficiency in patients (Sanz et al, 2012). Furthermore, together with pharmacokinetic properties, the speed of action will determine whether a drug will be used for acute treatment or chemoprotection. Assessing the risk of *in vitro* resistance selection will help to estimate whether the effectiveness of a drug will be compromised easily by resistance development in the field. The risk of resistance development is further minimized by using drug combinations, which again renders the drug development more complex and time consuming.

3.2.1   Stage specificity of benzylMD 1c action

Depending on their mode of action, most antimalarials express a particular stage specificity by acting at different time points during the intraerythrocytic development of the parasite. Most of the antimalarials currently in use act against the trophozoite or schizont stages with the rare exception of artemisinin that effectively kills ring-stage parasites. In the last years, ring stages have obtained increasing attention as promising drug target to circumvent the adhesion of trophozoite-infected erythrocytes and related symptoms but also to decrease the formation of gametocytes, which differentiate from this stage. Two other events of the asexual development, namely schizont rupture and merozoite invasion, are suitable drug targets but technically challenging and therefore not yet fully exploited (Wilson et al, 2013). Knowing a drug's preferential target stage(s) contributes to
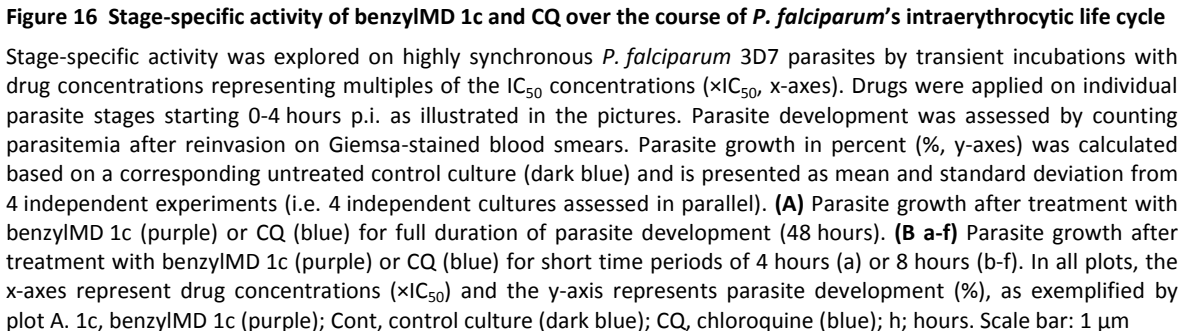
understand its mode of action and will help to estimate clinical efficiency in patients (Sanz et al, 2012). The experiments on stage specificity of benzylMD **1c** were conducted at the Museum National d'Histoire Naturelle in Paris. The culture conditions are described in the Materials and Methods chapter (see section 2.2.1.1). In these conditions, 3D7 parasites fulfill their development in 48 hours, although faster development was reported in other studies. Dr. Christiane Deregnaucourt [8] kindly contributed to the preparation, execution and analysis of the experiments presented in this section.

3.2.1.1 BenzylMD 1c's activity throughout the course of the intraerythrocytic parasite development

In order to reveal the preferential target stage(s) of benzylMD **1c**, its activity profile was explored throughout the course of the intraerythrocytic parasite development. Therefore, highly synchronous *P. falciparum* 3D7 parasites were transiently incubated with benzylMD **1c** concentrations representing $1\times IC_{50}$, $5\times IC_{50}$ and $10\times IC_{50}$ values for consecutive 8-hour periods (with the exception of a first, 4-hour period). Subsequently, cells were washed, resuspended in drug-free medium and maintained until reinvasion was completed. The parasite development under drug treatment was assessed by counting parasitemia after reinvasion on Giemsa-stained blood smears. The cultures were treated in the same way with chloroquine as a control agent.

The stage-specific activity of benzylMD **1c** was clearly different from that of chloroquine, with young ring stages being the most sensitive to the drug. The strongest inhibition of parasite development was observed after incubation of young ring stages for 8 hours (aged 8 h-16 h p.i.) with $5\times IC_{50}$ and $10\times IC_{50}$ concentrations of benzylMD **1c** (~60% and ~80% inhibition, respectively, Figure 16B, plot b). Remarkably, inhibition by benzylMD **1c** was detected also after short (4-hour) incubation of even younger parasites (aged 4 h-8 h p.i.) (~40% and ~55% inhibition, respectively, Figure 16B, plot a), whereas a 4-hour application of chloroquine had no effect on the development of such young ring-stage parasites. In these experimental conditions, parasites older than 12 h-16 h p.i. were not sensitive to benzylMD **1c** when incubated for 8 hours with the same concentrations of the drug: inhibition of reinvasion did not exceed 20%; only reinvasion of the $10\times IC_{50}$-treated schizonts was inhibited by approximately 35% (Figure 16B, plot f).

[8] Dr. Christiane Deregnaucourt, Equippe BAMEE, Museum National d'Histoire Naturelle, Paris, France

Figure 16 Stage-specific activity of benzylMD 1c and CQ over the course of *P. falciparum*'s intraerythrocytic life cycle

Stage-specific activity was explored on highly synchronous *P. falciparum* 3D7 parasites by transient incubations with drug concentrations representing multiples of the IC_{50} concentrations ($\times IC_{50}$, x-axes). Drugs were applied on individual parasite stages starting 0-4 hours p.i. as illustrated in the pictures. Parasite development was assessed by counting parasitemia after reinvasion on Giemsa-stained blood smears. Parasite growth in percent (%, y-axes) was calculated based on a corresponding untreated control culture (dark blue) and is presented as mean and standard deviation from 4 independent experiments (i.e. 4 independent cultures assessed in parallel). **(A)** Parasite growth after treatment with benzylMD 1c (purple) or CQ (blue) for full duration of parasite development (48 hours). **(B a-f)** Parasite growth after treatment with benzylMD 1c (purple) or CQ (blue) for short time periods of 4 hours (a) or 8 hours (b-f). In all plots, the x-axes represent drug concentrations ($\times IC_{50}$) and the y-axis represents parasite development (%), as exemplified by plot A. 1c, benzylMD 1c (purple); Cont, control culture (dark blue); CQ, chloroquine (blue); h; hours. Scale bar: 1 μm

Results obtained from chloroquine treated parasites were in good accordance with the well known specificity of chloroquine against the trophozoite stage. As expected, transient application of chloroquine ($5 \times IC_{50}$ and $10 \times IC_{50}$) on trophozoites fully prevented parasite development (Figure 16B, plot d and e), whereas application on rings (Figure 16B, plot b and c) and schizonts (Figure 16B, plot f) inhibited parasite development only slightly.

The selected IC_{50} values for benzylMD **1c** and chloroquine, were experimentally validated *a posteriori* by measurement of the re-invasion rate after a full cycle (48 h) application of the drugs: 48 hours application of the $1 \times IC_{50}$ concentration of benzylMD **1c** inhibited reinvasion by around 50%, whereas the $1 \times IC_{50}$ concentration of chloroquine induced almost 60% inhibition (Figure 16A). Given that chloroquine concentrations were slightly too high, the effect of the drug on the different parasite stages might be overestimated and the difference between trophozoites and the other stages artificially reduced. Though, it may be important to note that short time incubations with chloroquine showed generally higher effects on parasite development than with benzylMD **1c**.

Overall, these results demonstrated that chloroquine and benzylMD **1c** act on different blood stages, early ring-stage parasites being the preferential target of benzylMD **1c**.

3.2.1.2 BenzylMD 1c's activity against early or late developmental stages

In order to assess whether benzylMD **1c** targets young ring stages either preferentially or exclusively, its ability to inhibit the development of the mature parasite stages (i.e. trophozoites and schizonts) was tested by incubating rings or trophozoites with high drug concentrations for an extended period of time. Therefore, highly synchronous *P. falciparum* 3D7 parasites were transiently incubated with benzylMD **1c** concentrations representing $1 \times IC_{50}$, $5 \times IC_{50}$, $10 \times IC_{50}$ and $50 \times IC_{50}$ values for 22-24 hours starting at the ring stage (aged 0 h - 4 h p.i.) or at the trophozoite stage (aged 20 h – 24 h).

Using longer incubation times, it became clear that benzylMD **1c** activity was not restricted to early stages but occurred during the entire intraerythrocytic life cycle. A major inhibition (approx. 60%) of ring stage development was achieved using $1 \times IC_{50}$ concentrations; whereas $5 \times IC_{50}$ concentrations were necessary to observe the same effect on trophozoite and schizont stages (Figure 17). Similarly, a two-fold higher drug

concentration was required to fully inhibit development of mature parasites ($10 \times IC_{50}$) compared to ring stages ($5 \times IC_{50}$) (approx. 96% each). Interestingly, while a 24-hour application of $10 \times IC_{50}$ benzylMD **1c** leaded to almost full inhibition of trophozoite and schizont development, the same concentration applied for 8 hours had failed to inhibit parasites at the same stages (see Figure 16B, plots d-f). Compared to the former experiment, prolonged incubation times induced much higher inhibition of parasite development, independent of the affected stage. These results thus pointed towards dose and time dependent differences in drug susceptibility of individual intraerythrocytic stages.
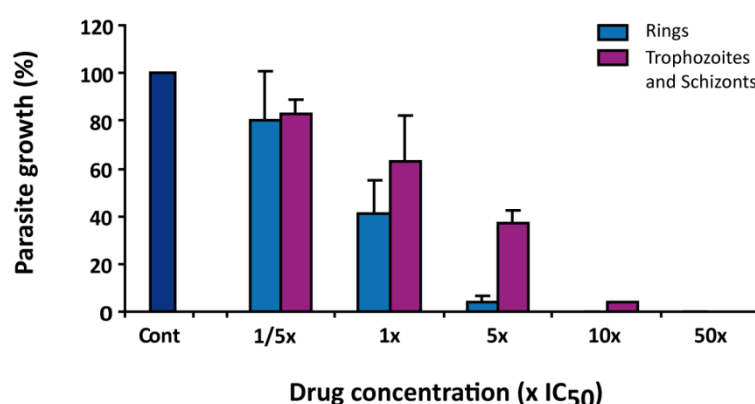

Figure 17 Activity of benzylMD 1c against early or late developmental stages

Activity of benzylMD 1c on different developmental stages was assessed on highly synchronous *P. falciparum* 3D7 parasites by successive incubations with drug concentrations representing multiples of the IC_{50} concentrations ($\times IC_{50}$). BenzylMD 1c was applied either on ring stages (aged 0-4 h p.i.) or on trophozoites (aged 20-24 h p.i.) for a duration of 22-24 hours. Parasite development was assessed by counting parasitemia after reinvasion on Giemsa-stained blood smears. Parasite growth in percent (%) was calculated based on a corresponding untreated control culture (cont) and is presented as mean and standard deviation from 3 independent experiments.

3.2.1.3 BenzylMD 1c's activity on parasite egress or invasion

Although benzylMD **1c** targets primarily young rings (as demonstrated before), a low inhibition of schizont development could be observed with high benzylMD **1c** concentrations (approx. 35% inhibition, $10 \times IC_{50}$ concentration, see Figure 16B, plot f). This observation suggests that the drug might also interfere with parasite egress from its host cell and / or invasion into new erythrocytes. To test this possibility, a culture highly enriched in mature schizonts (i.e. segmenters) was incubated for 8 hours with $5 \times IC_{50}$ and $10 \times IC_{50}$ concentrations of benzylMD **1c** and parasite reinvasion was analyzed by the number and proportion of remaining schizonts and newly invaded ring stages at the end of

the incubation period. The cysteine protease inhibitor E64 and mycotoxin cytochalasin D, an inhibitor of actin polymerization, were used as controls for inhibition of parasite egress and invasion, respectively (Bouillon et al, 2013).

As expected, treatment of mature schizonts with E64 and cytochalasin D resulted in a higher number of unruptered schizonts (E64) or a lower number of newly invaded ring stages (cytochalasin D), respectively, compared to untreated control cultures. In contrast, the number and proportion of schizont and ring stages in benzylMD **1c**-treated cultures were similar to the controls, indicating that benzylMD **1c** had no effect on parasite egress or reinvasion. The differences in total parasitemia between the two benzylMD **1c**-treated cultures (2.7% and 3.6%) and control culture (2.9%) were regarded to be in the range of experimental variation (e.g. disposition of culture on 96-well plate, preparation and coloration of blood smear).
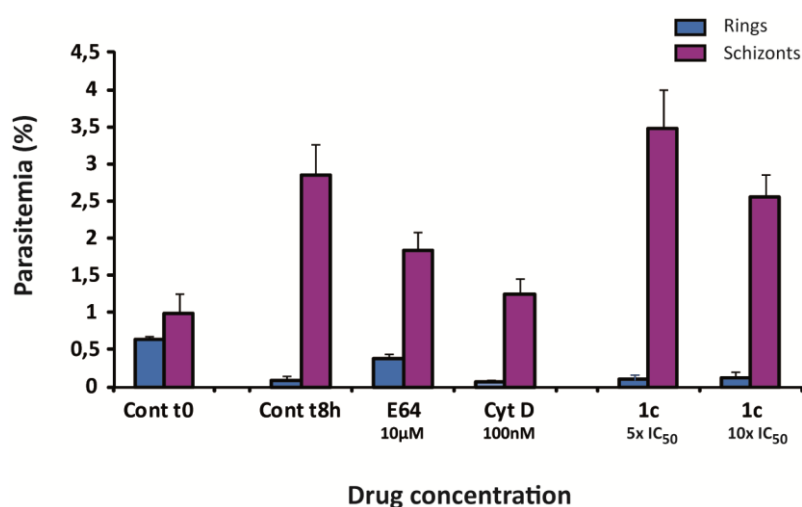

Figure 18 BenzylMD 1c activity against parasite egress or invasion

Activity of benzylMD 1c on parasite egress or invasion was assessed on highly synchronous *P. falciparum* 3D7 parasites by short-time incubation with drug concentrations representing multiples of the IC_{50} concentrations ($\times IC_{50}$). E64 and cytochalasin D (cyt D) were used as controls for inhibition of parasite egress and invasion, respectively. Drugs were applied on mature schizonts (segmenters) for a duration of 8 hours to cover the majority of the parasite's egress and invasion process. Subsequently, parasite development was assessed by counting numbers of ring and schizont stages on Giemsa-stained blood smears. Results from 3 independent experiments are presented as mean of parasitemia of the individual stages in percent (%) plus standard deviation (error bar). Graph demonstrates numbers of ring or schizonts stages present in a control culture at the beginning of drug treatment (cont t0) and after drug treatment (cont t8h) for comparison of parasite development.

All together, the results on stage specificity demonstrated a very strong activity of benzylMD **1c** against ring-stage parasites, especially young ring stages (aged 0-4 h p.i). This result is in agreement with the morphology of drug-treated parasite cultures. Indeed, several times it was observed that ring-stage parasites developed into residual pyknotic bodies (Müller et al, 2011; Ehrhardt et al, 2013) (see also section 3.3.2). Though, it is important to note that benzylMD **1c** activity was not restricted to these early stages. The full arrest of trophozoite and schizont development was observed using longer incubation times and higher drug concentrations. As the parasite develops, digestion of host's hemoglobin takes place, generating pulses of reactive oxygen species and redox-active heme (see Introduction, section 1.2.2.1). The concomitant destruction of drug molecules (e.g. by Fenton reactions) is an important process that has to be considered to explain the apparent lower activity of benzylMD **1c** in trophozoite and schizont stages (see also section 3.3.3.4).

The results on stage-specific activity of lead benzylMD **1c** presented in this section are currently prepared for publication (Ehrhardt et al, in preparation).

3.2.2 Speed of action

The efficiency of antimalarials to decrease blood parasitemia and cure patients is mediated in part by their speed of action. Recently, Sanz and colleagues (2012) developed an *in vitro* protocol to examine the speed of action of antimalarials in culture and to calculate the parasite reduction ratio as a predictive therapeutic index for clinical efficiency. The principle is based on determination of parasite viability in response to incubation with drug at a several-fold IC_{50} concentration for increasing periods of time. Parasite viability is assessed by examining re-growth of treated parasites over time. Accordingly, artemisinin and related endoperoxides were characterized as very fast acting drugs able to clear parasites within 48 hours, whereas atovaquone killed parasites very slowly after an extended cytostatic lag phase. Following this protocol, the speed of action (also called killing speed) profile of benzylMD **1c** was investigated on an asynchronous culture of *P. falciparum* 3D7 parasites. Atovaquone and artemisinin were used as a reference for slow- and fast-acting drugs, respectively. Different to the original protocol, a $5 \times IC_{50}$ concentration of each drug, instead of a $10 \times IC_{50}$ concentration, was used for treatment.

A $10 \times IC_{50}$ concentration of benzylMD **1c** was shown to fully inhibit parasite development within incubation times of only 20-24 hours (please refer to section 3.2.1.2) and was therefore considered too high for a treatment period of several days. Please note that the results (i.e. number of viable parasites after drug treatment) are presented in logarithmic form (log_{10}) as "viable parasites +1" (Figure 19). This presentation was adopted from the original protocol (Sanz et al, 2012) since only values greater than zero can be plotted on a logarithmic scale.

BenzylMD **1c** showed a very fast speed of action with an almost immediate onset of action and a rapid parasite clearance within 72 hours (Figure 19), similar to artemisinin and in contrast to the slow acting atovaquone. In contrast to artemisinin, a very short lag phase of 8 hours was observed for benzylMD **1c**, indicating an initial cytostatic drug effect. The lag phase describes the time period necessary to reach the maximal killing rate. However, this delay was rapidly compensated by the high killing rate observed in the following 40 hours.
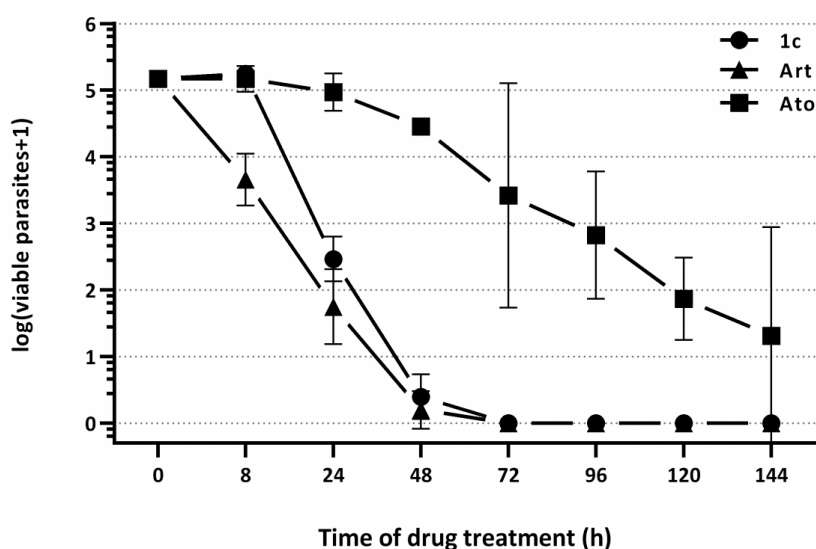

Figure 19 *In vitro* **speed of action profile of benzylMD 1c in comparison to antimalarial agents**

Graph displays numbers of viable parasites in response to drug treatment at $5 \times IC_{50}$ concentrations of lead benzylMD 1c (1c), artemisinin (ART) and atovaquone (ATO). Values are presented as mean of two independent experiments performed in triplicates and twofold detection of parasite growth on days 21 and 28, each. Error bars represent the standard deviation. According to the original protocol, results are presented in logarithmic form (log_{10}) as "viable parasites +1" (Sanz et al, 2012).

In our experimental set-up using $5 \times IC_{50}$ concentrations of the drug, atovaquone had a very pronounced lag phase of 72 hours and could not clear parasitemia within 144 hours. It is important to note that the killing speed profiles of atovaquone revealed from 2 independent experiments differed importantly from each other. A pronounced lag phase (> 48 hours) was observed in both experiments, but complete clearance of drug-treated parasites was only achieved in one experiment.

The parasite reduction ratio (PRR) accounts for the decrease of viable parasite numbers over 48 hours (i.e. one parasite's life cycle) in the phase of maximal killing speed. The PRR was $10^{4.8}$ parasites for benzylMD **1c**, 10^5 parasites for artemisinin and $10^{1.6}$ parasites for atovaquone (presented as $\log_{10}$ in Table 3). The parasite clearance time (PCT) describes the time needed to kill 99.9% of the initial parasite load. The PCT was determined by a linear regression of the time-response curve. Clearance of 99.9% parasites by benzylMD **1c** was achieved after 36 hours and thereby close to artemisinin, which was slightly faster (30 hours). In contrast, atovaquone exhibited substantially delayed clearance with a PCT of 115 hours (Table 3). In conclusion, benzylMD **1c** showed a very fast speed of action close to that of the endoperoxide artemisinin and can therefore be counted among the fastest compounds described so far *in vitro* (Sanz et al, 2012).

Table 3 Parameters of *in vitro* speed of action: lag phase, parasite reduction ratio (PRR) and parasite clearance time (PCT)

Agent	Lag phase (h)	Log(PRR)	99.9% PCT (h)
Artemisinin	0	5.0	30
BenzylMD 1c	8	4.8	36
Atovaquone	72	1.6	115

The results on benzylMD **1c**'s *in vitro* speed of action presented in this section are currently prepared for publication (Ehrhardt et al, in preparation).

3.2.3 Parasite resistance development

The rapid development of parasite resistance to new drugs is a major challenge in antimalarial drug design. Several *in vitro* protocols have been successfully used to reproduce resistance development observed in patients and to investigate the genetic basis and the molecular mechanisms underlying resistance (reviewed in Nzila & Mwai, 2010; Witkowski et al, 2010). It is considered as highly important to assess the risk of *de novo* resistance development as early as possible during drug development (Nzila & Mwai, 2010; Sanz et al, 2011; Ding et al, 2012). In the frame of this thesis, two different experimental settings were selected in order to (I) estimate the risk of resistance development under benzylMD **1c** treatment and (II) select for drug-adapted parasites as a tool to investigate the underlying mechanism.

Experiments on resistance development were performed with the *P. falciparum* Dd2 strain, owing to its ability to easily acquire resistance to drugs under *in vitro* conditions, commonly designated as *accelerated resistance to multiple drugs* (ARMD) phenotype (Rathod et al, 1997; Trotta et al, 2004; Castellini et al, 2011). The ARMD phenotype was linked to a defective DNA repair machinery, which could explain the acquisition of beneficial point mutations under drug pressure (Castellini et al, 2011). The results on *in vitro* parasite-resistance development under benzylMD **1c**-treatment presented in this section are currently prepared in modified form for publication (Ehrhardt et al, in preparation).

3.2.3.1 Risk of *de novo* resistance development

The intrinsic potential of benzylMD **1c** to induce parasite resistance was assessed by continual exposure of blood-stage parasites to lethal drug concentrations, based on the method established by Rathod and colleagues (1997). By using different parasite inocula, this experiment allows to determine the minimum number of parasites necessary for the development of resistant mutants (so-called frequency of resistance selection).

Therefore, a series of *P. falciparum* Dd2 blood-stage cultures with high parasite inocula (10^8, 10^7, 10^6, 10^5 infected erythrocytes) were maintained in the presence of $5\times IC_{50}$ or $10\times IC_{50}$ concentrations of benzylMD **1c** (i.e. approx. $2\times IC_{90}$ and $4\times IC_{90}$ concentrations). Similar to the original protocol (Rathod et al, 1997), 5-fluoroorotate treatment (100 nM)

was used as a positive control. For each condition, two independent cultures of synchronous ring-stage parasites were established from individual stock cultures.

During the first 2 days of benzylMD **1c** treatment, some parasites were able to continue their development, as observed by the formation of schizonts. The major developmental arrest occurred at the ring stage, which is in agreement with benzylMD **1c**'s stage specificity profile (section 3.2.1). After 5 days of continuous drug pressure, no living parasites were observed in any treated culture. Dead parasites presented a distinct condensed (i.e pyknotic) morphology that was first described by Dr. C. Deregnaucourt (in Müller et al, 2011) (see also section 3.3.2). It is interesting to note that erythrocytes harbouring such pyknotic parasites were present for several days and did not undergo lysis, as observed during a morphological study on benzylMD **1c** treated parasites (see also section 3.3.2).

Over 12 weeks of continuous drug pressure, no living parasites reappeared in any of the benzylMD **1c**-treated cultures (Table 4). In contrast, upon 5 weeks of 5-fluoroorotate treatment, parasites were able to grow under drug pressure in all cultures, indicating that drug treatment had raised resistant parasites (Table 4). Control cultures treated with 5-fluoroorotate were subsequently discarded without further investigation. By the end of week 12, cultures treated with benzylMD **1c** were washed and maintained drug free for another 4 weeks to allow the proliferation of possibly retained tolerant parasites (see following section).

Table 4 Frequency of resistance to benzylMD 1c or 5-fluoroorotate

Initial parasite population (iRBC per flask)	100 nM 5-fluoroorotate	250 nM ($5\times IC_{50}$) benzylMD 1c	500 nM ($10\times IC_{50}$) benzylMD 1c
10^8	2 / 2	0 / 2	0 / 2
10^7	2 / 2	0 / 2	0 / 2
10^6	2 / 2	0 / 2	0 / 2
10^5	2 / 2	0 / 2	0 / 2

Ratios represent the number of flasks yielding growing parasites after 12 weeks of drug treatment, divided by the number of initial cultures. iRBC, infected red blood cells.

Other studies using the same experimental setup reported a high frequency of spontaneous resistance for the antimalarial atovaquone (Rathod et al, 1997) and a lead cyclopropyl carboxamide (GSK2645947, Sanz et al, 2011).

Induction of parasite dormancy

At that time, recent studies with the first line antimalarial artemisinin reported the ability of parasites to tolerate drug pressure by arresting their cell cycle (Witkowski et al, 2010). Upon drug removal, some parasites succeeded in reactivating their cell cycle and continue development. Interestingly, these parasites did not present a decreased susceptibility to artemisinin, as reflected in their IC_{50} values. This phenomenon was originally described as "quiescence" (Witkowski et al, 2010) but is today generally designated as "dormancy" (Teuscher et al, 2012; Witkowski et al, 2013b). Only recently, novel phenotypic assays for the evidence of drug-induced cell cycle arrest were developed (Witkowski et al, 2013b) (see also Discussion, section 4.1.4).

Based on the observations of Witkowski et al. (2010), the question arose whether parasites could similarly tolerate benzylMD **1c** drug pressure and continue their development upon drug release. To address this possibility, cultures of the *P. falciparum* Dd2 strain that had been treated continuously for 12 weeks with high benzylMD **1c** concentrations were further maintained without drug treatment for another 4 weeks. Therefore, cells were washed twice and resuspended in drug-free medium.

Three weeks after benzylMD **1c** removal, growing parasites were observed in 2 of 16 flasks (Table 5). These cultures initially contained high parasite inocula (10^8 and 10^7 infected erythrocytes, respectively) and were, surprisingly, both treated with the highest ($10 \times IC_{50}$) benzylMD **1c** concentration. No more growing parasites were observed in any other culture over the last week of the experiment. Those cultures with no re-emerging parasites were discarded at the end of the 4-weeks period.

Table 5 Frequency of reappearing parasites after removal of benzylMD 1c drug pressure

Initial parasite population (iRBC per flask)	250 nM ($5\times IC_{50}$) benzylMD 1c	500 nM ($10\times IC_{50}$) benzylMD 1c
10^8	0 / 2	**1 / 2**
10^7	0 / 2	**1 / 2**
10^6	0 / 2	0 / 2
10^5	0 / 2	0 / 2

Ratios represent the number of flasks yielding growing parasites within 4 weeks after drug removal, divided by the number of initial cultures. Initially, cultures were treated continuously with specified benzylMD **1c** concentrations for a total period of 12 weeks. No living parasites were observed during this time.

Parasites from the 2 positive flasks were allowed to grow to a higher density in order to assess their susceptibilities to benzylMD **1c**. They showed no altered susceptibilities to benzylMD **1c** or to the control drug chloroquine. The IC_{50} values were comparable to the ones determined before drug selection and to that of a culture of Dd2 parasites assessed in parallel (Table 6).

Table 6 Susceptibility of reappearing parasites to benzylMD 1c

	Antimalarial agent IC_{50} ± SD (nM)	
Culture	benzylMD 1c	chloroquine
Flask 1 (10^8)	71 ± 22	93 ± 15
Flask 2 (10^7)	69 ± 25	92 ± 7
Control Dd2	67 ± 9	111 ± 22

IC_{50} values are presented as mean ± standard deviation (SD) determined from 3 independent experiments using the SYBR® green technique.

In conclusion, this experiment clearly showed that benzylMD **1c** has a very low potential to induce drug resistance of cultured blood-stage parasites. This was proven with two different lethal concentrations, representing $5\times IC_{50}$ and $10\times IC_{50}$ concentrations. A reappearance of growing parasites was observed in 2 of 16 cultures (2 of 20 flasks in total) upon drug release. However, these parasites showed no altered susceptibility to

benzylMD **1c** as reflected in their IC_{50} values. Whether these parasites acquired a tolerance mechanism, as it was shown for artemisinin, would need further investigation.

A second observation on parasite dormancy was attained during the experiment on generation of drug-adapted parasites (see section 3.2.3.2). In this experiment, a culture of parasites (drug-adapted $Dd2^{MD1}$ F3) was maintained in the presence of sublethal benzylMD **1c** concentrations (800 nM corresponds to approx. $1 \times IC_{90}$ concentration). Similar to the cultures challenged with $5 \times IC_{50}$ or $10 \times IC_{50}$ concentrations (described above), no living parasites were observed over 12 weeks culturing with constant drug pressure. In order to test for the reappearance of dormant parasites, cells were washed and cultures were maintained without drug treatment for further 4 weeks. In contrast to the cultures challenged with $5 \times IC_{50}$ or $10 \times IC_{50}$ concentrations (described above), these 4 cultures revealed no growing parasites upon drug removal (section 3.2.3.2).

3.2.3.2 Selection of drug-adapted parasites

In vitro selection of drug-resistant parasites provides a powerful tool for the investigation of genetic or molecular determinants accounting for resistance development. In patients, parasites are often exposed to inappropriately low (i.e. sublethal) drug concentrations, which are regarded to favor the selection of resistant parasites (White & Pongtavornpinyo, 2003). Consequently, the second experiment on resistance development intended to induce adaptation or resistance to benzylMD **1c** by exposing a high parasite inoculum to sublethal drug concentrations (modified after Beez et al, 2011).

For selection of drug-adapted parasites, a culture of *P. falciparum* strain Dd2 with high parasite inoculum was maintained in the presence of sublethal concentrations of benzylMD **1c** until the reappearance of normally growing parasites under drug pressure. Subsequently, concentrations for drug pressure were increased according to the altered susceptibility of drug selected parasites. BenzylMD **1c** concentrations for selection were chosen in the order of the IC_{90} concentration of the respective parasite population.

First selection cycle:

The selection of drug-adapted parasites was initiated from a culture of synchronous ring stage *P. falciparum* strain Dd2 with high parasite inoculum (3.6×10^9 iRBC). The initial culture was challenged with 125 nM of benzylMD **1c.** The mean IC_{50} and IC_{90} values of benzylMD **1c** on original Dd2 parasites, as assessed prior to drug selection, were 51 nM and 138 nM, respectively (see Appendix, Table A5). During the first week of drug treatment, parasites continued to multiply and therefore the initial culture was divided stepwise into 5 culture flasks that were subsequently treated identically.

Parasites were slowly killed over the first 10-14 days of drug treatment, as monitored on Giemsa-stained blood smears. After 5 weeks of continuous drug pressure, living parasites reappeared in 2 of 3 flasks, indicating successful adaptation of parasites to drug pressure. Drug-adapted parasites (hereafter designated Dd2^{MD1} F2 and F3 [9]) were allowed to grow to a higher density before dividing the cultures in halves. One part of the culture was maintained in the presence of benzylMD **1c** in order to initiate a second selection cycle. The other half was further cultured without drug pressure in order to assess the susceptibility of drug-selected parasites to benzylMD **1c**. At the same moment, several samples of parasites were prepared for cryopreservation. The 3 remaining cultures were discarded; two because of bacterial contamination, while the last one did not reveal living parasites.

The susceptibility of drug-selected parasites (Dd2^{MD1} F2 and F3) was regularly assessed over a period of 6 weeks after treatment stop. Over the first 3 weeks after drug removal, both parasite cultures Dd2^{MD1} F2 and F3 showed a 3-4 fold decreased susceptibility to benzylMD **1c** compared to progenitor Dd2 parasites, indicating successful adaptation of parasites to drug pressure. The measured IC_{50} values were 162 nM (Dd2^{MD1} F2) or 208 nM (Dd2^{MD1} F3) and the IC_{90} values 703 nM (Dd2^{MD1} F2) and 983 nM (Dd2^{MD1} F3) (Table 7). It is important to note that the IC_{50} values determined post-selection were only slightly higher than the benzylMD **1c** concentration used for selection. The susceptibility to chloroquine was unaffected compared to original Dd2 parasites (see Appendix, Table A5). Cultures Dd2^{MD1} F2 and F3 were used to initiate a 2nd selection cycle using higher drug concentrations (see below).

---

[9] Drug adapted parasites, raised after the 1st selection cycle with 125 nM benzylMD 1c, were designated as follows: Dd2^{MD1} F2 or F3. This denotation stands for: Dd2, progenitor parasite strain; MD, selected with benzylMD 1c; 1, 1st selection cycle; F2, F3, growing parasites were recovered from flasks number 2 and 3.

However, the described phenotype was not stable over time. Around 4 weeks after treatment stop, parasites no longer presented altered susceptibilities to benzylMD **1c**. The IC_{50} values measured 4-6 weeks after drug removal were comparable to the ones determined before drug selection and to a culture of Dd2 parasites that was assessed in parallel (Table 7 and Table A5, Appendix).

Table 7 Susceptibility of drug-adapted parasites to benzylMD 1c after 1st selection cycle

	Weeks 1-3 after drug removal		Weeks 4-6 after drug removal	
Culture	IC_{50} (nM) ± SD	IC_{90} (nM) ± SD	IC_{50} (nM) ± SD	IC_{90} (nM) ± SD
Dd2^{MD1} F2	162 ± 15 (3)	703 ± 250 (3)	52 ± 9 (2)	105 ± 21 (2)
Dd2^{MD1} F3	208 ± 17 (3)	983 ± 125 (3)	57 ± 0,4 (2)	110 ± 14 (2)
Dd2	55 ± 20 (3)	180 ± 52 (3)		

Susceptibility to benzylMD 1c was assessed on Dd2^{MD1} parasites after removal of drug pressure and over a total period of 6 weeks. Susceptibility of progenitor Dd2 parasites was assessed in parallel. IC_{50} and IC_{90} values are presented as mean ± standard deviation (SD) determined from (n) independent experiments using the SYBR® green technique.

Culturing of drug-adapted parasites Dd2^{MD1} F2 and F3 under continuous drug pressure was attended by difficulties. At first, parasites showed a normal multiplication rate under drug treatment (no quantification of multiplication rate performed). However, after several cycles, parasites started to suffer visibly and died. Parasites died particularly fast in cultures with low parasite inoculum concentrations (e.g. culture dilution before weekends). This observation might indicate a selective uptake of the drug by infected erythrocytes, a so-called inoculum effect, that was previously reported for other antimalarial drugs (e.g. chloroquine and artemisinin derivatives) (Gluzman et al, 1987; Duraisingh et al, 1999).

The 1st selection cycle was independently repeated with a culture of synchronous ring stages of progenitor Dd2 parasites with high parasite inoculum (3.6×10^{9} iRBC). The initial culture was challenged with 125 nM of benzylMD **1c.** During the first week of drug treatment, parasites continued to multiply to high parasitemia. Consequently, drug concentration was increased to 150 nM and the cultures were divided into 6 culture flasks in total that were subsequently treated identically. This selection cycle revealed growing

parasites in all 6 culture flasks. Similar to the first experiment, parasite susceptibility to benzylMD **1c** was 3-4 fold decreased (IC_{50} values ranging from 104 nM to 223 nM, IC_{90} values ranging from 227 nM to 947 nM, Table A6 in the Appendix). The IC_{50} values measured on different days varied importantly and most cultures were difficult to maintain. For the latter reason, it was not possible to use drug-adapted parasites for further experiments or another selection cycle. In conclusion, the independent repetition of the 1st selection cycle confirmed the selection of drug-adapted parasites with 3-4 fold decrease in susceptibility to benzylMD **1c**.

Second selection cycle:

A 2nd selection cycle with increased benzylMD **1c** concentrations was initiated from cultures $Dd2^{MD1}$ F2 and F3. Therefore, parasites were allowed to grow to a high density in the presence of benzylMD **1c**. For $Dd2^{MD1}$ F2 and F3 each, one initial culture of ring-stage parasites at high inoculum (1.1×10^9 and 1.1×10^9 infected erythrocytes, respectively) was set up and challenged with 550 nM ($Dd2^{MD1}$ F2) or 800 nM ($Dd2^{MD1}$ F3) benzylMD **1c**, respectively. This culture was subsequently divided into 4 culture flasks that were treated identically.

Parasites were slowly killed over the first 10-14 days of drug treatment, as monitored on Giemsa-stained blood smears. The first reappearing parasites were observed after 5 weeks in all 4 flasks challenged with 550 nM benzylMD **1c** ($Dd2^{MD1}$ F2). However, parasites developed very slowly, thus insufficient to perform growth-inhibition assays. After another 3 - 4 weeks culturing with constant benzylMD **1c** concentration, parasites multiplied normally in all 4 cultures. Drug adapted parasites are hereafter designated as $Dd2^{MD2}$ F1, F2, F3 and F4 [10]. Subsequently, the experiment was proceeded as described before for cultures of the 1st selection cycle.

The susceptibility of the selected parasites ($Dd2^{MD2}$ F1 - F4) was regularly assessed over a period of 10 weeks. After the 2nd selection cycle, all selected parasites presented a 4-5 fold decreased susceptibility to benzylMD **1c** compared to the original Dd2 strain (Table 8).

---

[10] Drug adapted parasites, raised after the 2nd selection cycle with 550 nM benzylMD 1c, were designated as follows: $Dd2^{MD2}$ F1 to F4. This denotation stands for: Dd2, progenitor parasite strain; MD, selected with benzylMD 1c; 2, 2nd selection cycle; F1 – F4, growing parasites were recovered from flasks number 1 to 4.

Remarkably, parasite adaptation to increased benzylMD **1c** concentrations (550 nM) was less pronounced than adaptation observed after the 1st selection cycle (125 nM). The IC_{50} and IC_{90} values ranged from 178 nM to 259 nM or from 495 nM to 917 nM, respectively (Table 8). Thus, IC_{50} values were only slightly higher than before selection ($Dd2^{MD1}$ F2, Table 7) and moreover, below the benzylMD **1c** concentration applied during drug pressure (550 nM). This observation could partially explain the slow parasite development under drug pressure.

Similarly to their progenitors ($Dd2^{MD1}$ F2), drug adaptation was not stable over time. This time, the reverse of phenotype occurred after 5-6 weeks following drug removal (compared to 3 weeks after the 1st selection cycle). $Dd2^{MD2}$ F1 - F4 parasites presented then the same susceptibility to benzylMD **1c** as before drug selection and compared to a culture of Dd2 parasites that was assessed in parallel (Table 8 and Table A5 in the Appendix). The susceptibility of $Dd2^{MD2}$ F1 - F4 parasites to chloroquine was slightly lower compared to Dd2 parasites, though this might be no real effect (Table A5 in the Appendix). The IC_{50} values of chloroquine were consistent during the complete duration of the experiment and not affected by the reverse of adaptation observed with benzylMD **1c**. In addition, culturing of parasites under continuous drug pressure was attended by the same difficulties as observed for parasites raised after the 1st selection cycle ($Dd2^{MD1}$ F2 and F3).

Table 8 Susceptibility of drug-adapted parasites to benzylMD 1c after 2nd selection cycle

Culture	Weeks 1-6 after drug removal		Weeks 7-10 after drug removal	
	IC_{50} (nM) ± SD	IC_{90} (nM) ± SD	IC_{50} (nM) ± SD	IC_{90} (nM) ± SD
$Dd2^{MD2}$ F1	178 ± 68 (4)	495 ± 306 (4)	74 (1)	170 (1)
$Dd2^{MD2}$ F2	250 ± 30 (3)	917 ± 76 (3)	90 ± 22 (3)	213 ± 40 (3)
$Dd2^{MD2}$ F3	197 ± 58 (5)	586 ± 176 (5)	67 ± 18 (3)	145 ± 40 (3)
$Dd2^{MD2}$ F4	259 ± 63 (5)	812 ± 250 (5)	86 ± 9 (3)	183 ± 42 (3)
Dd2	63 ± 17 (8)	176 ± 45 (8)		

Susceptibility to benzylMD 1c was assessed on $Dd2^{MD2}$ parasites after removal of drug pressure and over a total period of 10 weeks. Susceptibility of progenitor Dd2 parasites was assessed in parallel. IC_{50} and IC_{90} values are presented as mean ± standard deviation (SD) determined from (n) independent experiments using the SYBR® green technique.

In contrast to cultures Dd2^{MD1} F2, Dd2^{MD1} F3 parasites were not able to acquire adaptation to high drug concentrations of 800 nM benzylMD **1c.** No living parasites could be recovered from any of the 4 cultures after 12 weeks of constant drug pressure. Subsequently, the drug treatment was stopped; cells were washed and resuspended in drug-free medium. The cultures were maintained for another 4 weeks without drug pressure to allow the reappearance of possibly retained tolerant parasites. However, no living parasites appeared in any of the 4 cultures. As described before (section 3.2.3.1), reappearance of living parasites upon drug removal was observed after drug pressure with 500 nM benzylMD **1c** for 12 weeks.

The protocol used for growth-inhibition assays includes one step to measure the background fluorescence of the assay contents (e.g. autofluorescence of compounds) (see Materials and Methods, section 2.2.2). Interestingly, the background fluorescence of drug-adapted parasites was notably increased compared to progenitor Dd2 parasites. This observation was done repeatedly on several days and did not stem from different benzylMD **1c** concentrations. An increase of autofluorescence yielded from drug-adapted parasites might point towards differences in the formation of drug metabolites or heme catabolites that are both known to be fluorescent. Alternatively, the signal might stem from intrinsic intracellular fluorophores, for instance NAD(P)H and flavoproteins, as reported before in a study with *Leishmania* parasites (Eckers & Deponte, 2012).

Cloning of drug-adapted parasites:

It should be assumed that drug selected parasite cultures comprise a mixture of parasites with different phenotypes. Accordingly, clonal parasite lines are required to explore the basis of altered drug susceptibility. Two cultures, Dd2^{MD2} F2 and F4, were selected for further analysis, as they presented the lowest susceptibility to benzylMD **1c**, as reflected in their IC$_{50}$ values (Table 8).

Cloning of drug-adapted parasites was performed by limiting dilution on 96-well plates, either in the absence or presence of 550 nM benzylMD **1c**. Unfortunately, no parasite clone with decreased susceptibility to benzylMD **1c** was retained. After 4 weeks of culturing, ten clonal parasite lines were obtained in the absence of benzylMD **1c** treatment, whereas none were obtained in the presence of the drug. These parasites were isolated and frozen for further analysis. The drug susceptibility of 3 clonal lines was assessed directly after

isolation. The IC_{50} values of all cultures were comparable to a culture of original Dd2 parasites that was assessed in parallel (data not shown). This outcome confirmed that drug-adapted Dd2^{MD2} parasites easily reverted to their original phenotype (as Dd2) upon removal of drug pressure as observed before. Cloning of parasites under drug treatment was unsuccessful: even after 6 weeks of culturing, no parasitic DNA was detected by SYBR$^{®}$ green in any well of the two 96-well plates. Possibly, drug concentration of 550 nM was too high regarding the very low starting parasitemia of the cloning procedure. Once again, this observation would suggest an inoculum effect of benzylMD **1c**.

In conclusion, the selection of drug-adapted parasites under continuous exposure to sublethal benzylMD **1c** concentrations revealed that parasites succeeded at counteracting drug pressure, although to a very limited extent. Parasites were able to multiply in the presence of up to 550 nM benzylMD **1c** but failed to recover from higher drug concentrations (800 nM). However, this adaptation was lost after short time upon drug release. This observation is similarly reflected in the failure to obtain clonal parasites with decreased susceptibility to benzylMD **1c** or to recover them after freezing. Several attempts to thaw parasites in the presence of different drug concentrations or to apply drug pressure only 24 to 48 hours after freezing were unsuccessful, parasites were killed rapidly by benzylMD **1c** (data not shown). Moreover, no prolonged survival of drug selected parasites was achieved under continuous benzylMD **1c** treatment, which also prevented to recover clonal parasites under drug pressure. Together, these observations suggested a selective uptake of benzylMD **1c** by infected erythrocytes (inoculum effect). Altogether, these results suggest that the decreased susceptibility to benzylMD **1c** might be caused by a metabolic adaptation rather than a stable genetic mutation.

3.2.4 *In vitro* drug interactions with clinical antimalarial agents

For treatment of malaria, drug-combination therapies are preferred to monotherapies in order to prevent the emergence and spread of drug resistance (White & Olliaro, 1996; WHO, 2010). In the search for a possible future co-formulation partner, we investigated the *in vitro* interactions of benzylMD **1c** with clinically used antimalarials from different subclasses and with different modes of action.

The interaction profiles were assessed on the *P. falciparum* 3D7 or K14 strain using the fixed-ratio isobologram method (Fivelman et al, 2004). This approach is based on determining the IC_{50} values of two individual drugs alone and the IC_{50} values of these two drugs in combination at different concentration ratios. In principle, the shift of a drug's IC_{50} value assessed in combination compared to the one determined for this drug alone is indicative for the nature of drug-drug interaction. The *in vitro* interactions were evaluated based on arithmetical and graphical analyses.

For arithmetical analysis, the mean sum of fractional 50% inhibitory concentrations (mean $\sum FIC_{50}$ value) was calculated based on the shift of a drug's IC_{50} value observed in several combinations with a second agent (for more details please refer to Materials and Methods, section 2.2.6). The inherent variability of the experimental set-up was estimated by combining two separate (or: individual) working solutions of lead compound **1c**. Those tests revealed a clear indifferent interaction (mean $\sum FIC_{50}$: 1.0) with very low variation (SD: 0.02, n=3) (Figure 21 A-C). Based on the observed inherent variability, we defined the cut-off values for synergistic and antagonistic interactions as follows: Synergy was classified as a mean $\sum FIC_{50} \leq 0.7$, antagonism as a mean $\sum FIC_{50} \geq 1.3$ and any value in between as indifferent interaction (in other words no interaction, formerly described as additive interaction). These definitions are in agreement with the ones applied in other studies (for instance Bell, 2005; Schleiferbock et al, 2013). Arithmetical results of the complete set of combinations are reported in Table 9. Graphical analysis was performed on isobolograms, which were established by plotting pairs of FIC_{50} values of drug A and drug B for each combination. Figure 20 illustrates the characteristic isoboles for different drug-drug interactions, as they have been assessed during this project. A straight line indicated an indifferent interaction, a concave curve towards the origin of the axes represented synergy and a convex curve towards the opposite indicated antagonism. To provide an example for *in vitro* synergy, the partners of the antimalarial co-formulation Malarone[®]

(atovaquone and proguanil, GlaxoSmithKline) were tested in combination. Indeed, the interaction between atovaquone and proguanil was found to exhibit the strongest synergy amongst all the tested combinations, with a mean $\sum \text{FIC}_{50}$ of 0.2 (Table 9) and a characteristic concave shaped isobole (Figure 21A).
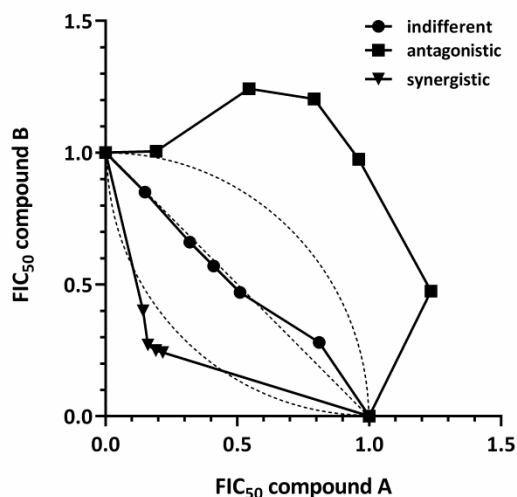

Figure 20 Isobologram illustrating characteristic curves ("isoboles") for different *in vitro* drug-drug interactions

Interaction profiles were assessed on *P. falciparum* 3D7 strain according to the fixed-ratio isobologram method. Indifferent interaction is indicated by a straight line, synergy by a concave curve and antagonism by a convex curve. Graph displays pairs of FIC_{50} values of compound A (x axis) and compound B (y axis) tested at different combinations. Depicted isoboles are representative plots for indifferent, synergistic or antagonistic interactions, as they have been assessed in this study. The dotted lines represent theoretical isoboles.

Combinations of benzylMD **1c** with the 4-methanolquinoline quinine and the current first line drug artemisinin were found synergistic (mean $\sum \text{FIC}_{50}$: 0.7 and 0.8, respectively), although for the latter one, it appeared like a tendency to synergism rather than true synergism (Table 9). A pronounced synergistic effect was however observed using the active metabolite of artemisinin, dihydroartemisinin (mean $\sum \text{FIC}_{50}$: 0.6). Synergistic effects of benzylMD **1c** in combination with dihydroartemisinin was also observed with the CQ-resistant strain K14 (mean $\sum \text{FIC}_{50}$: 0.7), whereas the combination of benzylMD **1c** and quinine behaved indifferently on strain K14 (mean $\sum \text{FIC}_{50}$: 1.1, Table 9). The isobolograms of quinine and dihydroartemisinin combinations determined on *P. falciparum* strain 3D7 show the concave shape characteristic for synergistic interactions (Figure 21A).

In contrast to quinine, 4-aminoquinolines chloroquine and amodiaquine showed no interaction when combined to benzylMD **1c** (Table 9, no graphical representation). The 4-aminoquinoline amodiaquine and ferroquine, an organometallic analogue of chloroquine, both showed a slight trend towards antagonism when combined with benzylMD **1c** (mean $\sum FIC_{50}$: 1.2), as further indicated by weakly convex shaped isoboles (Figure 21B). Though based on the mean $\sum FIC_{50}$ values, we have to consider it to be an indifferent interaction.

Antagonistic interactions with benzylMD **1c** were found for the antibiotic fosmidomycin (mean $\sum FIC_{50}$: 1.4), the purine analogue allopurinol (mean $\sum FIC_{50}$: 1.5) and for the antifolate proguanil (mean $\sum FIC_{50}$: 1.4). The respective isobolograms showed characteristic convex shaped curves (Figure 21C). Other antimetabolite compounds (pyrimethamine, cycloguanil) showed a trend towards antagonism (mean $\sum FIC_{50}$: 1.2- 1.3) with weakly convex isoboles (Table 9, Figure 21).

Recently, we demonstrated that benzylMD **1c** and the structurally related antimalarial atovaquone do not share the same mode of action (see section 3.3.1) (Ehrhardt et al, 2013). In line with these results, atovaquone and benzylMD **1c** revealed a clear indifferent interaction when tested in combination (mean $\sum FIC_{50}$: 1.0, Table 9, Figure 21D). Based on the same study (Ehrhardt et al, 2013), we expected to obtain a similar result for the combination of atovaquone with the redox-cycler methylene blue. While a slight trend towards an antagonistic interaction was observed, the result was classified as indifferent interaction (mean $\sum FIC_{50}$: 1.2; no graphical representation). Interestingly, the combination of benzylMD **1c** with methylene blue, that is supposed to follow a similar mode of action as redox-cycler, was also found indifferent (mean $\sum FIC_{50}$: 1.1, Table 9, Figure 21D). Both compounds are supposed to be reduced by the GR, which represents an essential step in their activation as redox-cyclers.

The experiments on *in vitro* drug interactions with amodiaquine, chloroquine, quinine, ferroquine, dihydroartemisinin, atovaquone and methylene blue were kindly provided by Dr. Christiane Deregnaucourt (MNHN, Paris). The experiments were performed under the routine culture conditions described in Materials and Methods, section 2.2.1.1. The synergistic interactions between benzylMD **1c** and quinine or artemisinin were experimentally confirmed at the Department of Parasitology, Heidelberg (data not shown).
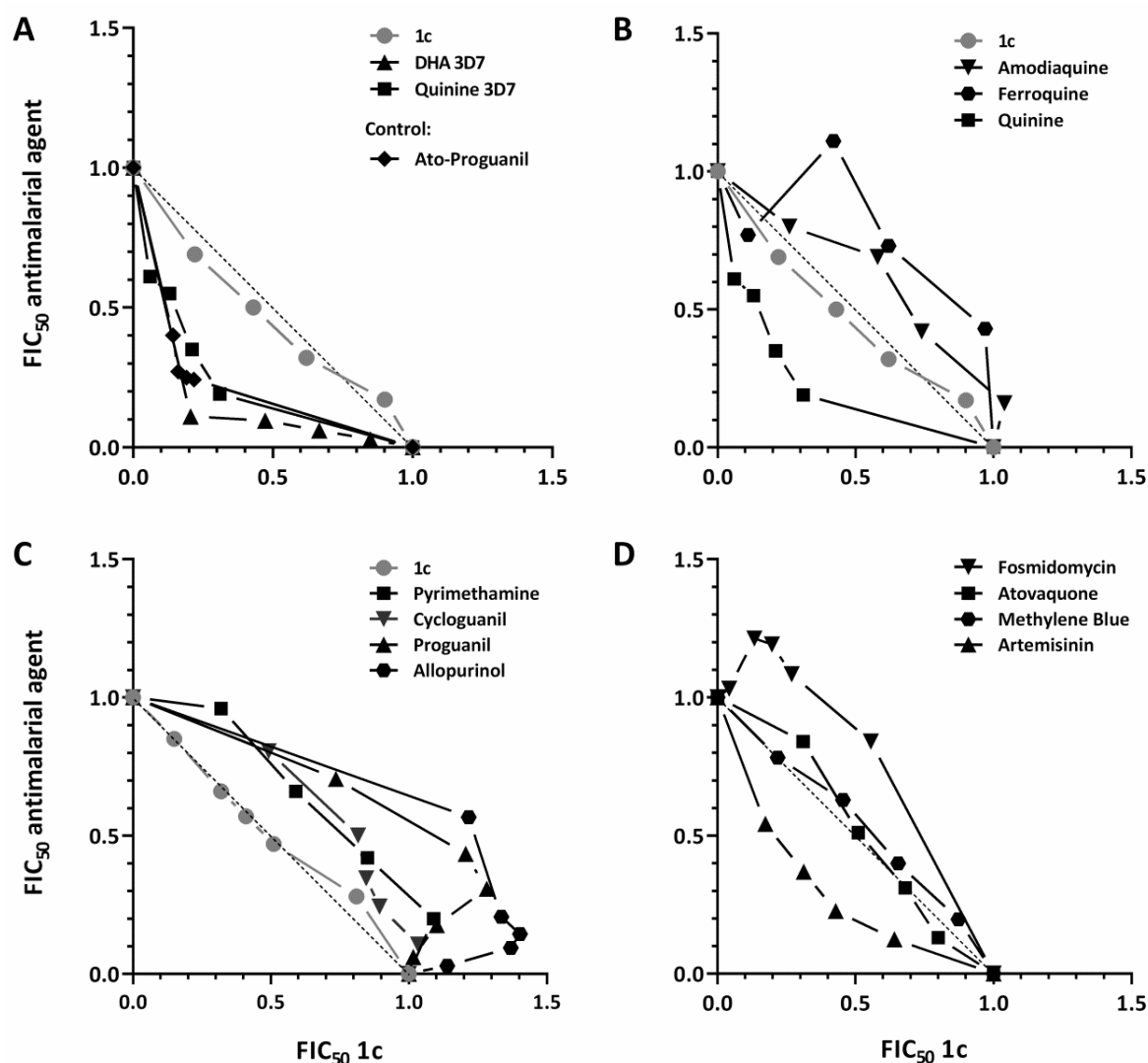
Figure 21 Isobolograms illustrating *in vitro* interactions of benzylMD 1c with clinically used antimalarials

Interaction profiles were assessed on *P. falciparum* 3D7 strain according to the fixed-ratio isobologram method. **(A)** Synergistic interactions of benzylMD **1c** with 4-methanolquinoline quinine and endoperoxide dihydroartemisinin (DHA) and synergistic interactions of atovaquone with proguanil for comparison **(B)** Interactions with quinoline antimalarials: amodiaquine and ferroquine (trend to antagonism) and quinine (synergistic) **(C)** Interactions with antimetabolite compounds: allopurinol and proguanil (antagonistic), pyrimethamine and cycloguanil (trend to antagonism) **(D)** Interactions with further antimalarial agents: antibiotic fosmidomycin (antagonistic), naphthoquinone atovaquone (indifferent), redox-cycler methylene blue (indifferent) and endoperoxide artemisinin (trend to synergy). Graphs display pairs of FIC_{50} values of benzylMD **1c** (x axis) and the antimalarial agent (y axis) tested at different combinations. Plots are from one representative experiment, arithmetical values from 3-4 independent experiments are reported in Table 9. The dotted line indicates theoretical indifferent interaction; indifferent interaction of benzylMD **1c** with itself (control of variability, grey) is shown for comparison. FIC_{50}, fractional 50% inhibitory concentration; DHA, dihydroartemisinin. Experiments with amodiaquine, chloroquine, quinine, ferroquine, dihydroartemisinin, atovaquone and methylene blue were performed by Dr. C. Deregnaucourt, Muséum National d'Histoire Naturelle, Paris. A selection of the presented isobolograms is currently prepared for publication (Ehrhardt et al, in preparation).

Results on *in vitro* interactions of lead benzylMD **1c** and clinical antimalarials are currently prepared for publication (Ehrhardt et al, in preparation).

Table 9 *In vitro* interactions between benzylMD 1c and clinical antimalarial agents

Antimalarial agent tested in combination with benzylMD 1c	Mean ∑ FIC_{50} ± SD (n) *P. falciparum* 3D7 (K14) strain	*In vitro* interaction
Quinolines [a]		
Amodiaquine	1.2 ± 0.1 (3)	indifferent
Chloroquine	1.0 ± 0.2 (4)	indifferent
Quinine	0.7 ± 0.1 (4) 1.1 ± 0.3 (4) (K14)	synergistic indifferent (K14)
Ferroquine	1.2 ± 0.1 (3)	indifferent
Mefloquine	1.0 (1)	indifferent
Divers modes of action		
Artemisinin	0.8 ± 0.1 (4)	indifferent
Dihydroartemisinin [a]	0.6 ± 0.1 (3); 0.7 ± 0.1 (4) (K14)	synergistic
Atovaquone [a]	1.1 ± 0.1 (3)	indifferent
Methylene blue [a]	1.1 ± 0.1 (3)	indifferent
Fosmidomycin	1.4 ± 0.1 (3)	antagonistic
Antimetabolites		
Allopurinol	1.5 ± 0.3 (3)	antagonistic
Pyrimethamine	1.3 ± 0.2 (3)	antagonistic
Proguanil	1.4 ± 0.1 (3)	antagonistic
Cycloguanil	1.2 ± 0.1 (3)	indifferent
Control combinations		
Control of variability [b]	1.0 ± 0.02 (3)	indifferent
Atovaquone + Proguanil	0.2 ± 0.1 (2)	synergistic
Atovaquone + Methylene Blue	1.2 ± 0.1 (3)	indifferent

In vitro drug-drug interactions were assessed on *P. falciparum* 3D7 strain according to the fixed-ratio isobologram method. Results are presented as mean sum of fractional 50% inhibitory concentration (mean ∑ FIC_{50}) ± standard deviation (SD) determined from (n) independent experiments. Calculation of mean ∑ FIC_{50} values is detailed in the Materials and Methods chapter, section 2.2.6. [a] Results were kindly provided by Dr. C. Deregnaucourt, Muséum National d'Histoire Naturelle, Paris; [b] Control of variability: benzylMD **1c** tested in combination to itself. Graphical visualization of individual *in vitro* interactions is presented in Figure 21. The results presented in this table are currently prepared for publication (Ehrhardt et al, in preparation).

3.3 Studies on the mode of action of lead compound benzylMD 1c

3.3.1 BenzylMD 1c activity against transgenic atovaquone resistant parasites

The presented work on lead benzylMD **1c**'s activity against transgenic atovaquone resistant *P. falciparum* strain 3D7attB-yDHODH and control strains 3D7attB and 3D7 was recently published (Ehrhardt et al, 2013). The following section is a full citation from this article. Tables are presented in modified form. Dr. Marcel Deponte [11] proposed the use of this transgenic parasite strains and contributed to this study.

"The commercial drug atovaquone (a 3-hydroxy-1,4-naphthoquinone) as well as other non-approved agents and compounds under development block complex III of the mitochondrial electron transport chain (mETC) (Fry & Pudney, 1992; Srivastava et al, 1997; Srivastava et al, 1999; Vaidya & Mather, 2009; Biagini et al, 2012) [...]. The major function of the mETC in asexual blood-stage cultures of P. falciparum is to regenerate ubiquinone as the electron acceptor of the mitochondrial dihydroorotate dehydrogenase (DHODH), which catalyzes a key step in pyrimidine biosynthesis (Painter et al, 2007). [...] Since pyrimidine biosynthesis is essential, a functional DHODH and mETC are necessary for parasite survival (Painter et al, 2007; Vaidya & Mather, 2009; Booker et al, 2010). Accordingly, atovaquone was demonstrated to loose its antimalarial activity in the presence of an episomal (Painter et al, 2007; Biagini et al, 2012) or chromosomal copy (Ke et al, 2011) of a yeast gene encoding an alternative cytosolic DHODH (yDHODH) that does not require the mETC as an electron acceptor. Transgenic P. falciparum strains with or without yDHODH therefore provide an excellent tool for the study of potential inhibitors of the mETC. [...]

*Methylene blue and benzylMD were proposed to act as redox-cyclers. [...] However, owing to their redox properties and structural similarities with mETC inhibitors, both agents might also alter or inhibit the mETC. [...] Consequently, the importance of the P. falciparum mETC to the antimalarial activities of methylene blue and lead benzylMD **1c** was investigated using the transgenic atovaquone resistant P. falciparum strain 3D7attB-yDHODH, such as control strains 3D7attB and 3D7. The first two strains contain a chromosomal attB site for the site-specific integration of a segment of DNA, which disrupts the gene encoding glutaredoxin-like protein 3 (PfGlp3) (Deponte et al, 2005; Nkrumah et*

---

[11] Apl. Prof. Dr. Marcel Deponte, Department of Parasitology, University Hospital Heidelberg, Germany

al, 2006). The first strain, 3D7attB-yDHODH, contains the gene encoding yDHODH (Ke et al, 2011), which confers resistance to atovaquone as well as other mETC inhibitors, whereas the second strain, 3D7attB, has no insert at the attB site. The wild type strain 3D7 was included as a control to assess the possibility that the agents affect a PfGlp3-dependent redox pathway. The IC$_{50}$ values of chloroquine and atovaquone were determined in parallel as a negative and positive control, respectively.

*The IC$_{50}$ values for the negative control chloroquine were very similar for all three strains (Table 10). In contrast, the antimalarial activity of the positive control atovaquone was significantly reduced against the strain 3D7attB-yDHODH, and the IC$_{50}$ value increased by almost four orders of magnitude. Methylene blue and benzylMD **1c** displayed potent antiplasmodial activities against all of the strains. The IC$_{50}$ values for atovaquone, methylene blue, and chloroquine presented in Table 10 correspond well with values reported elsewhere (Vennerstrom et al, 1995; Baniecki et al, 2007; Ke et al, 2011; Biagini et al, 2012). [...] It is worth noting that the presence or absence of PfGlp3 did not affect the IC$_{50}$ values of the redox-active agents (strains 3D7 and 3D7attB, respectively). Of particular importance, the presence of cytosolic yDHODH altered the activity of the mETC inhibitor atovaquone, but had no effect on the antimalarial activities of chloroquine, methylene blue, or benzylMD **1c**. Hence, the latter three agents do not exert their activity as inhibitors of the mETC in asexual blood-stage parasites.*" (Ehrhardt et al, 2013).

Table 10 *In vitro* **activities of redox-cyclers benzylMD 1c and methylene blue and control agents against transgenic atovaquone resistant *P. falciparum* 3D7attB-yDHODH and control strains**

Agent	Antimalarial activity (IC$_{50}$ (nM) ± SD)		
	3D7 [a]	3D7attB	3D7attB-yDHODH
Atovaquone	0.2 ± 0.05	0.5 ± 0.06	2230 ± 726
Methylene blue	3.1 ± 0.4	4.7 ± 0.5	3.3 ± 0.2
BenzylMD 1c	46 ± 3.5	48 ± 8.3	55 ± 5.6
Chloroquine	10 ± 0.6	11 ± 1.9	8.6 ± 2.1

Activity against cultured *P. falciparum* blood-stage parasites is presented as mean IC$_{50}$ values ± standard deviation determined from 3 independent experiments using the SYBR® green technique. [a] IC$_{50}$ values of all agents determined on *P. falciparum* 3D7 strain are presented in identical form in section 3.1.1. Results were previously published in (Ehrhardt et al, 2013).

3.3.2 Morphological investigation of benzylMD 1c treated parasites in comparison to atovaquone and methylene blue

The morphological investigation of benzylMD **1c**, atovaquone or methylene blue-treated parasites was recently published (Ehrhardt et al, 2013). The following section is a full citation from this article. Figures are presented in modified form. Dr. Marcel Deponte kindly contributed to the performance of this study.

"*Certain antimalarial agents and oxidants such as hydrogen peroxide can alter the morphology of P. falciparum (Deponte & Becker, 2004), which can sometimes provide clues to the mode of action of the drug.* [The morphology of drug-treated parasites was analyzed for lead compound **1c** in comparison to antimalarials methylene blue and atovaquone. Therefore, a synchronous *P. falciparum* 3D7attB-yDHODH culture was incubated over 46 hours with IC_{50} and IC_{90} concentrations of each drug and morphology of treated and untreated parasites was assessed at different time points on Giemsa-stained blood smears. Figure 22 illustrates the morphologies of blood-stage parasites after treatment with atovaquone, methylene blue or benzylMD **1c**.] *The morphologies of atovaquone-treated parasites were very similar to the untreated controls, which is in agreement with previous reports (Painter et al, 2010). In contrast, the growth of parasites that were treated with benzylMD 1c was retarded, and an important increase of abnormal parasite morphologies was observed (Figure 22A). After 14 hours of drug treatment, fewer trophozoite-stage parasites and more ring-stage parasites were detected than in the control culture. Some of the abnormal ring-stage parasites had a distorted mesh-like morphology, which has been previously observed in stressed cultures and usually indicates that the parasite is incapable of further development (Deponte & Becker, 2004). Others ring-stage parasites developed into residual pyknotic bodies as previously described (Müller et al, 2011) (Figure 22A). After 24 hours of drug treatment, trophozoites and schizonts appeared to be younger than in the control, which contained predominantly older mid- to late-stage schizonts (Figure 22B). After 46 hours, the benzylMD-treated culture contained remaining schizonts from the first infection cycle and numerous very small ring-stage parasites from the second infection cycle, whereas the controls did not contain schizonts and instead consisted of late ring-stage parasites from the second infection cycle (Figure 22C). The effect was more pronounced at higher drug concentrations, resulting in a significant increase of residual pyknotic bodies and*

*disordered schizont stage-parasites (Figure 22D). Thus, parasites treated with benzylMD **1c** presented a distinct morphology and became predominantly pyknotic at the ring stage.* [A detailed investigation of the stage-specific activity of benzylMD **1c** during the intraerythrocytic development was conducted separately and is presented in section 3.2.1 of this thesis. The observations on parasite morphology after drug treatment are in agreement to the benzylMD **1c**'s pronounced activity against ring-stage parasites compared to later stages (see section 3.2.1).]

An even more pronounced effect on ring-stage parasites was observed for methylene blue as indicated by the clearance of these parasite stages after 24 hours of drug treatment (Figure 22B). In addition, for methylene blue, the ratio between mesh-like and pyknotic ring-stage parasites seemed to be shifted towards the mesh-like morphology. Another difference between the methylene blue parasites and the other cultures was that numerous trophozoite- and schizont-stage parasites were surrounded by faintly stained erythrocytes after methylene blue treatment at IC_{90} concentrations (Figure 22D). Since the surrounding uninfected erythrocytes in the blood smears remained intact, the results suggest a selective lysis of infected red blood cells after prolonged treatment with methylene blue.

In summary, [the morphological differences observed for parasites treated with either atovaquone, methylene blue or benzylMD **1c**] *might be indicative of differences in drug action* [...]. [Together with the results on transgenic atovaquone resistant *P. falciparum* strains (section 3.3.1),] *these observations support the conclusion that atovaquone, methylene blue, and benzylMD **1c** do not share a common mechanism of action."* *(Ehrhardt et al, 2013).*
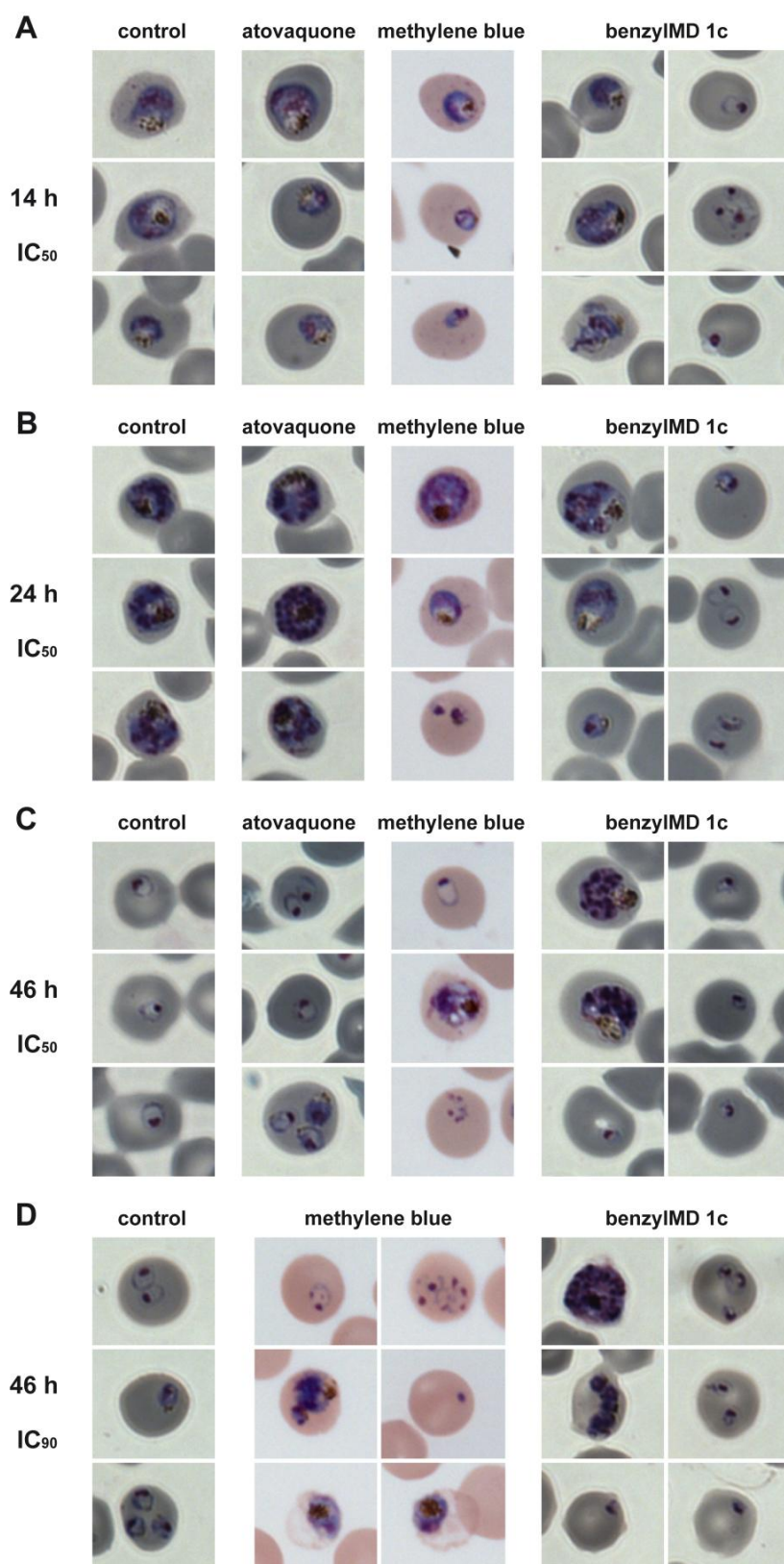
Figure 22 Parasite morphology after treatment with atovaquone, methylene blue or benzylMD 1c

Synchronous *P. falciparum* 3D7attB-yDHODH parasites were treated with one of the drugs starting at the ring stage (approx. 16 h post infection). An untreated control culture was analyzed in parallel. **(A)-(C)** Treatment with the IC_{50} concentrations for 14, 24, and 46 h. **(D)** Treatment with the IC_{90} concentration for 46 h. Color differences between the microscopic images are due to white balance settings and were not adjusted in order to avoid image manipulation. This figure was recently published in modified form (Ehrhardt et al, 2013).

3.3.3 Identifying key factors behind benzylMD 1c's redox-cycling using *in vitro* drug interaction studies with experimental molecules

The postulated mechanism of action of the benzylMD series involves a continuous cascade of redox reactions leading to the formation of several redox-active drug metabolites, which interact with different intracellular components and altogether contribute to the global antimalarial activity (see Introduction, section 1.4.1 for more details).

Direct proof that this redox cycling occurs *in situ* in the parasite, as well as evidence of the proposed metabolites, is difficult to find and technically complicated to measure, because (i) conventional approaches disrupt the cellular integrity thereby leading to oxidation of drug species and (ii) redox-cyclers are supposed to act as catalysts, existing only in trace amounts. To overcome these limitations, *in vitro* drug interaction studies were chosen as a tool to explore key features of benzylMD **1c's** mode of action in a whole cell assay. Drug-drug interactions are commonly explored in the frame of mechanistic studies on antimicrobial drugs and provide information about molecular drug targets, the relationships between different drug targets and / or the cellular consequences of drug action (Bell, 2005; Jia et al, 2009).

Several experimental molecules were carefully selected in order to explore the role of (i) GR activity, (ii) NADPH flux, (iii) interaction with iron and (iv) Fenton reactions for benzylMD **1c**'s antimalarial activity. Another set of compounds was selected to shed light on the influence of (v) intracellular GSH balance on drug activity.

In vitro interaction profiles were assessed on *P. falciparum* 3D7 strain using the fixed-ratio isobologram method (Fivelman et al, 2004) and based on arithmetical and graphical analyses of results as described in detail in section 3.2.4 of this chapter. The cut-off values for synergistic and antagonistic interactions were defined as follows: Synergy was classified as a mean $\sum \text{FIC}_{50} \leq 0.7$, antagonism as a mean $\sum \text{FIC}_{50} \geq 1.3$ and any value in between as indifferent interaction. The IC_{50} values determined for the experimental molecules, together with their chemical structures, are given in the Appendix (Table A7).

The following results on *in vitro* interactions of benzylMD **1c** with the agents benzylMD **7a**, nicotinamide, 6-aminonicotinamide, CB83, ML276 and desferrioxamine B are presented in the article of Bielitza et al. that was recently submitted (Bielitza et al, submitted, 2014.).

3.3.3.1 Redox-cycling: the role of the glutathione reductase

The oxidoreductase GR is proposed to play a crucial role in the benzylMD's mechanism of action by reducing benzoylMD species and thereby activating them for further redox-cycling. To test this hypothesis, the prodrug of a GR suicide inhibitor was selected for *in vitro* interaction studies, namely the difluoromethyl analogue of a bromo benzylMD, the benzylMD **7a** (structure see Table A7, Appendix). BenzylMD **7a** is the postulated prodrug form of an effective suicide substrate of both GRs of the infected erythrocyte (hGR and *Pf*GR) (so-called benzoylMD **8a**), both described in Müller et al., 2011. In contrast to other benzylMD derivatives, benzylMD **7a** has lost its antimalarial activity, as evidenced by IC$_{50}$ values in the high micromolar range.

The *in vitro* interaction of lead benzylMD **1c** and benzylMD **7a** was found antagonistic (mean $\sum$ FIC$_{50}$: 1.3, Table 12), though this effect was rather weak compared to the antagonistic interactions with other compounds, such as desferrioxamine B or ascorbic acid (see below). Figure 23A illustrates the resulting isobologram. This result would rather indicate towards an alternative or supplementary drug activation pathway upon inactivation of the GR by suicide inhibitors.

3.3.3.2 Redox-cycling: the role of NADPH

NADPH is an important reducing agent of the intracellular antioxidant defense and is the essential electron donor for GR and other oxidoreductases. BenzylMD-derived metabolites are proposed to be continuously recycled (or: regenerated) in a NADPH-dependent reaction. To test this hypothesis, different precursors of the NAD$^+$ / NADP$^+$ biosynthesis and inhibitors of the NADPH regeneration pathways were selected for *in vitro* interaction studies.

In higher eukaryotes, two major biochemical pathways, the salvage and the *de novo* pathway, are involved in the biosynthesis of NAD$^+$, which is consequently phosphorylated to generate NADP$^+$. Recent studies revealed important differences in the NAD$^+$ / NADP$^+$ metabolisms of non-infected and *P. falciparum*-infected erythrocytes. While nicotinamide is apparently not utilized in the normal erythrocyte for NAD$^+$ / NADP$^+$ synthesis, it is consumed by *P. falciparum*-infected erythrocytes, accounting for a substantial increase in NAD$^+$ levels and slight increases in NADP$^+$ levels compared to non-infected cells (Zerez et

al, 1990; Olszewski et al, 2009; O'Hara et al, 2014). Likewise, the antimetabolite of nicotinamide, 6-aminonicotinamide, was shown to decrease NAD^+ levels of parasitized erythrocytes (Zerez et al, 1990).

Nicotinic acid, nicotinamide and 6-aminonicotinamide showed no effect on *in vitro P. falciparum* proliferation even in high concentrations, consistent with observations by Zerez et al. (1990). Hence, it was not possible to establish the IC_{50} values of these compounds, which is essential to perform the fixed-ratio isobologram method. Therefore, *in vitro* interactions between these compounds and benzylMD **1c** were established differently: the IC_{50} value of benzylMD **1c** was determined in the presence of a fixed concentration of nicotinic acid, nicotinamide or 6-aminonicotinamide, which had no effect on parasite multiplication by themselves (Table 11). In the presence of of nicotinamide (3 mM), a ca. 50%-decreased IC_{50} value was measured for benzylMD **1c**, suggesting a synergistic interaction of nicotinamide and the lead compound. This observed effect was counteracted by the according antimetabolite 6-aminonicotinamide (ca. 40% increased IC_{50} value). Addition of up to 2 mM nicotinic acid had no affect on benzylMD **1c**'s IC_{50} value (data not shown).

Table 11 *In vitro* interaction of benzylMD 1c with NAD^+/$NADP^+$ precursor or respective antimetabolite

Compounds tested in combination	IC_{50} (nM) ± SD (n)	Mean IC_{50} shift (%)	*In vitro* interaction
BenzylMD **1c**	68.2 ± 17.5 (6)		
+ nicotinamide	35.3 ± 13.9 (3)	- 48.2	synergistic
+ 6-aminonicotinamide	95.4 ± 19.2 (3)	+ 39.9	antagonistic

IC_{50} values of benzylMD 1c were determined in the absence or presence of 3 mM nicotinamide or 0.5 mM 6-aminonicotinamide on *P. falciparum* 3D7 parasites using the SYBR® green technique. Results are presented as mean IC_{50} values ± standard deviation (SD) determined from (n) independent experiments. Results are presented in modified form in Bielitza et al. (Bielitza et al, submitted, 2014.).

Taken together, only NAD^+ / $NADP^+$ precursor nicotinamide, which is preferentially used by infected erythrocytes, showed an effect on benzylMD **1c**'s activity that is furthermore confirmed by the use of nicotinamide's antimetabolite 6-aminonicotinamide.

In *P. falciparum* and its hosting erythrocyte, NADPH is mainly generated in the PPP with the key enzymes *Pf*GluPho and hG6PD, respectively (see also Introduction, section 1.2.3). The small molecule CB83 was recently identified as a selective irreversible inhibitor of the human G6PD, which was shown to inhibit parasite development *in vitro* (Preuss et al, 2012a). High-throughput screening of a NIH compound library identified a series of benzothiazinones as highly selective inhibitors of *Pf*GluPho and a lead compound (ML276) with antiparasitic *in vitro* activity (Preuss et al, 2012a; Preuss et al, 2012c). The *in vitro* interactions were assessed using the fixed-ratio isobologram method.

Tested in combination with benzylMD **1c**, the *h*G6PD inhibitor CB83 showed a strong antagonistic interaction (mean $\sum$ FIC$_{50}$: 2.3, Table 12), possibly explained by the decreased rate of NADPH-dependent bioactivation of benzylMD **1c** in the host cell. The combination of *Pf*GluPho inhibitor ML276 with benzylMD **1c** showed a clearly indifferent interaction (mean $\sum$ FIC$_{50}$: 1.0, Table 12). The isobolograms of *in vitro* interactions of benzylMD **1c** with CB83 or ML276 are illustrated in Figure 23.
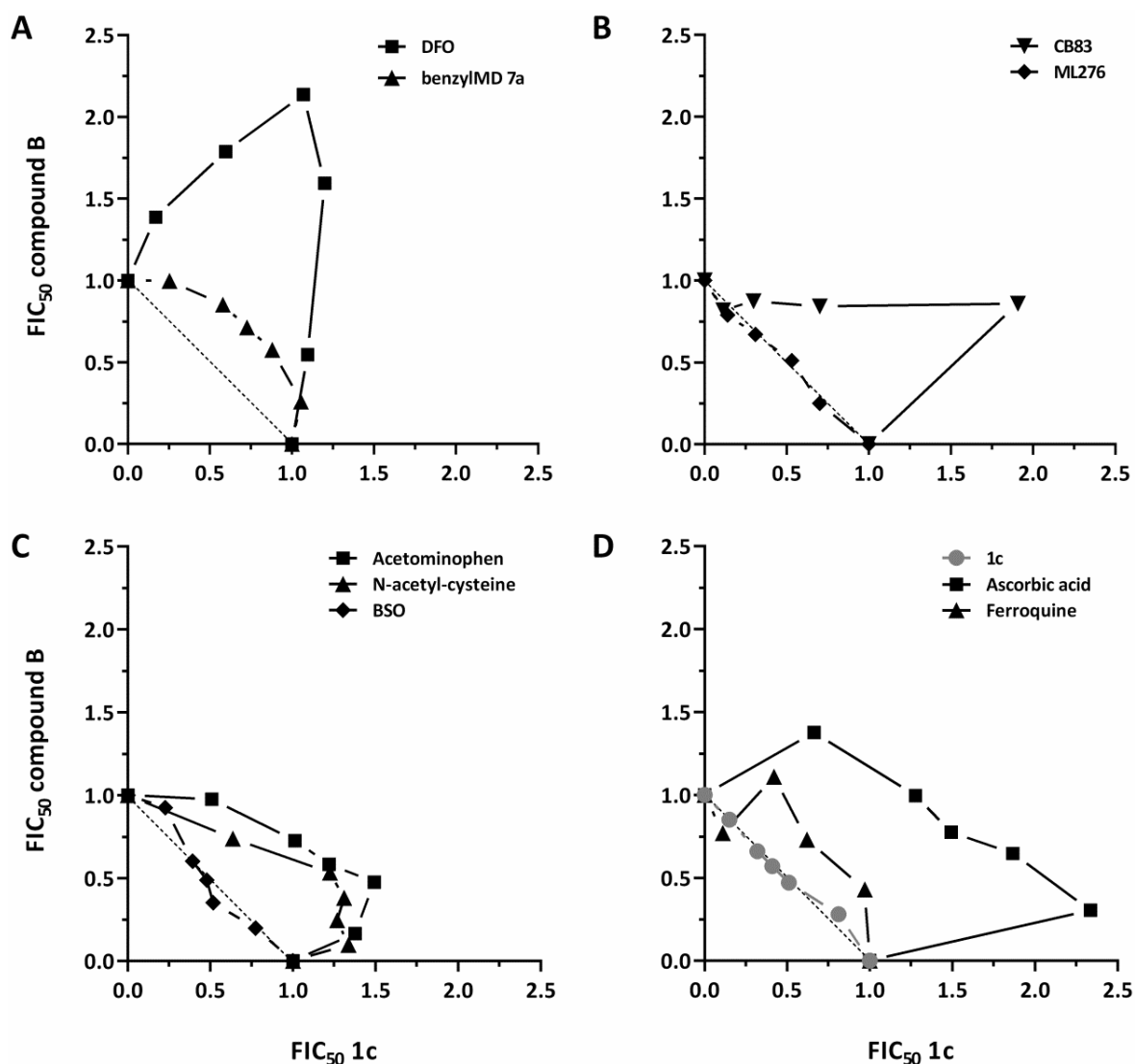
Figure 23 Isobolograms illustrating *in vitro* interactions of benzylMD 1c with experimental molecules

Interaction profiles were assessed on *P. falciparum* 3D7 strain according to the fixed-ratio isobologram method. **(A)** Interaction of benzylMD 1c with GR suicide inhibitor benzoylMD 8a (indifferent) or respective prodrug benzylMD 7a (antagonistic); interaction with iron chelator desferrioxamine B (DFO, antagonistic) **(B)** Interactions of benzylMD 1c with hG6PD inhibitor CB83 (antagonistic) or *Pf*GluPho inhibitor ML276 (indifferent) **(C)** Interactions with GSH depletor acetaminophen (antagonistic), precursor of GSH synthesis acetylcysteine (antagonistic) or inhibitor of γ-GCS BSO (indifferent) **(D)** Interactions with inducers of Fenton reactions ferroquine (slightly antagonistic) or ascorbic acid (antagonistic). Indifferent interaction of benzylMD 1c with itself (control of variability, grey) is shown for comparison. Graphs display pairs of FIC$_{50}$ values of benzylMD **1c** (x axes) and the experimental molecule (y axes) tested at different combinations. Plots are from one representative experiment, arithmetical values from 3-4 independent experiments are reported in Table 12. The dotted line indicates theoretical indifferent interaction. BSO, Buthionine sulfoximine; DFO, desferrioxamine B; FIC$_{50}$, fractional 50% inhibitory concentration; γ-GCS, γ-glutamyl-cysteine synthetase.

3.3.3.3   Iron complexation as a key factor of benzylMD 1c global activity

Numerous sources of iron (ferrous iron Fe^{2+}, ferric iron Fe^{3+}) are present within the parasitized erythrocyte (methemoglobin, hemoglobin, heme, hemozoin, hemichrome, labile iron pool) and play an important role in metabolic reactions (reviewed in Scholl et al, 2005). Iron is a transition metal that exists in different oxidation states and can transfer electrons between molecules, thereby participating in redox reactions. It was considered that benzylMD **1c**-derived metabolites act as metal chelators, which could play a critical role for the global drug activity (Müller et al, 2011). Chelation of ferric iron (Fe^{3+}) might catalyse key bioactivation steps or assist in drug transport within the pathogen's main compartments (siderophore-like transport).

In order to explore the importance of iron complexation for global benzylMD **1c** antiparasitic activity, benzylMD **1c** was tested in combination with the iron chelator desferrioxamine B (DFO). DFO is a bacterial siderophore from actinobacteria *Streptomyces* that strongly binds ferric iron (Fe^{3+}) species (structures see Table A7, Appendix). Along with other iron chelators, DFO was characterized as antimalarial compound with modest antiparasitic activity (reviewed in Mabeza et al, 1999). The *in vitro* interaction of DFO and benzylMD **1c** revealed a very strong antagonistic effect (mean $\sum FIC_{50}$: 2.4), thus indicating that chelation of iron species by benzylMD **1c**-derived metabolites is crucial for benzylMD **1c**'s antimalarial activity. The resulting isobole had a pronounced convex shape (Figure 23A). A modest antimalarial activity of DFO was confirmed in this test (IC_{50}: 12.3 µM, Table A7, Appendix). Interestingly, the observed antagonism between benzylMD **1c** and DFO was, together with ascorbic acid, the strongest interaction among all tested drug combinations.

3.3.3.4   Fenton reactions as a cause of intracellular drug degradation

Pro-oxidative Fenton reactions are generally occurring under oxidative conditions in the presence of transition metals like copper or iron. Thereby, hydrogen peroxide reacts with ferrous iron (Fe^{2+}) leading to reduction to ferric iron (Fe^{3+}) under generation of reactive hydroxyl radicals ($H_2O_2 + Fe^{2+} \rightarrow Fe^{3+} + OH^{\bullet} + OH^{-}$). In the presence of reductants, ferric iron (Fe^{3+}) can be easily reduced to ferrous iron (Fe^{2+}), providing additional electron acceptors for Fenton reactions. Several endogenous reductants are known to accelerate these reactions, such as ascorbic acid, GSH, or reduced redox-drugs (e.g. benzoylMD).

108

Fenton reactions are prone to occur in the digestive vacuole of the parasite, where they could contribute to the formation of harmful reactive oxygen species and the degradation of macromolecules like hemoglobin or heme. These reactions could also cause a degradation of drug molecules in the digestive vacuole, as it has been reported for ferrocenic dual molecules (Chavain et al, 2009). The observation that benzylMD **1c** exerted a lower activity against trophozoites raises the question whether Fenton reactions might cause degradation of drug molecules.

In order to test this hypothesis, lead compound **1c** was tested in combination with ferroquine or ascorbic acid, two compounds reported to trigger Fenton reactions in the parasite's digestive vacuole. The increase of hydroxyl radical formation by a Fenton-like mechanism was proposed to be a considerable part of the mode of action of ferroquine (Chavain et al, 2008). Ascorbic acid (also called vitamin C) is broadly known as antioxidant. Though, in the presence of iron and oxygen in the parasite's digestive vacuole, ascorbic acid turns into a pro-oxidant agent by acting as reductant of ferric iron (Fe^{3+}), thereby accelerating Fenton reactions (Marva et al, 1989; Winter et al, 1997). Similarly, the sterilizing effect of ascorbic acid on *Mycobacterium tuberculosis* could be explained by its pro-oxidant activity and induction of Fenton reactions (Vilcheze et al, 2013).

As described in section 3.2.4, ferroquine showed an indifferent interaction in combination with benzylMD **1c**, with a slight tendency towards antagonism (mean $\sum FIC_{50}$: 1.2, Table 12, Figure 23D). In contrast, the combination of benzylMD **1c** with ascorbic acid revealed a strong antagonistic interaction (mean $\sum FIC_{50}$: 2.4) with a convex shaped isobole (Table 12, Figure 23D). Ascorbic acid itself showed no effect on parasite survival or multiplication with IC_{50} values in the millimolar concentration range (IC_{50}: 7 mM, Table A7, Appendix). The latter result indicates that Fenton reactions occurring in the digestive vacuole of the parasite could contribute to degradation of benzylMD **1c**-derived drug species, thereby explaining the reduced activity of benzylMD **1c** against mature parasite stages (i.e. trophozoite and schizont stages).

3.3.3.5   Influence of intracellular GSH levels on benzylMD 1c's activity

BenzylMD redox-cyclers are proposed to disturb the redox equilibrium of the host-parasite unit and would therefore be expected to affect the level of the major antioxidant thiol GSH. The cytosolic GSH:GSSG ratio of the parasite is maintained by GSSG efflux to the host

cell or by regulating expression levels of GR and enzymes of GSH *de novo* biosynthesis (Patzewitz et al, 2012). Increase or depletion of intracellular GSH levels was shown to affect drug activity or parasites resistance of others antimalarials, such as ellagic acid and chloroquine (Ginsburg & Golenser, 2003; Soh et al, 2009). One could speculate that modulations of the intracellular GSH levels might similarly affect the activity of the pro-oxidant benzylMD **1c**.

To address this hypothesis, different compounds known to either deplete or increase intracellular GSH levels were selected for *in vitro* drug combination assays. The 4-aminoquinoline amodiaquine and acetaminophen (more precisely its metabolite N-acetyl-*p*-benzoquinone) were shown to deplete GSH stocks in cells (Moore et al, 1985; Tingle et al, 1995). Buthionine sulfoximine (BSO) is an inhibitor of the parasite's γGCS, the first enzyme of the GSH *de novo* synthesis pathway. BSO was shown to reduce GSH levels in iRBC and parasite compartments upon application to culture medium (Luersen et al, 2000; Meierjohann et al, 2002). N-acetyl-cysteine is intracellular converted to cysteine, which is used for GSH synthesis. Based on its capacity to increase intracellular GSH levels, N-acetyl-cysteine is, amongst others, clinically applied as an antidote of acetaminophen intoxications (reviewed in Rushworth & Megson, 2014) and was used for former *in vitro* studies of cultured *P. falciparum* parasites (Soh et al, 2009; Njomnang Soh et al, 2012; Patzewitz et al, 2013).

The *in vitro* interaction of benzylMD **1c** and amodiaquine was found to be indifferent (mean $\sum FIC_{50}$: 1.2, Table 12, Figure 21B). The antioxidant N-acetyl-cysteine behaved antagonistic in combination with benzylMD **1c** (mean $\sum FIC_{50}$: 1.8, Table 12), suggesting that increased GSH levels might neutralize the pro-oxidative effects of benzylMD **1c**. Alternatively, one might speculate that increased GSH levels induce Fenton reactions in the digestive vacuole and consequently lead to drug degradation, as discussed in the section before. The according isobole, which is characteristic for an antagonistic interaction, is illustrated in Figure 23C. Conversely, an antagonistic interaction was also observed for the GSH-depleting agent acetaminophen (mean $\sum FIC_{50}$: 1.8, Table 12, Figure 23C), which were expected to act in an opposite way than N-acetyl-cysteine. In contrast to the latter result, *in vitro* interaction of benzylMD **1c** with BSO, which was similarly shown to reduce GSH levels in iRBC, was found clearly indifferent (mean $\sum FIC_{50}$: 1.1, Table 12, Figure 23C).

Table 12 *In vitro* interactions between lead benzylMD 1c and experimental molecules

Compounds tested in combination with benzylMD 1c		Mean ∑ FIC$_{50}$ ± SD (n)	*In vitro* interaction
Glutathione reductase activity			
benzylMD **7a** [a]	Prodrug of a GR suicide substrate (hGR and *Pf*GR)	1.3 ± 0.1 (4)	slightly antagonistic
Iron complexation			
DFO [a]	Iron chelator	2.4 ± 0.6 (3)	antagonistic
Fenton reactions			
Ferroquine	Inducer of Fenton reactions	1.2 ± 0.1 (3)	indifferent
Ascorbic acid	Inducer of Fenton reactions	2.4 ± 0.3 (3)	antagonistic
NADPH balance of the infected erythrocyte			
ML276 [a]	*Pf*GluPho inhibitor	1.0 ± 0.1 (3)	indifferent
CB83 [a]	hG6PDH inhibitor	2.3 ± 0.6 (4)	antagonistic
GSH balance of the infected erythrocyte			
Amodiaquine	GSH depletor	1.2 ± 0.1 (3)	indifferent
Acetaminophen	GSH depletor	1.8 ± 0.2 (3)	antagonistic
BSO	γ-GCS inhibitor	1.1 ± 0.1 (3)	indifferent
N-acetyl-cysteine	Precursor of GSH synthesis	1.8 ± 0.3 (3)	antagonistic
Control combination			
Control of variability [b]		1.0 ± 0.02 (3)	indifferent

In vitro drug-drug interactions were assessed on *P. falciparum* 3D7 strain according to the fixed-ratio isobologram method. Results are presented as mean sum of fractional 50% inhibitory concentration (mean ∑ FIC$_{50}$) ± standard deviation (SD) determined from (n) independent experiments. Calculation of mean ∑ FIC$_{50}$ values is detailed in Materials and Methods, section 2.2.6. Structures of compounds and individual IC$_{50}$ values are presented in the Appendix (Table A7).a Results are presented in modified form in Bielitza et al. (submitted, 2014.); b Control of variability: benzylMD 1c tested in combination to itself. Graphical visualization of individual *in vitro* interactions is presented in Figure 23. BSO, Buthionine sulfoximine; DFO, desferrioxamine B; γ-GCS, γ-glutamyl-cysteine synthetase; GSH, glutathione; hGR, human glutathione reductase; *Pf*GR, *P. falciparum* GR.

4 DISCUSSION

4.1 Lead benzylMD 1c possesses a very attractive *in vitro* activity profile

The presented doctoral project represents an essential part of the lead evaluation stage of the benzylMD drug-development process. One major focus of this was dedicated to exploring in detail the *in vitro* potency of lead benzylMD **1c** on cultured *P. falciparum* blood-stage parasites. Next to antiparasitic activity and cytotoxicity on human cells, this comprises further safety aspects such as the risk of resistance development. Not less important are the properties of drug action, which help to predict the clinical efficacy of a drug (i.e. the speed of action and stage specificity). Particular attention was directed to identifying potential combination partners for lead benzylMD **1c** in the portfolio of existing antimalarial drugs.

Based on the characterization of its *in vitro* activity profile, benzylMD **1c** fulfills the requirements of a first-line treatment and is best described as target candidate profile 1 (TCP1), as classified by MMV (Burrows et al, 2013). Most importantly, benzylMD **1c** showed an excellent *in vitro* speed of action with an immediate and rapid clearance of parasites. Therefore it could be expected to significantly decrease the initial parasite burden, as well as reduce related symptoms. The drug's pronounced activity against ring-stage parasites might be an important factor for good clinical efficacy (further discussed in the following sections). In addition, benzylMD **1c** has been shown to effectively inhibit the development of drug-sensitive and multiple drug-resistant *P. falciparum* isolates, which represent common resistance-mechanisms to clinical antimalarials. The outcomes of *in vitro* drug-pressure experiments suggest a low probability of parasite-resistance development.

As a fast-killing compound (TCP 1), benzylMD **1c** should be combined with a long-acting companion with a prolonged plasma half-life that would kill residual parasites in the patient (TCP 2) (Burrows et al, 2013). Several clinical antimalarials showed synergistic or indifferent *in vitro* interactions with benzylMD **1c,** including long-acting compounds currently used as artemisinin partner-drugs, such as mefloquine, atovaquone and cycloguanil. The lack of pre-existing cross-resistance to those antimalarials increases the chance of finding a suitable drug partner in the portfolio of existing antimalarials.

Further pharmacological and pharmacokinetic studies are essential to determining the oral bioavailability and plasma half-life of lead compound **1c** and additional benzylMD derivatives of the second generation. Additionally, it is of obvious importance to test the activity of lead **1c** in mouse models, for instance the humanized *P. falciparum* model.

In conclusion, this work elucidated the attractive *in vitro* activity profile of lead benzylMD **1c** and supports further development of the benzylMD series as antimalarial drug candidates. The individual aspects of benzylMD **1c**'s *in vitro* activity profile are discussed in more detail in the following sections of the discussion.

4.1.1 BenzylMD 1c is selectively active against *P. falciparum* parasites and strongly inhibits the development of drug-sensitive and drug-resistant strains

Consistent with former studies (Müller et al, 2011), lead benzylMD **1c** was demonstrated to be a potent inhibitor of *P. falciparum* blood-stage development, with IC_{50} values in the low nanomolar range (section 3.1.1). Moreover, Dr. B. Pradines has shown that benzylMD **1c** is also active in the low nanomolar range against a panel of drug-sensitive and drug-resistant *P. falciparum* strains of different geographical origins (section 3.1.2). A statistical correlation analysis revealed the lack of cross-resistance with a set of clinically used antimalarials, namely chloroquine, quinine, monodesethylamodiaquine and mefloquine. These data suggests that the observed variation of benzylMD **1c**'s antimalarial activity might be attributable to natural phenotypic variations of the different *P. falciparum* strains. Furthermore, the lack of pre-existing resistance to benzylMD **1c** supports its specific mechanism of action, which is unaffected by the resistance mechanisms to common clinical antimalarials.

114

Lead benzylMD **1c** presented a low cytotoxicity against several human cell lines, as reflected in the micromolar IC_{50} values. The cytotoxicity against buccal carcinoma cells (KB) and lung fibroblasts (MRC-5) have been published previously (Müller et al, 2011). Ms. T. Tzanova and Dr. D. Bragel further tested the cytotoxicity of benzylMD **1c** against a liver carcinoma cell line (HepG2) (see Results, section 3.1.1). It is of interest to note, that further toxicity studies revealed no risk of geno- or cardiotoxicity and a lack of intrinsic mutagenic potential of lead benzylMD **1c**. These results will be presented and further discussed in a future publication (Ehrhardt et al, in preparation). Despite its elusive pro-oxidative activity in infected erythrocytes, benzylMD **1c** exerts no risk of hemolysis or intrinsic toxicity on uninfected G6PD-deficient or G6PD-sufficient cells. The latter observation could be further confirmed in a humanized G6PD-deficient mouse model (Rochford et al, 2013).

4.1.2 Lead benzylMD 1c inhibited the development of all intra-erythrocytic stages but was most effective against ring-stage parasites

The stage-specific activity of benzylMD 1c was found to be clearly different from most others antimalarials, with young ring stages being the most sensitive to the drug (Results, section 3.2.1). This observation is supported by a morphological investigation of drug-treated parasites, which revealed that mainly drug-affected ring stages presented a characteristic pyknotic morphology under benzylMD **1c** treatment (Results, section 3.3.2), as it was first described by Dr. Christiane Deregnaucourt (Müller et al, 2011; Ehrhardt et al, 2013). Still, it is indispensable to highlight that benzylMD **1c** activity was not restricted to early stages, as the development of mature-parasite stages (trophozoites and schizonts) was completely inhibited by prolonged drug treatment, as shown in further experiments. The drug's potency against all stages is similarly reflected in the high parasite reduction ratio that was assessed over 48 hours using a mixed-stage culture (Results, section 3.2.2).

Together, these results thus point towards dose- and time-dependent differences in drug susceptibility among individual intraerythrocytic stages. The observation that benzylMD **1c** was less active against trophozoites could be partially explained as a result of drug degradation by Fenton reactions. This hypothesis was addressed by assessing the *in vitro* interactions of benzylMD **1c** in combination with ferroquine and ascorbic acid, both of which were shown to induce Fenton reactions in the digestive vacuole of the

parasite (section 3.3.3.4) (Marva et al, 1989; Winter et al, 1997; Chavain et al, 2008). Indeed, the latter combination revealed a strong antagonistic interaction, indicating that Fenton reactions can contribute to drug destruction in the digestive vacuole and thereby explaining the reduced activity of benzylMD **1c** against mature parasite stages.

The majority of antimalarial compounds, with the rare exceptions of artemisinin and methylene blue, act on the trophozoite or schizont stages. Several authors have stressed the importance of developing new drugs with novel modes of action that affect parasite stages other than the trophozoite (Burrows et al, 2013; Wilson et al, 2013). The redox-cycler methylene blue has a stage-specificity profile very similar to that of benzylMD **1c**, with a pronounced activity against ring-stage parasites (section 3.3.2) (Akoachere et al, 2005; Ehrhardt et al, 2013). Interestingly, the third group of antimalarial redox-cyclers, namely INODs, has also been shown to preferentially inhibit the development of ring-stage parasites. Therefore one might speculate that ring stages are particularly vulnerable to an overload of oxidative stress. Only recently, very young ring stages (< 4 hours p.i.) were shown to be hypersensitive to artemisinin (Klonis et al, 2013) and an altered *ex vivo* response of those stages to artemisinin pulses was correlated with prolonged *in vivo* parasite clearance times (Witkowski et al, 2013a) (please also refer to the discussion on parasite dormancy in the following section).

Compounds killing ring stages can be expected to be beneficial for patients. Several arguments support this hypothesis. First, in the course of infection, a subpopulation of ring-stage parasites differentiates to sexual gametocytes, which are responsible for the transmission of the parasite to the mosquito vector (Baker, 2010). In the idea that a given compound will kill the sexually committed ring-stage parasites before differentiation to gametocytes, this drug would decrease the gametocyte load in patients and parasite transmission. Secondly, erythrocytes infected with trophozoite or schizont stages adhere to endothelia of small blood vessels in important organs and consequently cause severe forms of the disease, including cerebral and placental malaria or respiratory distress (White et al, 2014). Any drug treatment leading to increased killing or phagocytosis of ring-stage infected erythrocytes can be expected to prevent the attachment of infected erythrocytes to the endothelium and would consequently lower related symptoms and prevent progression of the disease to severe forms (previously discussed in more detail in Ayi et al, 2004). In support of this hypothesis is the observation that several genetic disorders of the

erythrocyte, such as G6PD-deficiency, confer resistance against severe forms of malaria. The resistance of G6PD-deficient patients was shown to be related to a rapid removal of ring-stage infected erythrocytes by phagocytosis. Parasite development in G6PD-deficient cells encounters an enormous oxidative stress on the host cell, which results in the increased denaturation of hemoglobin species and membrane binding of hemichromes, a key determinant for phagocytosis (Cappadoro et al, 1998) (see also Introduction, section 1.2.2.3). Recent spectrophotometric studies with benzylMD **1c**-derived metabolites (benzoylMD **2c** and dihydrobenzoylMD **3c**) and hemoglobin species in solution approved the degradation of different hemoglobin species accompanied by the formation of reactive oxygen species and ferrylhemoglobin upon extended redox-cycling (Bielitza et al, submitted, 2014.) (described in detail in the Introduction, section 1.4.1). Of particular importance for drug activity was the evidence of ferrylhemoglobin formation and the precipitation of irreversible hemichromes. In support of this finding, treating ring-stage infected erythrocytes with benzylMD **1c** induced a significantly increased binding of hemichromes to the host cell membrane, as it was shown before for ring-stage infected G6PD-deficient cells (in collaboration with Dr. P. Arese, Bielitza et al, submitted, 2014.). Early hemichrome deposition and subsequent opsonisation in ring-stage infected erythrocytes is considered to be advantageous for the phagocytic removal of infected cells (Turrini et al, 2003). First of all, circulating ring-stage infected erythrocytes can be recognized by residual macrophages in the liver or spleen and secondly, those cells contain only few hemozoin, which was shown to inhibit macrophage functions in higher amounts as present in trophozoites (previously discussed in more detail in Turrini et al, 2003; Ayi et al, 2004).

Thus, it can be expected that benzylMD **1c**-induced hemichrome formation will be a key factor in triggering phagocytosis of drug-treated cells *in vivo*. As stated before, the phagocytosis of drug-treated infected erythrocytes can be expected to contribute significantly to parasite clearance *in vivo* and can be expected to protect from severe malaria. Therefore it would be of particular interest to further explore this topic in adequate *in vitro* and *in vivo* experiments (e.g. Chan et al, 2012).

4.1.3 Lead 1c can be counted among the fastest compounds described so far

The efficiency of antimalarials in decreasing blood parasitemia and curing patients is mediated in part by their speed of action. Lead compound **1c** showed a very fast speed of action comparable to artemisinin, one of the fastest compounds described so far (section 3.2.2). A quick onset of action is considered to be necessary for first-line treatment because the drug will rapidly decrease blood parasitemia and consequently related symptoms (Sanz et al, 2012; Burrows et al, 2013). Still, a slightly delayed onset of benzylMD **1c** action (< 24 h, 8 h lag phase) was observed and may indicate an initial cytostatic drug effect. On the basis of our proposed mechanism of action, this observation might point towards an exponential formation of drug metabolites, reactive oxygen species and / or degradation of hemoglobin species. Regardless, this short delay was rapidly compensated by the high parasite killing rate observed in the following 40 hours. In conclusion, the fast speed of action of benzylMD **1c** promises a high therapeutic efficacy and furthermore minimizes the time window for parasites to develop drug resistance (White & Pongtavornpinyo, 2003; Sanz et al, 2012; Burrows et al, 2013).

4.1.4 Lead benzylMD 1c showed a low potential to induce drug resistance

The rapid development of parasite resistance to new drugs is a major challenge for antimalarial drug design. Whether the emergence of drug resistance will be slow or fast is depending on several factors and *in vitro* protocols may only give limited predictions of resistance development in the field (White & Pongtavornpinyo, 2003; Nzila & Mwai, 2010). However, it has been clearly shown that some compounds induce resistance more easily than others. In the case of atovaquone, treatment failure related to resistant parasites was already observed with its first clinical use (Looareesuwan et al, 1996). The genetic basis of the parasite's resistance to spiroindolone NITD609 (2012 in clinical Phase IIa, Anthony et al, 2012) was already resolved during preclinical studies (Rottmann et al, 2010) and the extremely fast selection of resistant parasites by cyclopropyl carboxamides stopped their further development as antimalarial drug candidates (Sanz et al, 2011; Ding et al, 2012). All these examples highlight the importance of assessing the risk of *de novo* resistance development as early as possible during drug development (Sanz et al, 2011; Ding et al, 2012).

Recently, MMV proposed a framework to evaluate the risk of resistance development of new antimalarial compounds (Ding et al, 2012). This strategy covers several aspects of drug resistance, such as potential cross-resistance with clinical antimalarials, the risk of *de novo* resistance development or the elucidation of molecular mechanisms underlying resistance. As discussed before, benzylMD **1c**'s activity was not impaired by one of the pre-existing resistances to single or multiple antimalarials in the tested parasite strains, for instance resistance to chloroquine, quinine, mefloquine or monodesethylamodiaquine (see also section 4.1.1).

Drug-pressure experiments conducted with lethal benzylMD **1c** concentrations failed to select for resistant parasites, indicating a very low intrinsic potential of the drug to induce *de novo* resistance (Results, section 3.2.3.1). The lack of intrinsic mutagenic potential observed in genotoxicity studies supports this conclusion (Müller et al, 2011). Other studies using the same experimental setup, reported a high frequency of spontaneous resistance to 5-fluoroorotate, atovaquone and a lead cyclopropyl carboxamide (GSK2645947) (Rathod et al, 1997; Sanz et al, 2011). Moreover, this protocol was successfully used to select for chloroquine resistant parasites and to reveal the responsible mutation in the *pfcrt* gene (Cooper et al, 2002).

Molecules with multiple drug targets or a pleiotropic mode of action are considered to be less prone to select for resistance (Ding et al, 2012 and others). This is expected to account for redox-active drugs, such as benzylMD **1c**, that interfere with a highly complex and tightly regulated redox network in the host-parasite unit (Nepveu & Turrini, 2013). So far, there are almost no reports about resistance to methylene blue, the only redox-active antimalarial currently in clinical use (Schirmer et al, 2003).

Within this work, the selection of drug-adapted or resistant parasites was further encountered by exposing a high parasite inoculum to sublethal benzylMD **1c** concentrations (in the range of IC_{90} values), as this is regarded to favor the selection of resistant parasites (White & Pongtavornpinyo, 2003; Walliker et al, 2005). Indeed, the ARMD strain Dd2 was able to adapt to constant drug exposure but only to a very limited extent (section 3.2.3.2). Using a selection strategy with stepwise increasing drug concentrations, parasites succeeded to multiply in the presence of 550 nM benzylMD **1c** but failed to recover from higher drug concentrations (800 nM). Drug-adapted parasites presented a 4-5 fold decrease in susceptibility to benzylMD **1c** compared to progenitor

Dd2 parasites, as reflected in their IC_{50} values. However, this phenotype was not stable over time and parasite susceptibility reversed to original levels 4-6 weeks after drug removal. In addition, a prolonged culturing of drug-adapted parasites under continuous drug pressure was not possible, parasites suffered visibly and died rapidly. These observations are similarly reflected in the loss of drug adaptation during cloning or cryopreservation. Unstable drug-resistant phenotypes arising from *in vitro* drug selections were observed frequently (discussed in Nzila & Mwai, 2010), even in cases of prolonged drug pressure for as long as 16 months, as reported in a study on lumefantrine (Mwai et al, 2012). The transient nature of drug resistance might be explained by reduced parasite fitness, such that upon drug removal, resistant mutants are outnumbered by sensitive ones (Walliker et al, 2005; Nzila & Mwai, 2010). Alternatively, one might assume that adaptation to benzylMD **1c** pressure may not originate from a stable genetic mutation but from metabolic adaptations, such as changes in enzymatic activities (i.e. NADPH-dependent flavoenzymes), protein expression levels (Prieto et al, 2008), protein *S*-glutathionylation (Kehr et al, 2011) or epigenetic regulation (Merrick & Duraisingh, 2010). Very recently, epigenetic histone modifications were reported for the first time as being responsible for the development of drug resistance (Sharma et al, 2013).

In line with Ding et al. (2012), it can be concluded that the lack of pre-existing resistance and the inability to select for stable *de novo* resistance indicates that benzylMD **1c**'s effectiveness may not be easily compromised by resistance development in the field. Nevertheless, from a basic research perspective, it would be interesting to further explore the mechanisms underlying the observed parasite adaptation to benzylMD **1c** drug pressure. Regarding the increasing frequency of reports about treatment failures with artemisinin, it would be of particular interest to explore a possible cross-resistance with artemisinin-resistant field isolates. Artemisinin tolerance is partly related to the transient dormancy of drug-treated ring stages, which is discussed in more detail in the next section.

Parasite dormancy as a mode of drug resistance

Previous *in vitro* studies reported about a mechanism of artemisinin tolerance, by which parasites resisted drug pressure and continued their development after drug removal (Witkowski et al, 2010; Teuscher et al, 2012). This phenomenon, which is referred to as dormancy, was attributed to temporary cell cycle arrest within ring-stage parasites under drug pressure (Witkowski et al, 2010). Novel phenotypic assays characterizing

120

P. falciparum field isolates and mathematical simulations provided further understanding of this resistance mechanism (Klonis et al, 2013; Witkowski et al, 2013a; Witkowski et al, 2013b). Culture-adapted *P. falciparum* field isolates from regions of artemisinin resistance were characterized by an altered drug susceptibility of young ring-stage parasites, as assessed with a recently established ring-stage survival assay (RSA) (Witkowski et al, 2013b). In addition, artemisinin resistance was correlated with a high proportion of dormant ring stages that successfully resumed growth after drug removal (Witkowski et al, 2013b). The RSA assay was successfully implemented to identify artemisinin-resistant clinical parasite isolates (i.e. slow clearing parasites) in *ex vivo* conditions (Witkowski et al, 2013a).

It might be speculated that other antimalarials, for instance lead compound **1c**, might also induce dormant parasites. Accordingly, the possible reappearance of benzylMD **1c**-treated parasites was monitored in cultures from drug pressure experiments after drug removal (sections 3.2.3.1 and 3.2.3.2). Occurrence of growing parasites was observed 3 weeks after stopping treatment in only 2 out of 20 flasks in total. Similar to artemisinin-tolerant parasites, these parasites showed no altered susceptibility to benzylMD **1c** compared to progenitor parasites. However, this observation does not provide sufficient evidence to conclude whether the parasites tolerated benzylMD **1c** by entering a dormancy state, as described for artemisinin. This assumption should be further pursued using adequate *in vitro* protocols, which have been developed in the meantime. Witkowski and colleagues established a panel of *in vitro* assays for the identification of artemisinin-tolerant parasite strains (Witkowski et al, 2013b). In contrast to classical *in vitro* drug susceptibility assays, which are performed over 48 to 72 hours of drug incubation, novel *in vitro* assays are based on a short-time exposure of ring or mature parasite stages to pulses of high artemisinin concentrations. Culture-adapted artemisinin-resistant *P. falciparum* field isolates and the simple RSA assay provide an excellent tool for the identification of possible cross-resistance between artemisinin and novel drug candidates. It would be of particular importance to test compounds that share the same stage specificity with artemisinin (i.e. the ring stage), such as benzylMD **1c** and methylene blue. In addition to the RSA assay, the authors proposed a standardized setup for detecting drug-induced cell cycle arrest, which relies on morphological identification of persistent ring stages and their unresponsiveness to sorbitol-induced lysis (so-called ring stage growth arrest assay, RGA, Witkowski et al, 2013b). Alternatively, the presence of dormant ring-stage parasites in

drug-treated cultures can be shown by flow cytometry analysis using DAPI (staining of DNA) and rhodamine 123 (mitochondria) staining (Witkowski et al, 2010). The RGA assay would be particularly suitable to screen other drugs, such as benzylMD **1c**, for their potential to induce dormancy and could be easily adapted for large panels of drugs (medium throughput) by the use of flow cytometry analysis, thus eliminating the need of time consuming microscopical read-out.

4.1.5 Antimalarial combination partners for lead benzylMD 1c

Our investigations on the *in vitro* drug interactions between benzylMD **1c** and clinical antimalarials revealed synergistic interactions with quinine and artemisinin and a pronounced synergy with dihydroartemisinin, the active metabolite of artemisinin (section 3.2.4). The nature of drug interactions between benzylMD **1c** and dihydroartemisinin was independent of the drug-resistance pattern of the tested *P. falciparum* strain. Companions for drug combinations should preferably interact synergistically to allow for smaller doses and prevent potentially toxic side effects, but also a combination based on indifferently interacting partners could be favored (Bell, 2005; Burrows et al, 2013). BenzylMD **1c** interacted indifferently with amodiaquine, chloroquine, atovaquone, cycloguanil and methylene blue. Owing to its fast speed of action, lead **1c** could most likely be combined to a compound with long serum half-life, such as combination partners of artemisinin (e.g. amodiaquine, mefloquine, atovaquone or cycloguanil).

A potential partner drug cannot be chosen without complete knowledge of the *in vivo* pharmacokinetic and pharmacodynamic behavior of all candidates (White & Olliaro, 1996; Bell, 2005; Jia et al, 2009). Thus, potential drug combinations should be further tested using *in vivo* models to confirm the nature of their interaction and to explore possible pharmacological interactions, as well as additional toxicity (White & Olliaro, 1996; Bell, 2005). Until now, the pharmacokinetic and pharmacological properties of benzylMD **1c** have been little explored, but the synergistic interactions with existing antimalarials and the lack of cross-resistance to clinically used antimalarials increase the chance of finding a suitable drug partner in the portfolio of existing drugs.

4.3 Unraveling benzylMD 1c's mechanism of action

Compounds of the benzylMD series are postulated to act as pro-oxidative redox-cyclers that degrade hemoglobin species, consume intracellular NADPH and ultimately perturb the sensitive redox homeostasis of the parasite-host unit (Müller et al, 2011; Bielitza et al, submitted, 2014.). Results of previous electrochemical, biochemical and physicochemical studies have provided important insights into the functions of predicted benzylMD **1c**-derived metabolites (Müller et al, 2011; Johann et al, 2012; Bielitza et al, submitted, 2014.). Moreover, recent studies in *P. falciparum*-infected erythrocytes have evidenced the denaturation of hemoglobin species and the perturbation of the GSH-redox equilibrium and therefore provided further support for the postulated mechanism of action (see Introduction, section 1.4.1) (Bielitza et al, submitted, 2014.).

4.3.1 Identifying key factors behind benzylMD 1c's redox-cycling

As described in detail in the introduction, antimalarial benzylMDs are proposed to act as redox-cyclers. However, direct proof that this redox cycling occurs *in situ* in a parasite, as well as evidence of the proposed metabolites, is technically highly complicated and remained so far without success. To overcome this limitation, *in vitro* drug interaction studies were chosen as a tool to explore key features of benzylMD **1c's** mode of action in a whole cell assay. Drug-drug interactions are commonly explored in the framework of mechanistic studies on antimicrobial drugs (Bell, 2005; Jia et al, 2009). Synergistic or antagonistic interactions provide information about molecular drug targets, the relationships between different drug targets and / or the cellular consequences of drug action. Thus, they might also, but rarely, originate from actual physical or chemical contact between combined molecules. In agreement with Bell (2005), it is important to emphasize that a mechanistic interpretation of drug interaction data might provide only limited proof of any given hypothesis.

At this point, it is important to mention that the identification of benzylMD **1c**-derived metabolites in treated infected erythrocytes was attempted during this doctoral thesis by using a high resolution mass spectrometry approach. Even after cells were treated with high concentrations of benzylMD **1c**, only considerably low drug signals (from either benzylMD **1c** or derived metabolites) were detected. This result might indicate that

benzylMD **1c** or its metabolites are only present in very low amounts (in unbound forms) but could also be explained by technical reasons. Preliminary studies indicated a high affinity of benzylMD **1c** and metabolites to human serum proteins. In the near future, the search for benzylMD **1c**-derived metabolites will be further realized with a fully C^{13}-enriched **1c** molecule and the use of optimized extraction procedures.

Is glutathione reductase the only electron donor for benzylMD bioactivation?

A continuous GR-catalyzed reduction of benzylMD-derived metabolites was proposed to be an essential pre-requisite for further redox-cycling and thus for the antimalarial activity of benzylMDs. This hypothesis was initially supported by the loss of the antimalarial activity of benzylMD analogues that act as suicide substrates of both GRs of the infected erythrocyte (hGR and *Pf*GR), namely benzylMD **7a** and benzoylMD **8a** (Müller et al, 2011). Moreover, benzylMD **1c** and its predicted metabolites were characterized as substrates of hGR and *Pf*GR. While benzylMD **1c** itself has been shown to be a poor GR substrate (Müller et al, 2011), metabolite benzoylMD **2c** possesses a markedly altered redox property and therefore significantly enhanced efficiency to act as a substrate of both GRs (i.e. hGR and *Pf*GR). The redox-cycler could therefore act synergistically in different compartments of the parasite-host unit (Müller et al, 2011; Blank et al, 2012; Bielitza et al, submitted, 2014.). As emphasized before, in all biochemical studies carried out with benzylMD **1c** and predicted metabolites, the metabolite benzoylMD **2c** was shown to be the key player in NADPH-dependent GR-mediated redox-cycling and drug-induced hemoglobin catabolism. Similar to benzylMDs, the redox-cycler methylene blue has been described as an inhibitor and / or subversive substrate of human and parasitic GR (Färber et al, 1998; Buchholz et al, 2008b).

The question whether the GR is the crucial electron donor for methylene blue and benzylMD **1c** *in vivo* was discussed in our recent publication (Ehrhardt et al, 2013).

"*Is GR the electron donor for methylene blue and benzylMD* **1c** *in vivo? A key study by Pastrana-Mena et al. revealed that the absence of P. berghei GR has no significant effect on the sensitivity of the rodent malaria parasite to methylene blue (2010). Even though these findings point to an alternative electron donor for this drug, it is important to note that there seems to be substantial differences between the glutathione metabolisms of human and rodent malaria parasites. For example, a recent study by Patzewitz et al.*"

*suggests that glutathione biosynthesis is essential for the asexual blood stages of P. falciparum in contrast to P. berghei (2012). To date, there is no P. falciparum GR knock-out strain. Thus, we could not analyze the IC$_{50}$ values for methylene blue and benzylMD **1c** in such a genetic background. [...]"* (Ehrhardt et al, 2013)

In the absence of a *P. falciparum* GR knock-out strain, *in vitro* drug interaction studies with GR suicide substrates were regarded as a valuable tool for providing further evidence of the aforementioned hypothesis (section 3.3.3.1). The rather weak antagonistic interaction observed between benzylMD **1c** and benzylMD **7a** suggests that another NADPH-dependent oxidoreductase could partially bioactivate benzylMD **1c** upon irreversible GR inactivation. However, it might also be possible that the intracellular GR activity (hGR and / or *Pf*GR) is not fully inhibited upon treatment with benzylMD **7a** and the remaining enzyme activity would still contribute to drug bioactivation. Such a scenario could explain the observation of only a weak antagonistic interaction. Therefore, this result does not fully exclude the possibility that GR acts as an electron donor *in situ,* but raises doubts about its being the sole electron donor responsible for accomplishing continuous redox-cycling of benzylMD-derived metabolites. As already mentioned, a *Plasmodium* GR knock-out strain would be the ideal tool to address this question. Therefore, Alice-Anne Goetz, a PhD student under Dr. Stephanie Blandin's [12] supervision, is currently assessing the activity of benzylMD **1c** against the *P. berghei* GR knock-out strain under *ex vivo* conditions.

In the case of methylene blue, alternative disulfide reductases were identified as putative drug targets, such as *P. falciparum* thioredoxin reductase (TrxR) or parasitic and human mitochondrial dihydrolipoamide dehydrogenase (LipDH) (Buchholz et al, 2008b). Furthermore, methylene blue's trypanocidal activity might be explained by a similar mechanism, meaning by acting as subversive substrate of disulfide reductase orthologues from *Trypanosoma cruzi* (trypanothione reductase, TR and LipDH) (Buchholz et al, 2008a). *P. falciparum* thioredoxin reductase and *T. cruzi* trypanothione reductase are important components of the parasitic antioxidant systems (Müller et al, 2003; Jortzik & Becker, 2012).

---

[12] Dr. Stephanie Blandin and Ms. Alice-Anne Goetz, Institut de Biologie Moléculaire et Cellulaire, Université de Strasbourg, France

Furthermore, based on their redox state, benzylMD **1c** and methylene blue could also act as electron donors (after being reduced) and acceptors at various sites in the mETC, as we previously discussed (Ehrhardt et al, 2013).

"*If methylene blue or benzylMD **1c** target the mETC as a subversive substrate, the mETC could act as their electron donor/acceptor regardless of the presence or absence of cytosolic yDHODH. For instance, both inhibitors might be suited to accept electrons from the endogenous type 2 DHODH or from complex III. The reduced redox-cycler could subsequently catalyze the formation of reactive oxygen species - and / or of Fe^{2+} species as suggested earlier (Müller et al, 2011) - without depletion of the pyrimidine pool. Reduced menadione species with antitrypanosomal activities were, for example, shown to generate superoxide anions and to reduce cytochrome c (Fe^{3+}) in vitro (Blumenstiel et al, 1999; Salmon-Chemin et al, 2001). Future work is needed to address whether methylene blue or benzylMD **1c** are subversive substrates of the mETC of malaria parasites.*" (Ehrhardt et al, 2013)

In conclusion, although this study did not exclude the possibility of GR acting as an electron donor, it provided a basis to speculate about alternative drug activation pathways. Several oxidoreductases would be valuable candidates, for instance *P. falciparum* thioredoxin reductase or other flavorenzymes like DOX reductase or lipoamide dehydrogenase. Future work is needed to elucidate the activation of benzylMD-metabolites for intracellular redox cycling.

The role of NADPH in benzylMD 1c's activity

NADPH is an important reducing agent of intracellular antioxidant defense and is the essential electron donor for GR and other oxidoreductases. BenzylMD-derived metabolites have been proposed to be continuously regenerated in a NADPH-dependent reaction. Consequently, one might speculate that benzylMD **1c** activity is depending on available NADPH, which would be consumed by prolonged drug action. This would substantially contribute to the perturbation of the redox homeostasis upon drug treatment. *In vitro* interaction studies with compounds that presumably affect intracellular NADPH flux have not revealed a clear perspective (Results, section 3.3.3.2). Interestingly, the antiparasitic activity of benzylMD **1c** increased in the presence of nicotinamide, an effect that was counteracted by the antimetabolite 6-aminonicotinamide.

Augmentation of NAD^+ levels by nicotinamide supply and the resulting fortification of benzylMD **1c** activity might be indicative of increased drug bioactivation in NADPH dependent reactions. Moreover, in a recent study nicotinamide was shown to inhibit the histone deacetylase activity of the *P. falciparum* Sir2 protein (stands for *silent information regulator 2*), which was recently identified as essential for epigenetic regulation of virulence genes (Prusty et al, 2008). In support of the observed synergy with nicotinamide, a strong antagonistic effect was observed in combination with the *h*G6PD inhibitor CB83 that targets the NADPH regeneration in erythrocyte. In addition, the latter result suggests that the host-cell cytosol is involved in benzylMD bioactivation and / or benzylMD action. In contrast, combining benzylMD **1c** with the *Pf*GluPho inhibitor ML276 resulted in a clear indifferent interaction.

As emphasized before, it can be difficult to verify conclusions drawn from *in vitro* interaction studies. This is particularly important for compounds that target single components of complex intracellular networks. In the cases of NADPH or GSH balance, the regulatory mechanism and the complex interactions between host cell and parasite are not fully understood. Nevertheless, it might be interesting to point out that parasite's NAD^+ and glucose-6-phosphate metabolisms are of interest for the development of new antimalarial drugs (Preuss et al, 2012b; O'Hara et al, 2014). With this in mind, both synergistic and indifferent interactions between benzylMD **1c** and compounds targeting these pathways could be further exploited as potential drug combinations.

Iron complexation is crucially involved in benzylMD 1c's activity

BenzylMD **1c**-derived metabolites are thought to act as metal chelators, which could play a critical role in global drug activity (Müller et al, 2011). The chelation of ferric iron (Fe^{3+}) might catalyze key bioactivation steps or assist in drug transport within different compartments of the infected erythrocyte (siderophore-like transport). Recent biochemical studies identified the reduced benzoylMD **3c** metabolite as effective Fe^{3+} chelator, while benzoylMD **2c** only ineffectively bound to Fe^{3+} species (Bielitza et al, submitted, 2014.). These results prompted further investigations to explore the importance of iron complexation for benzylMD **1c**'s antiparasitic activity. Therefore, benzylMD **1c** was tested in combination with the iron chelator DFO (section 3.3.3.3).

The role of iron complexation for benzylMD **1c's** global activity was discussed in detail in an article that was recently submitted (Bielitza et al, submitted, 2014.).

"*Regarding iron complexation, we propose that the metal binding properties of reduced benzylMD-derived metabolites, as benzoylMD **3c**, play a critical role in the global activity of the lead benzylMD **1c**. This was evidenced by the antagonistic interaction between benzylMD **1c** and a powerful Fe^{3+} chelator from Streptomyces, DFO. Interestingly, the observed antagonist effect mediated by DFO on the antimalarial activity of the lead benzylMD **1c** is the highest among all compound combinations to benzylMD **1c** tested. As suggested in our previous study (Müller et al, 2011), the benzoylMD **3c** was proposed to cycle in and out of the acidic vesicles, upon iron complexation / release and drug oxido-reduction by GR. It is noteworthy to mention the strong antagonistic effect exerted by DFO with semisynthetic and synthetic endoperoxide antimalarial drugs (Stocks et al, 2007). The study suggested a common non-heme chelatable iron-dependent activation mechanism for endoperoxide drugs via Fe^{3+}-Fe^{2+} redox cycling. Taking into account the central role of DFO as an iron chelator in fungi, we expected that DFO might inhibit the transport of drug metabolites:iron complexes in and out the parasite compartments, similarly to microbial siderophores upon iron complexation..*" (Bielitza et al, submitted, 2014.)

In addition, DFO exerts antioxidative effects by scavenging free iron sources and consequently preventing Fenton reactions (Reeder et al, 2008). These reactions can be considered to counteract the oxidative stress induced by benzylMD **1c**. Most importantly, DFO was reported to reduce ferrylhemoglobin to methemoglobin and thereby prevents the denaturation of hemoglobin, in forms of a cross-linking of the protein structure and formation of hemichromes (Reeder et al, 2008). Interestingly, this reaction was observed at physiological conditions of pH 7.4 and moreover at acidic conditions of pH 5, as found in acidic vesicles and the digestive vacuole of the parasite. In line with Reeder et al, the reactions employed by DFO (i.e reduction of ferrylhemoglobin to methemoglobin and prevention of Fenton reactions) can be expected to counteract the over-oxidation and denaturation of hemoglobin species induced by continuous redox-cycling of benzylMD **1c**-derived metabolites. This hypothesis is currently investigated in the prolonged methemoglobin reduction assay (UV-Vis spectrophotometric assay), which was formerly used to evidence the formation of ferrylhemoglobin and precipitation of hemichrome by metabolite benzoylMD **2c** in the presence of the NADPH-based GR system and

methemoglobin (as described before, Introduction, section 1.4.1). In conclusion, the strong *in vitro* antagonism between DFO and benzylMD **1c** provides valuable support for the postulated mode of action. Based on the evidence of hemichrome formation in biochemical assays and furthermore in *P. falciparum*-infected benzylMD **1c**-treated erythrocytes, this result strongly indicates that the oxidation and denaturation of hemoglobin species, together with increase of ROS-formation upon drug treatment, accounts, at least in parts, for the intracellular mechanism of action of benzylMD **1c**.

Redox homeostasis of the parasite reflected in levels of reduced GSH

BenzylMD **1c** are proposed to lead to the disruption of intracellular redox homeostasis. The redox homeostasis in infected erythrocytes largely depends on the glutathione systems of both, host and parasite, with reduced GSH as a major component of those systems.

In vitro interaction studies with compounds affecting either GSH *de novo* synthesis (BSO or acetylcysteine) or levels of reduced GSH (acetaminophen, amodiaquine) have been inconclusive (section 3.3.3.5). In contrast, both the GSH-depleting agent acetaminophen and GSH precursor acetylcysteine behaved antagonistically in combination with benzylMD **1c**.

More convincing insight into benzylMD **1c**'s effect on the glutathione-dependent redox potential of living *P. falciparum* blood-stage parasites was recently acquired when the genetically encoded real-time redox sensitive GFP biosensor hGrx1-roGFP2 was used (developed by Kasozi et al, 2013). Microscopical analysis of the cytosolic expression of hGrx1-roGFP2 in trophozoites detected a change of the GSH:GSSG equilibrium towards GSSG, indicative of a shift towards a more oxidizing redox potential in the cytosol (Bielitza et al, submitted, 2014.). This finding is a first evidence for the perturbation of intracellular redox homeostasis upon treatment with benzylMD **1c** and provides important support for the proposed mechanism of action. Further studies aimed at investigating the perturbation of the redox homeostasis in other parasite's compartments are currently ongoing. Given the demonstrated binding of hemichromes to the membrane of infected erythrocytes upon treatment with benzylMD **1c**, it would be of particular interest to investigate the perturbation of the redox homeostasis in the cytosol of the host cell. This could be realized using a roGFP2-tagged protein that will be exported into the erythrocyte cytosol.

4.3.2 Lead 1c is not an inhibitor of the mitochondrial electron transport chain

One antimalarial drug apparently related to benzylMD **1c** is atovaquone, that shares the common 1,4-naphthoquinone core. In this work, it was shown that lead benzylMD **1c** is not an inhibitor of the mETC, in contrast to atovaquone, by using a transgenic *P. falciparum* strain (section 3.3.1) (Ehrhardt et al, 2013). This strain expresses a cytosolic bypass of the mETC, in form of the yDHODH, which confers resistance to atovaquone and other inhibitors of the mETC (Ke et al, 2011).

Apart from structural differences, further biochemical or physicochemical compound properties seem to be important to explain the different modes of action of these two 1,4-naphthoquinones: first the enzymatic substrate capacities and secondly the redox potential. Both aspects were discussed in detail in our previous publication (Ehrhardt et al, 2013). *"When we recently studied the ability of human and P. falciparum GR to reduce either atovaquone or 2-hydroxy-1,4-naphthoquinone at substrate concentrations of up to 25 μM or 100 μM, respectively, no NADPH consumption was observed (Davioud-Charvet & Lanfranchi, 2011; Lanfranchi et al, 2012a). By contrast, methylene blue and predicted benzylMD metabolites were shown to be effective substrates with catalytic efficiencies - i.e., the k_{cat}/K_m values - as high as 13.7 mM^{-1}s^{-1} for the blue dye and 12.5 mM^{-1}s^{-1} for the predicted 3-[4-(substituted)benzoyl]-menadione metabolites (Morin et al, 2008; Müller et al, 2011; Blank et al, 2012). [...] Another important property seems to be the redox potential. The low redox potential of atovaquone (-0.51 V) indicates that, under physiological conditions, atovaquone reduction is considerably less favored compared to menadione reduction (-0.14 V) (Lopez-Shirley et al, 1994). Even under highly reducing intracellular conditions with an estimated half-cell redox potential for NADPH around -0.34 V (Deponte, 2013), the redox potential for atovaquone will be too low for efficient reduction by two-electron reduced GRs, which have redox potentials around -0.24 V at pH 7 (Veine et al, 1998). In contrast, the two-electron reduction potentials for methylene blue and menadione at pH 7 are +0.01 V (Impert et al, 2003) and -0.23 V (Patriarche & Lingane, 1970), respectively, and cyclic voltammetry measurements show that one-electron and two-electron-transfer reactions are kinetically reversible (Morin et al, 2008). These properties allow a continuous reduction and oxidation under physiological conditions, which is a prerequisite for a subversive substrate-driven redox cycle."* (Ehrhardt et al, 2013)

5 CONCLUSIONS AND OUTLOOK

The presented work on the *in vitro* activity of lead compound **1c** represents a part of the lead evaluation stage of the benzylMD drug-development process. Overall, the presented findings demonstrate the promising *in vitro* potency of lead benzylMD **1c** and furthermore emphasize its very attractive *in vitro* antimalarial activity profile. This work highly supports the further development of the benzylMD series as antimalarial drug candidates.

In accordance with TCPs postulated by MMV (Burrows et al, 2013), benzylMD **1c** would be a suitable drug candidate for first-line treatment mainly owing to its fast speed of action. Preliminary studies in the mouse model indicated that lead benzylMD might have a poor bioavailability or be rapidly eliminated from the bloodstream (Müller et al, 2011). Consequently, detailed pharmacological and pharmacokinetic studies are essential to determine the oral bioavailability and plasma half-life of lead compound **1c** in order to assure that those fulfill the according requirements. At the same time, it would be of interest to assess the pharmacokinetic properties of benzylMD derivatives with similar *in vitro* antiparasitic potency. A short plasma half-life of benzylMD compounds would exclude their use as a combination partner for fast-acting compounds (TCP 2), their use as chemoprotection (TCP 4) and possibly also for blocking parasite transmission to the mosquito vector (Burrows et al, 2013).

So far, the benzylMD drug design project focused mainly on the intraerythrocytic stages of *P. falciparum.* This is partly based on the relative accessibility and ease of using of blood-stage cultures for standardized *in vitro* studies. Now, it would be timely to test selected benzylMD derivatives against other *P. falciparum* stages from the vertebrate host or mosquito vector. Alice-Anne Goetz, a PhD student under Dr. Stephanie Blandin's supervision, is currently performing a detailed characterization of lead benzylMD **1c**'s

activity in the *Anopheles* vector and the *P. berghei* mouse model. Prof. Katja Becker [13] could preliminarily show that lead benzylMD **1c** inhibits the development of *P. falciparum* gametocytes, which should be confirmed soon. Conversely, lead compound **1c** and a panel of eight derivatives were recently shown to have no impact on the motility of *P. berghei* sporozoites, as investigated in the laboratory of Prof. Freddy Frischknecht [14]. Another interesting aspect would be to test the activity of benzylMDs against *P. vivax* and *P. ovale* blood stages and dormant liver stages (hypnozoites), though respective *in vitro* cultures are not easy to establish (Burrows et al, 2013; Dembele et al, 2014).

To provide further support of benzylMDs as drug candidates, it is of clear importance to test the activity of selected derivatives in *P. berghei*-infected mice and moreover in the humanized *P. falciparum* mouse model. A previous study using *P. berghei*-infected mice demonstrated a moderate antiparasitic activity of lead compound **1c** and four analogues following intraperitoneal or oral administration (Müller et al, 2011). This observation might be explained by poor pharmacokinetic properties of benzylMDs, as mentioned before, but could also stem from a low antiparasitic drug activity against *P. berghei* parasites. The latter possibility will be addressed by Alice-Anne Goetz by assessing the activity of benzylMD **1c** against *P. berghei* blood-stage development *ex vivo*.

The second part of this work was dedicated to exploring the mechanism of action of lead benzylMD **1c**. Most importantly, the possibility that benzylMD **1c** inhibits the mETC, as suggested based on its structural similarities to atovaquone, can be clearly excluded (Ehrhardt et al, 2013). One important shortcoming of our work on the mode of action of benzylMDs is the lack of direct evidence that the proposed redox-cycling occurs *in situ* in the parasite or likewise any evidence that the proposed metabolites are formed intracellularly. The *in vitro* drug interaction studies conducted in this work provided interesting insights into different aspects of benzylMD **1c**'s redox-cycling and antimalarial activity. In spite of this work, future attempts are necessary to provide a proof of concept for the proposed intracellular benzylMD **1c** redox-cycling.

Hopefully, the findings of this work could not only highlight the potential of benzylMDs as antimalarial drug candidates, but moreover emphasize the innovative approach of targeting *P. falciparum* parasites with redox-cycling agents.

---

[13] Prof. Katja Becker, Interdisciplinary Research Centre (IFZ), Justus Liebig University, Giessen, Germany.

[14] Prof. Freddy Frischknecht, Department of Parasitology, University Hospital Heidelberg, Germany

References

Akoachere M, Buchholz K, Fischer E, Burhenne J, Haefeli WE, Schirmer RH, Becker K (2005) *In vitro* assessment of methylene blue on chloroquine-sensitive and -resistant Plasmodium falciparum strains reveals synergistic action with artemisinins. *Antimicrob Agents Chemother* **49:** 4592-4597

Alonso PL, Brown G, Arevalo-Herrera M, Binka F, Chitnis C, Collins F, Doumbo OK, Greenwood B, Hall BF, Levine MM, Mendis K, Newman RD, Plowe CV, Rodriguez MH, Sinden R, Slutsker L, Tanner M (2011) A research agenda to underpin malaria eradication. *PLoS Med* **8:** e1000406

Anthony MP, Burrows JN, Duparc S, Moehrle JJ, Wells TN (2012) The global pipeline of new medicines for the control and elimination of malaria. *Malar J* **11:** 316

Arama C, Troye-Blomberg M (2014) The path of malaria vaccine development: challenges and perspectives. *J Intern Med* **275:** 456-466

Atamna H, Ginsburg H (1995) Heme degradation in the presence of glutathione. A proposed mechanism to account for the high levels of non-heme iron found in the membranes of hemoglobinopathic red blood cells. *J Biol Chem* **270:** 24876-24883

Atamna H, Krugliak M, Shalmiev G, Deharo E, Pescarmona G, Ginsburg H (1996) Mode of antimalarial effect of methylene blue and some of its analogues on *Plasmodium falciparum* in culture and their inhibition of *P. vinckei petteri* and *P. yoelii nigeriensis in vivo*. *Biochem Pharmacol* **51:** 693-700

Ayi K, Turrini F, Piga A, Arese P (2004) Enhanced phagocytosis of ring-parasitized mutant erythrocytes: a common mechanism that may explain protection against *falciparum* malaria in sickle trait and beta-thalassemia trait. *Blood* **104:** 3364-3371

Baker DA (2010) Malaria gametocytogenesis. *Mol Biochem Parasitol* **172:** 57-65

Baniecki ML, Wirth DF, Clardy J (2007) High-throughput *Plasmodium falciparum* growth assay for malaria drug discovery. *Antimicrob Agents Chemother* **51:** 716-723

Bauer H, Fritz-Wolf K, Winzer A, Kuhner S, Little S, Yardley V, Vezin H, Palfey B, Schirmer RH, Davioud-Charvet E (2006) A fluoro analogue of the menadione derivative 6-[2'-(3'-methyl)-1',4'-naphthoquinolyl]hexanoic acid is a suicide substrate of glutathione reductase. Crystal structure of the alkylated human enzyme. *J Am Chem Soc* **128:** 10784-10794

Becker K, Rahlfs S, Nickel C, Schirmer RH (2003) Glutathione-functions and metabolism in the malarial parasite *Plasmodium falciparum. Biol Chem* **384:** 551-566

Becker K, Tilley L, Vennerstrom JL, Roberts D, Rogerson S, Ginsburg H (2004) Oxidative stress in malaria parasite-infected erythrocytes: host-parasite interactions. *Int J Parasitol* **34:** 163-189

Becuwe P, Gratepanche S, Fourmaux MN, Van Beeumen J, Samyn B, Mercereau-Puijalon O, Touzel JP, Slomianny C, Camus D, Dive D (1996) Characterization of iron-dependent endogenous superoxide dismutase of *Plasmodium falciparum. Mol Biochem Parasitol* **76:** 125-134

Beez D, Sanchez CP, Stein WD, Lanzer M (2011) Genetic predisposition favors the acquisition of stable artemisinin resistance in malaria parasites. *Antimicrob Agents Chemother* **55:** 50-55

Bell A (2005) Antimalarial drug synergism and antagonism: mechanistic and clinical significance. *FEMS Microbiol Lett* **253:** 171-184

Belorgey D, Lanfranchi DA, Davioud-Charvet E (2013) 1,4-naphthoquinones and other NADPH-dependent glutathione reductase-catalyzed redox cyclers as antimalarial agents. *Curr Pharm Des* **19:** 2512-2528

Biagini GA, Fisher N, Shone AE, Mubaraki MA, Srivastava A, Hill A, Antoine T, Warman AJ, Davies J, Pidathala C, Amewu RK, Leung SC, Sharma R, Gibbons P, Hong DW, Pacorel B, Lawrenson AS, Charoensutthivarakul S, Taylor L, Berger O, Mbekeani A, Stocks PA, Nixon GL, Chadwick J, Hemingway J, Delves MJ, Sinden RE, Zeeman AM, Kocken CH, Berry NG, O'Neill PM, Ward SA (2012) Generation of quinolone antimalarials targeting the *Plasmodium falciparum* mitochondrial respiratory chain for the treatment and prophylaxis of malaria. *Proc Natl Acad Sci U S A* **109:** 8298-8303

Bielitza M, Belorgey D, Ehrhardt K, Johann L, Lanfranchi DAI, Gallo V, Schwarzer E, Mohring F, Jortzik E, Williams DL, Becker K, Arese P, Elhabiri M, Davioud-Charvet E (submitted, 2014.) Antimalarial NADPH-consuming redox-cyclers as superior G6PD deficiency copycats. *Manuscript submitted*

Biot C, Bauer H, Schirmer RH, Davioud-Charvet E (2004) 5-substituted tetrazoles as bioisosteres of carboxylic acids. Bioisosterism and mechanistic studies on glutathione reductase inhibitors as antimalarials. *J Med Chem* **47:** 5972-5983

Blank O, Davioud-Charvet E, Elhabiri M (2012) Interactions of the antimalarial drug methylene blue with methemoglobin and heme targets in *Plasmodium falciparum*: a physico-biochemical study. *Antioxidants & redox signaling* **17:** 544-554

Blumenstiel K, Schoneck R, Yardley V, Croft SL, Krauth-Siegel RL (1999) Nitrofuran drugs as common subversive substrates of *Trypanosoma cruzi* lipoamide dehydrogenase and trypanothione reductase. *Biochem Pharmacol* **58:** 1791-1799

Boddey JA, Cowman AF (2013) *Plasmodium* nesting: remaking the erythrocyte from the inside out. *Annu Rev Microbiol* **67:** 243-269

Bogreau H, Renaud F, Bouchiba H, Durand P, Assi SB, Henry MC, Garnotel E, Pradines B, Fusai T, Wade B, Adehossi E, Parola P, Kamil MA, Puijalon O, Rogier C (2006) Genetic diversity and structure of African *Plasmodium falciparum* populations in urban and rural areas. *Am J Trop Med Hyg* **74:** 953-959

Booker ML, Bastos CM, Kramer ML, Barker RH, Jr., Skerlj R, Sidhu AB, Deng X, Celatka C, Cortese JF, Guerrero Bravo JE, Crespo Llado KN, Serrano AE, Angulo-Barturen I, Jimenez-Diaz MB, Viera S, Garuti H, Wittlin S, Papastogiannidis P, Lin JW, Janse CJ, Khan SM, Duraisingh M, Coleman B, Goldsmith EJ, Phillips MA, Munoz B, Wirth DF, Klinger JD, Wiegand R, Sybertz E (2010) Novel inhibitors of *Plasmodium falciparum* dihydroorotate dehydrogenase with anti-malarial activity in the mouse model. *J Biol Chem* **285:** 33054-33064

Botte CY, Dubar F, McFadden GI, Marechal E, Biot C (2012) *Plasmodium falciparum* apicoplast drugs: targets or off-targets? *Chem Rev* **112:** 1269-1283

Bouillon A, Gorgette O, Mercereau-Puijalon O, Barale JC (2013) Screening and evaluation of inhibitors of *Plasmodium falciparum* merozoite egress and invasion using cytometry. *Methods Mol Biol* **923:** 523-534

Boyle MJ, Wilson DW, Beeson JG (2013) New approaches to studying *Plasmodium falciparum* merozoite invasion and insights into invasion biology. *Int J Parasitol* **43:** 1-10

Briolant S, Henry M, Oeuvray C, Amalvict R, Baret E, Didillon E, Rogier C, Pradines B (2010) Absence of association between piperaquine *in vitro* responses and polymorphisms in the pfcrt, pfmdr1, pfmrp, and pfnhe genes in *Plasmodium falciparum*. *Antimicrob Agents Chemother* **54:** 3537-3544

Buchholz K, Comini MA, Wissenbach D, Schirmer RH, Krauth-Siegel RL, Gromer S (2008a) Cytotoxic interactions of methylene blue with trypanosomatid-specific disulfide reductases and their dithiol products. *Mol Biochem Parasitol* **160:** 65-69

Buchholz K, Putrianti ED, Rahlfs S, Schirmer RH, Becker K, Matuschewski K (2010) Molecular genetics evidence for the *in vivo* roles of the two major NADPH-dependent disulfide reductases in the malaria parasite. *J Biol Chem* **285:** 37388-37395

Buchholz K, Schirmer RH, Eubel JK, Akoachere MB, Dandekar T, Becker K, Gromer S (2008b) Interactions of methylene blue with human disulfide reductases and their orthologues from *Plasmodium falciparum. Antimicrob Agents Chemother* **52:** 183-191

Burrows JN, van Huijsduijnen RH, Mohrle JJ, Oeuvray C, Wells TN (2013) Designing the next generation of medicines for malaria control and eradication. *Malar J* **12:** 187

Cappadoro M, Giribaldi G, O'Brien E, Turrini F, Mannu F, Ulliers D, Simula G, Luzzatto L, Arese P (1998) Early phagocytosis of glucose-6-phosphate dehydrogenase (G6PD)-deficient erythrocytes parasitized by *Plasmodium falciparum* may explain malaria protection in G6PD deficiency. *Blood* **92:** 2527-2534

Cappellini MD, Fiorelli G (2008) Glucose-6-phosphate dehydrogenase deficiency. *Lancet* **371:** 64-74

Castellini MA, Buguliskis JS, Casta LJ, Butz CE, Clark AB, Kunkel TA, Taraschi TF (2011) Malaria drug resistance is associated with defective DNA mismatch repair. *Mol Biochem Parasitol* **177:** 143-147

Cesar-Rodo E, Ehrhardt K, Lanzer M, Williams DL, Davioud-Charvet E, Lanfranchi DA (in preparation) Synthetic Engineering for Versatile Access to Polysubstituted 2-Methyl-3-benzyl-1,4-Naphthoquinones (Vitamin K3) Derivatives. *Manuscript in preparation*

Chan CL, Renia L, Tan KS (2012) A simplified, sensitive phagocytic assay for malaria cultures facilitated by flow cytometry of differentially-stained cell populations. *PLoS One* **7:** e38523

Chavain N, Davioud-Charvet E, Trivelli X, Mbeki L, Rottmann M, Brun R, Biot C (2009) Antimalarial activities of ferroquine conjugates with either glutathione reductase inhibitors or glutathione depletors via a hydrolyzable amide linker. *Bioorg Med Chem* **17:** 8048-8059

Chavain N, Vezin H, Dive D, Touati N, Paul JF, Buisine E, Biot C (2008) Investigation of the redox behavior of ferroquine, a new antimalarial. *Mol Pharm* **5:** 710-716

Chugh M, Sundararaman V, Kumar S, Reddy VS, Siddiqui WA, Stuart KD, Malhotra P (2013) Protein complex directs hemoglobin-to-hemozoin formation in *Plasmodium falciparum*. *Proc Natl Acad Sci U S A* **110:** 5392-5397

Combrinck JM, Mabotha TE, Ncokazi KK, Ambele MA, Taylor D, Smith PJ, Hoppe HC, Egan TJ (2013) Insights into the role of heme in the mechanism of action of antimalarials. *ACS Chem Biol* **8:** 133-137

Cooper RA, Ferdig MT, Su XZ, Ursos LM, Mu J, Nomura T, Fujioka H, Fidock DA, Roepe PD, Wellems TE (2002) Alternative mutations at position 76 of the vacuolar transmembrane protein PfCRT are associated with chloroquine resistance and unique stereospecific quinine and quinidine responses in *Plasmodium falciparum*. *Mol Pharmacol* **61:** 35-42

Coronado LM, Nadovich CT, Spadafora C (2014) Malarial hemozoin: From target to tool. *Biochim Biophys Acta* **1840:** 2032-2041

Coulibaly B, Zoungrana A, Mockenhaupt FP, Schirmer RH, Klose C, Mansmann U, Meissner PE, Muller O (2009) Strong gametocytocidal effect of methylene blue-based combination therapy against falciparum malaria: a randomised controlled trial. *PLoS One* **4:** e5318

Cyrklaff M, Sanchez CP, Frischknecht F, Lanzer M (2012) Host actin remodeling and protection from malaria by hemoglobinopathies. *Trends in parasitology* **28:** 479-485

Cyrklaff M, Sanchez CP, Kilian N, Bisseye C, Simpore J, Frischknecht F, Lanzer M (2011) Hemoglobins S and C interfere with actin remodeling in *Plasmodium falciparum*-infected erythrocytes. *Science* **334:** 1283-1286

Davioud-Charvet E, Delarue S, Biot C, Schwobel B, Boehme CC, Mussigbrodt A, Maes L, Sergheraert C, Grellier P, Schirmer RH, Becker K (2001) A prodrug form of a *Plasmodium falciparum* glutathione reductase inhibitor conjugated with a 4-anilinoquinoline. *J Med Chem* **44:** 4268-4276

Davioud-Charvet E, Lanfranchi DA (2011) Subversive Substrates of Glutathione Reductases from *Plasmodium falciparum*-Infected Red Blood Cells as Antimalarial Agents. In *Apicomplexan Parasites - Molecular approaches toward targeted drug development*, Ed: Becker K, Vol. 2, pp 375-396, from the series *Drug Discovery in Infectious Diseases*, Series Ed: Selzer PM. Weinheim: Wiley-VCH Verlag GmbH & Co. KGaA

Dembele L, Franetich JF, Lorthiois A, Gego A, Zeeman AM, Kocken CH, Le Grand R, Dereuddre-Bosquet N, van Gemert GJ, Sauerwein R, Vaillant JC, Hannoun L, Fuchter MJ, Diagana TT, Malmquist NA, Scherf A, Snounou G, Mazier D (2014) Persistence and activation of malaria hypnozoites in long-term primary hepatocyte cultures. *Nat Med* **20:** 307-312

Deponte M (2013) Glutathione catalysis and the reaction mechanisms of glutathione-dependent enzymes. *Biochim Biophys Acta* **1830:** 3217-3266

Deponte M, Becker K (2004) *Plasmodium falciparum* - do killers commit suicide? *Trends in parasitology* **20:** 165-169

Deponte M, Becker K, Rahlfs S (2005) *Plasmodium falciparum* glutaredoxin-like proteins. *Biol Chem* **386:** 33-40

Desjardins RE, Canfield CJ, Haynes JD, Chulay JD (1979) Quantitative assessment of antimalarial activity *in vitro* by a semiautomated microdilution technique. *Antimicrob Agents Chemother* **16:** 710-718

Ding XC, Ubben D, Wells TN (2012) A framework for assessing the risk of resistance for anti-malarials in development. *Malar J* **11:** 292

Dubar F, Khalife J, Brocard J, Dive D, Biot C (2008) Ferroquine, an ingenious antimalarial drug: thoughts on the mechanism of action. *Molecules* **13:** 2900-2907

Duraisingh MT, Jones P, Sambou I, von Seidlein L, Pinder M, Warhurst DC (1999) Inoculum effect leads to overestimation of *in vitro* resistance for artemisinin derivatives and standard antimalarials: a Gambian field study. *Parasitology* **119 (Pt 5):** 435-440

Eckers E, Deponte M (2012) No need for labels: the autofluorescence of *Leishmania tarentolae* mitochondria and the necessity of negative controls. *PLoS One* **7:** e47641

Egan TJ (2008) Recent advances in understanding the mechanism of hemozoin (malaria pigment) formation. *J Inorg Biochem* **102:** 1288-1299

Ehrhardt K, Davioud-Charvet E, Ke H, Vaidya AB, Lanzer M, Deponte M (2013) The antimalarial activities of methylene blue and the 1,4-naphthoquinone 3-[4-(trifluoromethyl)benzyl]-menadione are not due to inhibition of the mitochondrial electron transport chain. *Antimicrob Agents Chemother* **57:** 2114-2120

Ehrhardt K, Deregnaucourt C, Goetz A, Tzanova T, Pradines B, Adjalley S, Blandin S, Bagrel D, Lanzer M, Davioud-Charvet E (in preparation) The lead 3-[4-(trifluoromethyl)benzyl]-menadione is a potent antimalarial drug candidate with fast killing speed and transmission blocking activity. *Manuscript in preparation*

Färber PM, Arscott LD, Williams CH, Jr., Becker K, Schirmer RH (1998) Recombinant *Plasmodium falciparum* glutathione reductase is inhibited by the antimalarial dye methylene blue. *FEBS Lett* **422:** 311-314

Fivelman QL, Adagu IS, Warhurst DC (2004) Modified fixed-ratio isobologram method for studying *in vitro* interactions between atovaquone and proguanil or dihydroartemisinin against drug-resistant strains of *Plasmodium falciparum*. *Antimicrob Agents Chemother* **48:** 4097-4102

Freshney R. (1987) Culture of Animal Cells: A Manual of Basic Technique. Alan R. Liss, New York.

Friebolin W, Jannack B, Wenzel N, Furrer J, Oeser T, Sanchez CP, Lanzer M, Yardley V, Becker K, Davioud-Charvet E (2008) Antimalarial dual drugs based on potent inhibitors of glutathione reductase from *Plasmodium falciparum*. *J Med Chem* **51:** 1260-1277

Fromentin Y, Gaboriaud-Kolar N, Lenta BN, Wansi JD, Buisson D, Mouray E, Grellier P, Loiseau PM, Lallemand MC, Michel S (2013) Synthesis of novel guttiferone A derivatives: *in-vitro* evaluation toward *Plasmodium falciparum*, *Trypanosoma brucei* and *Leishmania donovani*. *Eur J Med Chem* **65:** 284-294

Fry M, Pudney M (1992) Site of action of the antimalarial hydroxynaphthoquinone, 2-[trans-4-(4'-chlorophenyl) cyclohexyl]-3-hydroxy-1,4-naphthoquinone (566C80). *Biochem Pharmacol* **43:** 1545-1553

Ginsburg H, Golenser J (2003) Glutathione is involved in the antimalarial action of chloroquine and its modulation affects drug sensitivity of human and murine species of *Plasmodium*. *Redox Rep* **8:** 276-279

Giribaldi G, Ulliers D, Mannu F, Arese P, Turrini F (2001) Growth of *Plasmodium falciparum* induces stage-dependent haemichrome formation, oxidative aggregation of band 3, membrane deposition of complement and antibodies, and phagocytosis of parasitized erythrocytes. *Br J Haematol* **113:** 492-499

Gluzman IY, Francis SE, Oksman A, Smith CE, Duffin KL, Goldberg DE (1994) Order and specificity of the *Plasmodium falciparum* hemoglobin degradation pathway. *J Clin Invest* **93:** 1602-1608

Gluzman IY, Schlesinger PH, Krogstad DJ (1987) Inoculum effect with chloroquine and *Plasmodium falciparum*. *Antimicrob Agents Chemother* **31:** 32-36

Goldberg DE, Slater AF, Beavis R, Chait B, Cerami A, Henderson GB (1991) Hemoglobin degradation in the human malaria pathogen *Plasmodium falciparum*: a catabolic pathway initiated by a specific aspartic protease. *J Exp Med* **173:** 961-969

Goldstein ST, Shapiro CN (1997) A recombinant circumsporozoite protein vaccine against malaria. *N Engl J Med* **336:** 1760; author reply 1760-1761

Grobusch MP, Kremsner PG (2005) Uncomplicated malaria. *Curr Top Microbiol Immunol* **295:** 83-104

Guttmannn P, Ehrlich P (1891) Über die Wirkung des Methylenblau bei Malaria. *Berl Klin Wochenschr* **28**

Henry M, Diallo I, Bordes J, Ka S, Pradines B, Diatta B, M'Baye PS, Sane M, Thiam M, Gueye PM, Wade B, Touze JE, Debonne JM, Rogier C, Fusai T (2006) Urban malaria in Dakar, Senegal: chemosusceptibility and genetic diversity of *Plasmodium falciparum* isolates. *Am J Trop Med Hyg* **75:** 146-151

Hillard EA, de Abreu FC, Ferreira DC, Jaouen G, Goulart MO, Amatore C (2008) Electrochemical parameters and techniques in drug development, with an emphasis on quinones and related compounds. *Chem Commun (Camb)***:** 2612-2628

Hogg T, Nagarajan K, Herzberg S, Chen L, Shen X, Jiang H, Wecke M, Blohmke C, Hilgenfeld R, Schmidt CL (2006) Structural and functional characterization of Falcipain-2, a hemoglobinase from the malarial parasite *Plasmodium falciparum*. *J Biol Chem* **281:** 25425-25437

Ibrahim H, Pantaleo A, Turrini F, Arese P, Nallet J-P, Nepveu F (2011) Pharmacological properties of indolone-N-oxides controlled by a bioreductive transformation in red blood cells? *MedChemComm* **2:** 860-869

140

Impert O, Katafias A, Kita P, Mills A, Pietkiewiez-Graczyk A, Wrzeszcz G (2003) Kinetics and mechanism of a fast leuco-Methylene Blue oxidation by copper(II)–halide species in acidic aqueous media. *Dalton Transactions* **3:** 348-353

Jani D, Nagarkatti R, Beatty W, Angel R, Slebodnick C, Andersen J, Kumar S, Rathore D (2008) HDP-a novel heme detoxification protein from the malaria parasite. *PLoS Pathog* **4:** e1000053

Jia J, Zhu F, Ma X, Cao Z, Li Y, Chen YZ (2009) Mechanisms of drug combinations: interaction and network perspectives. *Nat Rev Drug Discov* **8:** 111-128

Johann L, Lanfranchi DA, Davioud-Charvet E, Elhabiri M (2012) A physico-biochemical study on potential redox-cyclers as antimalarial and anti-schistosomal drugs. *Curr Pharm Des* **18:** 3539-3566

Jortzik E, Becker K (2012) Thioredoxin and glutathione systems in *Plasmodium falciparum*. *Int J Med Microbiol* **302:** 187-194

Jortzik E, Mailu BM, Preuss J, Fischer M, Bode L, Rahlfs S, Becker K (2011) Glucose-6-phosphate dehydrogenase-6-phosphogluconolactonase: a unique bifunctional enzyme from *Plasmodium falciparum*. *Biochem J* **436:** 641-650

Kanias T, Acker JP (2010) Biopreservation of red blood cells--the struggle with hemoglobin oxidation. *The FEBS journal* **277:** 343-356

Kasozi D, Mohring F, Rahlfs S, Meyer AJ, Becker K (2013) Real-time imaging of the intracellular glutathione redox potential in the malaria parasite *Plasmodium falciparum*. *PLoS Pathog* **9:** e1003782

Ke H, Morrisey JM, Ganesan SM, Painter HJ, Mather MW, Vaidya AB (2011) Variation among *Plasmodium falciparum* strains in their reliance on mitochondrial electron transport chain function. *Eukaryot Cell* **10:** 1053-1061

Kehr S, Jortzik E, Delahunty C, Yates JR, 3rd, Rahlfs S, Becker K (2011) Protein *S*-glutathionylation in malaria parasites. *Antioxidants & redox signaling* **15:** 2855-2865

Kehr S, Sturm N, Rahlfs S, Przyborski JM, Becker K (2010) Compartmentation of redox metabolism in malaria parasites. *PLoS Pathog* **6:** e1001242

Klonis N, Tan O, Jackson K, Goldberg D, Klemba M, Tilley L (2007) Evaluation of pH during cytostomal endocytosis and vacuolar catabolism of haemoglobin in *Plasmodium falciparum*. *Biochem J* **407:** 343-354

Klonis N, Xie SC, McCaw JM, Crespo-Ortiz MP, Zaloumis SG, Simpson JA, Tilley L (2013) Altered temporal response of malaria parasites determines differential sensitivity to artemisinin. *Proc Natl Acad Sci U S A* **110:** 5157-5162

Koncarevic S, Rohrbach P, Deponte M, Krohne G, Prieto JH, Yates J, 3rd, Rahlfs S, Becker K (2009) The malarial parasite *Plasmodium falciparum* imports the human protein peroxiredoxin 2 for peroxide detoxification. *Proc Natl Acad Sci U S A* **106:** 13323-13328

Krauth-Siegel RL, Bauer H, Schirmer RH (2005) Dithiol proteins as guardians of the intracellular redox milieu in parasites: old and new drug targets in *trypanosomes* and malaria-causing *plasmodia*. *Angew Chem Int Ed Engl* **44:** 690-715

Krugliak M, Zhang J, Ginsburg H (2002) Intraerythrocytic *Plasmodium falciparum* utilizes only a fraction of the amino acids derived from the digestion of host cell cytosol for the biosynthesis of its proteins. *Mol Biochem Parasitol* **119:** 249-256

Lambros C, Vanderberg JP (1979) Synchronization of *Plasmodium falciparum* erythrocytic stages in culture. *J Parasitol* **65:** 418-420

Lanfranchi DA, Belorgey D, Muller T, Vezin H, Lanzer M, Davioud-Charvet E (2012a) Exploring the trifluoromenadione core as a template to design antimalarial redox-active agents interacting with glutathione reductase. *Org Biomol Chem* **10:** 4795-4806

Lanfranchi DA, Cesar-Rodo E, Bertrand B, Huang HH, Day L, Johann L, Elhabiri M, Becker K, Williams DL, Davioud-Charvet E (2012b) Synthesis and biological evaluation of 1,4-naphthoquinones and quinoline-5,8-diones as antimalarial and schistosomicidal agents. *Org Biomol Chem* **10:** 6375-6387

Lelievre J, Berry A, Benoit-Vical F (2005) An alternative method for *Plasmodium* culture synchronization. *Exp Parasitol* **109:** 195-197

Lew VL, Macdonald L, Ginsburg H, Krugliak M, Tiffert T (2004) Excess haemoglobin digestion by malaria parasites: a strategy to prevent premature host cell lysis. *Blood Cells Mol Dis* **32:** 353-359

Lim L, McFadden GI (2010) The evolution, metabolism and functions of the apicoplast. *Philos Trans R Soc Lond B Biol Sci* **365:** 749-763

Looareesuwan S, Viravan C, Webster HK, Kyle DE, Hutchinson DB, Canfield CJ (1996) Clinical studies of atovaquone, alone or in combination with other antimalarial drugs, for treatment of acute uncomplicated malaria in Thailand. *Am J Trop Med Hyg* **54:** 62-66

Lopez-Shirley K, Zhang F, Gosser D, Scott M, Meshnick SR (1994) Antimalarial quinones: redox potential dependence of methemoglobin formation and heme release in erythrocytes. *J Lab Clin Med* **123:** 126-130

Low PS, Waugh SM, Zinke K, Drenckhahn D (1985) The role of hemoglobin denaturation and band 3 clustering in red blood cell aging. *Science* **227:** 531-533

Lucius R, Loos-Frank B (2008) *Biologie der Parasiten*, Berlin, Heidelberg: Springer Berlin Heidelberg.

Luersen K, Walter RD, Muller S (2000) *Plasmodium falciparum*-infected red blood cells depend on a functional glutathione *de novo* synthesis attributable to an enhanced loss of glutathione. *Biochem J* **346 Pt 2:** 545-552

Mabeza GF, Loyevsky M, Gordeuk VR, Weiss G (1999) Iron chelation therapy for malaria: a review. *Pharmacol Ther* **81:** 53-75

Maier AG, Cooke BM, Cowman AF, Tilley L (2009) Malaria parasite proteins that remodel the host erythrocyte. *Nature reviews Microbiology* **7:** 341-354

mal ERACGoD (2011) A research agenda for malaria eradication: drugs. *PLoS Med* **8:** e1000402

Marva E, Cohen A, Saltman P, Chevion M, Golenser J (1989) Deleterious synergistic effects of ascorbate and copper on the development of *Plasmodium falciparum*: an *in vitro* study in normal and in G6PD-deficient erythrocytes. *Int J Parasitol* **19:** 779-785

Meierjohann S, Walter RD, Muller S (2002) Regulation of intracellular glutathione levels in erythrocytes infected with chloroquine-sensitive and chloroquine-resistant *Plasmodium falciparum*. *Biochem J* **368:** 761-768

Merrick CJ, Duraisingh MT (2010) Epigenetics in *Plasmodium*: what do we really know? *Eukaryot Cell* **9:** 1150-1158

MMV Medicines for Malaria Venture - Essential information for scientists. http://www.mmv.org/research-development/essential-information-scientists

Mohring F, Pretzel J, Jortzik E, Becker K (2014) The redox systems of *Plasmodium falciparum* and *Plasmodium vivax*: comparison, *in silico* analyses and inhibitor studies. *Curr Med Chem* **21:** 1728-1756

Monti D, Vodopivec B, Basilico N, Olliaro P, Taramelli D (1999) A novel endogenous antimalarial: Fe(II)-protoporphyrin IX alpha (heme) inhibits hematin polymerization to beta-hematin (malaria pigment) and kills malaria parasites. *Biochemistry* **38:** 8858-8863

Moore M, Thor H, Moore G, Nelson S, Moldeus P, Orrenius S (1985) The toxicity of acetaminophen and N-acetyl-*p*-benzoquinone imine in isolated hepatocytes is associated with thiol depletion and increased cytosolic Ca^{2+}. *J Biol Chem* **260:** 13035-13040

Morin C, Besset T, Moutet JC, Fayolle M, Bruckner M, Limosin D, Becker K, Davioud-Charvet E (2008) The aza-analogues of 1,4-naphthoquinones are potent substrates and inhibitors of plasmodial thioredoxin and glutathione reductases and of human erythrocyte glutathione reductase. *Org Biomol Chem* **6:** 2731-2742

Müller S, Liebau E, Walter RD, Krauth-Siegel RL (2003) Thiol-based redox metabolism of protozoan parasites. *Trends in parasitology* **19:** 320-328

Müller T, Johann L, Jannack B, Bruckner M, Lanfranchi DA, Bauer H, Sanchez C, Yardley V, Deregnaucourt C, Schrevel J, Lanzer M, Schirmer RH, Davioud-Charvet E (2011) Glutathione reductase-catalyzed cascade of redox reactions to bioactivate potent antimalarial 1,4-naphthoquinones-a new strategy to combat malarial parasites. *J Am Chem Soc* **133:** 11557-11571

Mwai L, Diriye A, Masseno V, Muriithi S, Feltwell T, Musyoki J, Lemieux J, Feller A, Mair GR, Marsh K, Newbold C, Nzila A, Carret CK (2012) Genome wide adaptations of *Plasmodium falciparum* in response to lumefantrine selective drug pressure. *PLoS One* **7:** e31623

Nepveu F, Kim S, Boyer J, Chatriant O, Ibrahim H, Reybier K, Monje MC, Chevalley S, Perio P, Lajoie BH, Bouajila J, Deharo E, Sauvain M, Tahar R, Basco L, Pantaleo A, Turini F, Arese P, Valentin A, Thompson E, Vivas L, Petit S, Nallet JP (2010) Synthesis and antiplasmodial activity of new indolone N-oxide derivatives. *J Med Chem* **53:** 699-714

Nepveu F, Turrini F (2013) Targeting the redox metabolism of *Plasmodium falciparum*. *Future Med Chem* **5:** 1993-2006

Njomnang Soh P, Witkowski B, Gales A, Huyghe E, Berry A, Pipy B, Benoit-Vical F (2012) Implication of glutathione in the *in vitro* antiplasmodial mechanism of action of ellagic acid. *PLoS One* **7:** e45906

Nkrumah LJ, Muhle RA, Moura PA, Ghosh P, Hatfull GF, Jacobs WR, Jr., Fidock DA (2006) Efficient site-specific integration in *Plasmodium falciparum* chromosomes mediated by mycobacteriophage Bxb1 integrase. *Nat Methods* **3:** 615-621

Nzila A, Mwai L (2010) *In vitro* selection of *Plasmodium falciparum* drug-resistant parasite lines. *J Antimicrob Chemother* **65:** 390-398

O'Hara JK, Kerwin LJ, Cobbold SA, Tai J, Bedell TA, Reider PJ, Llinas M (2014) Targeting NAD+ Metabolism in the Human Malaria Parasite *Plasmodium falciparum*. *PLoS One* **9:** e94061

Oakley MS, Gerald N, McCutchan TF, Aravind L, Kumar S (2011) Clinical and molecular aspects of malaria fever. *Trends in parasitology* **27:** 442-449

Olszewski KL, Morrisey JM, Wilinski D, Burns JM, Vaidya AB, Rabinowitz JD, Llinas M (2009) Host-parasite interactions revealed by *Plasmodium falciparum* metabolomics. *Cell Host Microbe* **5:** 191-199

Painter HJ, Morrisey JM, Mather MW, Vaidya AB (2007) Specific role of mitochondrial electron transport in blood-stage *Plasmodium falciparum*. *Nature* **446:** 88-91

Painter HJ, Morrisey JM, Vaidya AB (2010) Mitochondrial electron transport inhibition and viability of intraerythrocytic *Plasmodium falciparum*. *Antimicrob Agents Chemother* **54:** 5281-5287

Pal C, Bandyopadhyay U (2012) Redox-active antiparasitic drugs. *Antioxidants & redox signaling* **17:** 555-582

Pantaleo A, Ferru E, Vono R, Giribaldi G, Lobina O, Nepveu F, Ibrahim H, Nallet JP, Carta F, Mannu F, Pippia P, Campanella E, Low PS, Turrini F (2012) New antimalarial indolone-N-oxides, generating radical species, destabilize the host cell membrane at early stages of *Plasmodium falciparum* growth: role of band 3 tyrosine phosphorylation. *Free Radic Biol Med* **52:** 527-536

Pastrana-Mena R, Dinglasan RR, Franke-Fayard B, Vega-Rodriguez J, Fuentes-Caraballo M, Baerga-Ortiz A, Coppens I, Jacobs-Lorena M, Janse CJ, Serrano AE (2010) Glutathione reductase-null malaria parasites have normal blood stage growth but arrest during development in the mosquito. *J Biol Chem* **285:** 27045-27056

Pasvol G, Wilson RJ, Smalley ME, Brown J (1978) Separation of viable schizont-infected red cells of *Plasmodium falciparum* from human blood. *Ann Trop Med Parasitol* **72:** 87-88

Patriarche GJ, Lingane JJ (1970) Electrochemical characteristics of 2-methyl-I,4-naphthoquinone (vitamin K3). A coulometric micromethod of determination. *Anal Chim Acta* **49:** 241-246

Patzewitz EM, Salcedo-Sora JE, Wong EH, Sethia S, Stocks PA, Maughan SC, Murray JA, Krishna S, Bray PG, Ward SA, Muller S (2013) Glutathione transport: a new role for PfCRT in chloroquine resistance. *Antioxidants & redox signaling* **19:** 683-695

Patzewitz EM, Wong EH, Müller S (2012) Dissecting the role of glutathione biosynthesis in *Plasmodium falciparum*. *Mol Microbiol* **83:** 304-318

Petersen I, Eastman R, Lanzer M (2011) Drug-resistant malaria: molecular mechanisms and implications for public health. *FEBS Lett* **585:** 1551-1562

Pradines B, Briolant S, Henry M, Oeuvray C, Baret E, Amalvict R, Didillon E, Rogier C (2010) Absence of association between pyronaridine *in vitro* responses and polymorphisms in genes involved in quinoline resistance in *Plasmodium falciparum*. *Malar J* **9:** 339

Preuss J, Hedrick M, Sergienko E, Pinkerton A, Mangravita-Novo A, Smith L, Marx C, Fischer E, Jortzik E, Rahlfs S, Becker K, Bode L (2012a) High-throughput screening for small-molecule inhibitors of *plasmodium falciparum* glucose-6-phosphate dehydrogenase 6-phosphogluconolactonase. *J Biomol Screen* **17:** 738-751

Preuss J, Jortzik E, Becker K (2012b) Glucose-6-phosphate metabolism in *Plasmodium falciparum*. *IUBMB Life* **64:** 603-611

Preuss J, Maloney P, Peddibhotla S, Hedrick MP, Hershberger P, Gosalia P, Milewski M, Li YL, Sugarman E, Hood B, Suyama E, Nguyen K, Vasile S, Sergienko E, Mangravita-Novo A, Vicchiarelli M, McAnally D, Smith LH, Roth GP, Diwan J, Chung TD, Jortzik E, Rahlfs S, Becker K, Pinkerton AB, Bode L (2012c) Discovery of a *Plasmodium falciparum* glucose-6-phosphate dehydrogenase 6-phosphogluconolactonase inhibitor (R,Z)-N-((1-ethylpyrrolidin-2-yl)methyl)-2-(2-fluorobenzylidene)-3-oxo-3,4-dihydr   o-2H-benzo[b][1,4]thiazine-6-carboxamide (ML276) that reduces parasite growth *in vitro*. *J Med Chem* **55:** 7262-7272

Prieto JH, Koncarevic S, Park SK, Yates J, 3rd, Becker K (2008) Large-scale differential proteome analysis in *Plasmodium falciparum* under drug treatment. *PLoS One* **3:** e4098

Prusty D, Mehra P, Srivastava S, Shivange AV, Gupta A, Roy N, Dhar SK (2008) Nicotinamide inhibits *Plasmodium falciparum* Sir2 activity *in vitro* and parasite growth. *FEMS Microbiol Lett* **282:** 266-272

Rathod PK, McErlean T, Lee PC (1997) Variations in frequencies of drug resistance in *Plasmodium falciparum*. *Proc Natl Acad Sci U S A* **94:** 9389-9393

Reeder BJ, Hider RC, Wilson MT (2008) Iron chelators can protect against oxidative stress through ferryl heme reduction. *Free Radic Biol Med* **44:** 264-273

Reeder BJ (2010) The redox activity of hemoglobins: from physiologic functions to pathologic mechanisms. *Antioxidants & redox signaling* **13:** 1087-1123

Rieckmann KH, Campbell GH, Sax LJ, Mrema JE (1978) Drug sensitivity of *Plasmodium falciparum*. An *in-vitro* microtechnique. *Lancet* **1:** 22-23

Riscoe M, Kelly JX, Winter R (2005) Xanthones as antimalarial agents: discovery, mode of action, and optimization. *Curr Med Chem* **12:** 2539-2549

Rochford R, Ohrt C, Baresel PC, Campo B, Sampath A, Magill AJ, Tekwani BL, Walker LA (2013) Humanized mouse model of glucose 6-phosphate dehydrogenase deficiency for *in vivo* assessment of hemolytic toxicity. *Proc Natl Acad Sci U S A* **110:** 17486-17491

Rottmann M, McNamara C, Yeung BK, Lee MC, Zou B, Russell B, Seitz P, Plouffe DM, Dharia NV, Tan J, Cohen SB, Spencer KR, Gonzalez-Paez GE, Lakshminarayana SB, Goh A, Suwanarusk R, Jegla T, Schmitt EK, Beck HP, Brun R, Nosten F, Renia L, Dartois V, Keller TH, Fidock DA, Winzeler EA, Diagana TT (2010) Spiroindolones, a potent compound class for the treatment of malaria. *Science* **329:** 1175-1180

Rushworth GF, Megson IL (2014) Existing and potential therapeutic uses for N-acetylcysteine: the need for conversion to intracellular glutathione for antioxidant benefits. *Pharmacol Ther* **141:** 150-159

Salmon-Chemin L, Buisine E, Yardley V, Kohler S, Debreu MA, Landry V, Sergheraert C, Croft SL, Krauth-Siegel RL, Davioud-Charvet E (2001) 2- and 3-substituted 1,4-naphthoquinone derivatives as subversive substrates of trypanothione reductase and lipoamide dehydrogenase from *Trypanosoma cruzi*: synthesis and correlation between redox cycling activities and *in vitro* cytotoxicity. *J Med Chem* **44:** 548-565

Sanz LM, Crespo B, De-Cozar C, Ding XC, Llergo JL, Burrows JN, Garcia-Bustos JF, Gamo FJ (2012) *P. falciparum in vitro* killing rates allow to discriminate between different antimalarial mode-of-action. *PLoS One* **7:** e30949

Sanz LM, Jimenez-Diaz MB, Crespo B, De-Cozar C, Almela MJ, Angulo-Barturen I, Castaneda P, Ibanez J, Fernandez EP, Ferrer S, Herreros E, Lozano S, Martinez MS, Rueda L, Burrows JN, Garcia-Bustos JF, Gamo FJ (2011) Cyclopropyl carboxamides, a chemically novel class of antimalarial agents identified in a phenotypic screen. *Antimicrob Agents Chemother* **55:** 5740-5745

Schindelin J, Arganda-Carreras I, Frise E, Kaynig V, Longair M, Pietzsch T, Preibisch S, Rueden C, Saalfeld S, Schmid B, Tinevez JY, White DJ, Hartenstein V, Eliceiri K, Tomancak P, Cardona A (2012) Fiji: an open-source platform for biological-image analysis. *Nat Methods* **9:** 676-682

Schirmer RH, Adler H, Pickhardt M, Mandelkow E (2011) "Lest we forget you--methylene blue...". *Neurobiol Aging* **32:** 2325 e2327-2316

Schirmer RH, Coulibaly B, Stich A, Scheiwein M, Merkle H, Eubel J, Becker K, Becher H, Muller O, Zich T, Schiek W, Kouyate B (2003) Methylene blue as an antimalarial agent. *Redox Rep* **8:** 272-275

Schleiferbock S, Scheurer C, Ihara M, Itoh I, Bathurst I, Burrows JN, Fantauzzi P, Lotharius J, Charman SA, Morizzi J, Shackleford DM, White KL, Brun R, Wittlin S (2013) *In vitro* and *in vivo* characterization of the antimalarial lead compound SSJ-183 in *Plasmodium* models. *Drug Des Devel Ther* **7:** 1377-1384

Scholl PF, Tripathi AK, Sullivan DJ (2005) Bioavailable iron and heme metabolism in *Plasmodium falciparum. Curr Top Microbiol Immunol* **295:** 293-324

Sharma P, Wollenberg K, Sellers M, Zainabadi K, Galinsky K, Moss E, Nguitragool W, Neafsey D, Desai SA (2013) An epigenetic antimalarial resistance mechanism involving parasite genes linked to nutrient uptake. *J Biol Chem* **288:** 19429-19440

Sienkiewicz N, Daher W, Dive D, Wrenger C, Viscogliosi E, Wintjens R, Jouin H, Capron M, Muller S, Khalife J (2004) Identification of a mitochondrial superoxide dismutase with an unusual targeting sequence in *Plasmodium falciparum*. *Mol Biochem Parasitol* **137:** 121-132

Smilkstein M, Sriwilaijaroen N, Kelly JX, Wilairat P, Riscoe M (2004) Simple and inexpensive fluorescence-based technique for high-throughput antimalarial drug screening. *Antimicrob Agents Chemother* **48:** 1803-1806

Soh PN, Witkowski B, Olagnier D, Nicolau ML, Garcia-Alvarez MC, Berry A, Benoit-Vical F (2009) *In vitro* and *in vivo* properties of ellagic acid in malaria treatment. *Antimicrob Agents Chemother* **53:** 1100-1106

Srivastava IK, Morrisey JM, Darrouzet E, Daldal F, Vaidya AB (1999) Resistance mutations reveal the atovaquone-binding domain of cytochrome b in malaria parasites. *Mol Microbiol* **33:** 704-711

Srivastava IK, Rottenberg H, Vaidya AB (1997) Atovaquone, a broad spectrum antiparasitic drug, collapses mitochondrial membrane potential in a malarial parasite. *J Biol Chem* **272:** 3961-3966

Stocks PA, Bray PG, Barton VE, Al-Helal M, Jones M, Araujo NC, Gibbons P, Ward SA, Hughes RH, Biagini GA, Davies J, Amewu R, Mercer AE, Ellis G, O'Neill PM (2007) Evidence for a common non-heme chelatable-iron-dependent activation mechanism for semisynthetic and synthetic endoperoxide antimalarial drugs. *Angew Chem Int Ed Engl* **46:** 6278-6283

Tahar R, Vivas L, Basco L, Thompson E, Ibrahim H, Boyer J, Nepveu F (2011) Indolone-N-oxide derivatives: *in vitro* activity against fresh clinical isolates of *Plasmodium falciparum*, stage specificity and in vitro interactions with established antimalarial drugs. *J Antimicrob Chemother* **66:** 2566-2572

Taylor SM, Cerami C, Fairhurst RM (2013) Hemoglobinopathies: slicing the Gordian knot of *Plasmodium falciparum* malaria pathogenesis. *PLoS Pathog* **9:** e1003327

Teuscher F, Chen N, Kyle DE, Gatton ML, Cheng Q (2012) Phenotypic changes in artemisinin-resistant *Plasmodium falciparum* lines *in vitro*: evidence for decreased sensitivity to dormancy and growth inhibition. *Antimicrob Agents Chemother* **56:** 428-431

Tingle MD, Jewell H, Maggs JL, O'Neill PM, Park BK (1995) The bioactivation of amodiaquine by human polymorphonuclear leucocytes *in vitro*: chemical mechanisms and the effects of fluorine substitution. *Biochem Pharmacol* **50:** 1113-1119

Trager W, Jensen JB (1976) Human malaria parasites in continuous culture. *Science* **193:** 673-675

Trotta RF, Brown ML, Terrell JC, Geyer JA (2004) Defective DNA repair as a potential mechanism for the rapid development of drug resistance in *Plasmodium falciparum*. *Biochemistry* **43:** 4885-4891

Turrini F, Ginsburg H, Bussolino F, Pescarmona GP, Serra MV, Arese P (1992) Phagocytosis of *Plasmodium falciparum*-infected human red blood cells by human monocytes: involvement of immune and nonimmune determinants and dependence on parasite developmental stage. *Blood* **80:** 801-808

Turrini F, Giribaldi G, Carta F, Mannu F, Arese P (2003) Mechanisms of band 3 oxidation and clustering in the phagocytosis of *Plasmodium falciparum*-infected erythrocytes. *Redox Rep* **8:** 300-303

Tuteja R (2007) Malaria - an overview. *The FEBS journal* **274:** 4670-4679

Urgin K, Lanfranchi DA, Müller T, Ehrhardt K, Davioud-Charvet E (in preparation) Synthesis of antiparasitic biaryls- and N-arylalkylamines in the 3-[(4-trifluoromethyl)benzyl)]-menadione series. *Manuscript in preparation*

Vaidya AB, Mather MW (2009) Mitochondrial evolution and functions in malaria parasites. *Annu Rev Microbiol* **63:** 249-267

vander Jagt DL, Hunsaker LA, Campos NM, Scaletti JV (1992) Localization and characterization of hemoglobin-degrading aspartic proteinases from the malarial parasite *Plasmodium falciparum*. *Biochim Biophys Acta* **1122:** 256-264

Veine DM, Arscott LD, Williams CH, Jr. (1998) Redox potentials for yeast, *Escherichia coli* and human glutathione reductase relative to the NAD+/NADH redox couple: enzyme forms active in catalysis. *Biochemistry* **37:** 15575-15582

Vennerstrom JL, Makler MT, Angerhofer CK, Williams JA (1995) Antimalarial dyes revisited: xanthenes, azines, oxazines, and thiazines. *Antimicrob Agents Chemother* **39:** 2671-2677

Vilcheze C, Hartman T, Weinrick B, Jacobs WR, Jr. (2013) *Mycobacterium tuberculosis* is extraordinarily sensitive to killing by a vitamin C-induced Fenton reaction. *Nat Commun* **4:** 1881

Walliker D, Hunt P, Babiker H (2005) Fitness of drug-resistant malaria parasites. *Acta Trop* **94:** 251-259

Wein S, Maynadier M, Tran Van Ba C, Cerdan R, Peyrottes S, Fraisse L, Vial H (2010) Reliability of antimalarial sensitivity tests depends on drug mechanisms of action. *J Clin Microbiol* **48:** 1651-1660

Wells TN, Burrows JN, Baird JK (2010) Targeting the hypnozoite reservoir of *Plasmodium vivax*: the hidden obstacle to malaria elimination. *Trends in parasitology* **26:** 145-151

Wenzel NI, Chavain N, Wang Y, Friebolin W, Maes L, Pradines B, Lanzer M, Yardley V, Brun R, Herold-Mende C, Biot C, Toth K, Davioud-Charvet E (2010) Antimalarial versus cytotoxic properties of dual drugs derived from 4-aminoquinolines and Mannich bases: interaction with DNA. *J Med Chem* **53:** 3214-3226

White NJ, Olliaro PL (1996) Strategies for the prevention of antimalarial drug resistance: rationale for combination chemotherapy for malaria. *Parasitol Today* **12:** 399-401

White NJ, Pongtavornpinyo W (2003) The *de novo* selection of drug-resistant malaria parasites. *Proc Biol Sci* **270:** 545-554

White NJ, Pukrittayakamee S, Hien TT, Faiz MA, Mokuolu OA, Dondorp AM (2014) Malaria. *Lancet* **383:** 723-735

WHO (2010) Guidelines for the treatment of malaria - Second edition. WHO Press, World Health Organization, Geneva, Switzerland.

WHO (2012) Map: Trends in reported malaria incidence 2000 - 2012. http://www.who.int/gho/malaria/en/

WHO (2013) World Malaria Report 2013. WHO Press, World Health Organization, Geneva, Switzerland.

Wilson DW, Langer C, Goodman CD, McFadden GI, Beeson JG (2013) Defining the timing of action of antimalarial drugs against *Plasmodium falciparum*. *Antimicrob Agents Chemother* **57:** 1455-1467

Winter RW, Ignatushchenko M, Ogundahunsi OA, Cornell KA, Oduola AM, Hinrichs DJ, Riscoe MK (1997) Potentiation of an antimalarial oxidant drug. *Antimicrob Agents Chemother* **41:** 1449-1454

Winterbourn CC, French JK, Claridge RF (1979) The reaction of menadione with haemoglobin. Mechanism and effect of superoxide dismutase. *Biochem J* **179:** 665-673

Witkowski B, Amaratunga C, Khim N, Sreng S, Chim P, Kim S, Lim P, Mao S, Sopha C, Sam B, Anderson JM, Duong S, Chuor CM, Taylor WR, Suon S, Mercereau-Puijalon O, Fairhurst RM, Menard D (2013a) Novel phenotypic assays for the detection of artemisinin-resistant *Plasmodium falciparum* malaria in Cambodia: *in-vitro* and *ex-vivo* drug-response studies. *Lancet Infect Dis* **13:** 1043-1049

Witkowski B, Khim N, Chim P, Kim S, Ke S, Kloeung N, Chy S, Duong S, Leang R, Ringwald P, Dondorp AM, Tripura R, Benoit-Vical F, Berry A, Gorgette O, Ariey F, Barale JC, Mercereau-Puijalon O, Menard D (2013b) Reduced artemisinin susceptibility of *Plasmodium falciparum* ring stages in western Cambodia. *Antimicrob Agents Chemother* **57:** 914-923

Witkowski B, Lelievre J, Barragan MJ, Laurent V, Su XZ, Berry A, Benoit-Vical F (2010) Increased tolerance to artemisinin in *Plasmodium falciparum* is mediated by a quiescence mechanism. *Antimicrob Agents Chemother* **54:** 1872-1877

Zerez CR, Roth EF, Jr., Schulman S, Tanaka KR (1990) Increased nicotinamide adenine dinucleotide content and synthesis in *Plasmodium falciparum*-infected human erythrocytes. *Blood* **75:** 1705-1710

Zhang J, Krugliak M, Ginsburg H (1999) The fate of ferriprotorphyrin IX in malaria infected erythrocytes in conjunction with the mode of action of antimalarial drugs. *Mol Biochem Parasitol* **99:** 129-141

Zoungrana A, Coulibaly B, Sie A, Walter-Sack I, Mockenhaupt FP, Kouyate B, Schirmer RH, Klose C, Mansmann U, Meissner P, Muller O (2008) Safety and efficacy of methylene blue combined with artesunate or amodiaquine for uncomplicated *falciparum* malaria: a randomized controlled trial from Burkina Faso. *PLoS One* **3:** e1630

Publications and Conference Presentations

The following publications emerged from this work.

Ehrhardt K, Davioud-Charvet E, Ke H, Vaidya AB, Lanzer M, Deponte M (2013) The antimalarial activities of methylene blue and the 1,4-naphthoquinone 3-[4-(trifluoromethyl)benzyl]-menadione are not due to inhibition of the mitochondrial electron transport chain. *Antimicrob Agents Chemother* **57:** 2114-2120

Ehrhardt K, Deregnaucourt C, Goetz A, Tzanova T, Pradines B, Adjalley S, Blandin S, Bagrel D, Lanzer M, Davioud-Charvet E. The lead 3-[4-(trifluoromethyl)benzyl]-menadione is a potent antimalarial drug candidate with fast killing speed and transmission blocking activity. *Manuscript in preparation*

Bielitza M, Belorgey D, Ehrhardt K, Johann L, Lanfranchi DAI, Gallo V, Schwarzer E, Mohring F, Jortzik E, Williams DL, Becker K, Arese P, Elhabiri M, Davioud-Charvet E (submitted, 2014.) Antimalarial NADPH-consuming redox-cyclers as superior G6PD deficiency copycats. *Manuscript submitted*

Cesar-Rodo E, Ehrhardt K, Lanzer M, Williams DL, Davioud-Charvet E, Lanfranchi DAI. Synthetic Engineering for Versatile Access to Polysubstituted 2-Methyl-3-benzyl-1,4-Naphthoquinones (Vitamin K3) Derivatives. *Manuscript in preparation*

Urgin K, Lanfranchi DA, Müller T, Ehrhardt K, Davioud-Charvet E. Synthesis of antiparasitic biaryls- and N-arylalkylamines in the 3-[(4-trifluoromethyl)benzyl)]-menadione series. *Manuscript in preparation*

Results of this work were presented at the following scientific conferences.

Tropical Medicine and Parasitology, 25th Annual Meeting of the German Society for Parasitology. 17 - 19 March 2012, Heidelberg, Germany. Conference Talk: Ehrhardt K, Kasozi DM, Deregnaucourt C, Becker K, Pradines B, Lanzer M, Davioud-Charvet E. *Subversive Glutathione Reductase Substrates as Redox-Cyclers: A New Strategy to Combat Malarial Parasites.*

3èmes Journées de Consortium anti-Parasitaire, "De la conception de molecule à l'effect biologique". 08 – 09 February 2013, Lille, France. Conference Talk: Ehrhardt K, Kasozi DM, Deregnaucourt C, Becker K, Deponte M, Pradines B, Lanzer M, Davioud-Charvet E. *Redox-active 1,4-naphthoquinones in a cascade of NADPH-consuming bioactivation – A new strategy to combat malarial parasites.*

Seminaire de Microbiologie de Strasbourg 2013. 11 April 2013, Strasbourg, France. Conference Talk: Ehrhardt K, Deregnaucourt C, Deponte M, Lanzer M, Davioud-Charvet E. *Redox-active 1,4-naphthoquinones in a cascade of NADPH-consuming bioactivation – A new strategy to combat malarial parasites.*

9th Annual BioMalPar Conference on the Biology and Pathology of the Malaria Parasite. 13. – 15 Mai 2013, Heidelberg, Germany. Poster: Ehrhardt K, Davioud-Charvet E, Ke H, Vaidya A, Lanzer M, Deponte M. *The antimalarial activities of methylene blue and the 1,4-naphthoquinone 3-[4- (trifluoromethyl)benzyl]-menadione are not due to inhibition of the mitochondrial electron transport chain.*

Appendix

Table A1 Definitions of hemoglobin catabolites and heme-containing molecules cited in this work

Heme compound	Oxidation state	Definition
Hemoglobin	ferrous – Fe^{2+}	Oxygen-carrying Fe^{2+} hemoprotein of erythrocytes made up of four different polypeptide globin chains that contain between 141 and 146 amino acids and a prosthetic group that consists of an iron atom contained in the center of a heterocyclic porphyrin ring, namely the protoporphyrin-IX (PPIX).
Oxyhemoglobin	ferrous – Fe^{2+}	Hemoglobin protein containing an oxygen molecule in its Fe^{2+} PPIX site
Methemoglobin	ferric – Fe^{3+}	Methemoglobin is formed from hemoglobin by oxidation of the iron atom from the ferrous to the ferric state. A small amount is found in the blood normally, but injury or toxic agents convert a larger proportion of hemoglobin into methemoglobin, which does not function as an oxygen carrier.
Heme or Fe^{3+}-protoporphyrin-IX or Fe^{3+}-PPIX	ferric - Fe^{3+}	Heme corresponds to the active protein-free unit of hemoglobin molecule, or the prosthetic group of hemoglobin that consists of an iron atom contained in the center of a heterocyclic porphyrin ring, namely the protoporphyrin-IX.
α-hematin or: Fe^{3+}-PPIX(OH$_2$) Fe^{3+}-PPIX(OH)	ferric - Fe^{3+}	Heme containing a water or and hydroxide molecule axially bound in the fifth position of the iron(Fe^{3+}) porphyrinic system.
β-hematin	ferric - Fe^{3+}	Synthetic hematin crystal standing for hemozoin pigment equivalent
Hemozoin or malarial pigment	ferric - Fe^{3+}	Disposal pigment – biocrystals which result from self-association of Fe^{3+}-protoporphyrin-IX - formed during the digestion of methemoglobin in several blood-feeding parasites (the Fe^{3+}-PPIX are held together mainly through π-π and μ-Pr interactions).
Ferrylhemoglobin	ferryl – Fe^{4+}	Oxidation product of hemoglobin following hydrogen peroxide treatment. Oxidation of the iron atom from the ferric to the ferryl state. Ferryl iron is reactive and unstable and can return to the ferric state by reacting with specific amino acids of the globin chains.
Hemichrome	ferric - Fe^{3+}	Hemichromes are low-spin Fe^{3+} species closely related to methemoglobin. Hemichromes mainly result from denaturation processes of hemoglobin. Hemichromes are characterized by the strong axial binding of two histidine residues to the ferric center, which prevent dioxygen or ligand binding. Hemichromes are considered as markers of the erythrocyte's senescence.

Table A2 Characterisation of lead benzylMD 1c and predicted benzylMD 1c-derived metabolites regarding their antimalarial activities against *P. falciparum* blood-stage parasites and physicochemical and biochemical parameters (unpublished data from Laboratory of Medicinal Chemistry, ECPM, Strasbourg and references cited below)
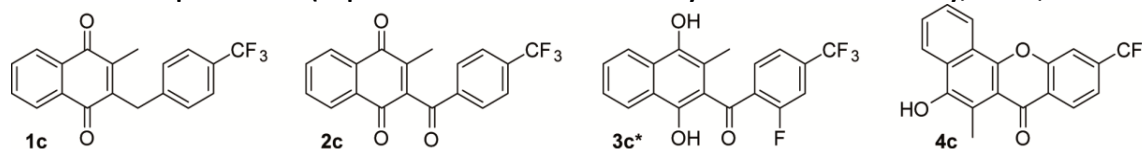
Agent:	*P. falciparum* strain IC$_{50}$ (nM) ± SD [a][1]		Heme binding [b]	β-Hematin inhibition [c]	Enzymatic properties (*h*GR *vs. Pf*GR/NADPH) [d]	metHb(Fe^{3+}) reduction (*h*GR/NADPH) [e]	Redox potentials [f]
	3D7 (nM)	Dd2 (nM)	[Heme]/K_D (µM)	IC$_{50}$ (%$_{max}$ inhib.)	K_m (µM)/k_{cat} (× 10^{-3} s^{-1})/ k_{cat}/K_m (mM^{-1} s^{-1})	k_{metHb} (× 10^{-2} s^{-1})	$E_{1/2}$ (mV) [ΔE (mV)]
benzylMD 1c	49.2 ± 6.1	69.2 ± 2.8	[1:1]/0.15	No inhibition	No substrate	No reduction	-0.61[84] -1.35[88]
benzylMD 2c	>1,000	>1,000	[1:1]/2.0	2.8 (52%)	16.6/44/2.7 *vs.* 42.4/56/1.3	0.12(3)	-0.43[80] -1.12[84] -1.62[60]
benzylMD 3c*	1,159 ± 136	1,290 ± 177	[1:1]/0.8	2.7 (57%)	No substrate	1.3(2) **	nd
benzylMD 4c	431 ± 120	613 ± 79	[1:1]/3.2	2.3 (70%)	No substrate	0.22(2) ***	E_{1pa} = -0.05[irr] E_{2pa} = 0.208[irr] -2.05[153] -1.71[146]
CQ	7.9 ± 1.5	134.0 ± 11.3	[2:1]/1.3	1.6 (86%) [2]	No substrate	No reduction	nd
AQ	10.2 ± 0.2 *	nd	[4:1]/10.7 [3]	0.5 (86%) [3]	No substrate	No reduction	nd
MD	16,000 [2]	nd	nd	-	31.2/160/5.1 vs. 82.2/160/2.0 [4]	Red at 100 µM [5]	-0.60[102] /-1.33[108]

Experimental conditions: **a)** ^{3}H-hypoxanthine incorporation assay (ref 1). * Dr. C. Deregnaucourt, MNHN, Paris, unpublished. **b)** 0.2 M sodium hepes buffer pH 7.5, the dimerization constant K_{Dim} of Fe^{3+}PPIX was fixed at $10^{6.82}$ (ref 3). **c)** [c]12.9 M sodium acetate buffer pH 4.5, 60 °C, 1 h then 0.2 M + 0.02 M sodium hepes buffer pH 7.5 containing 5% pyridine (v/v) as reporting reagent (ref 3). **d)** 100 mM phosphate buffer pH 6.9, 1 mM EDTA, 200 mM KCl; T = 25.0 °C, [*h*GR]$_0$ = 1.3-2.6 µM; [NADPH]$_0$ = 100 µM. **e)** 47 mM phosphate buffer pH 6.9, 1 mM EDTA, 200 mM KCl; T = 25.0 °C; [*h*GR]$_0$ = 81 nM; [NADPH]$_0$ = 121 µM; [metHb]$_{tot}$ = 7.96 µM; [S]$_0$ = 40 µM; **Direct reduction of metHb(Fe^{III}) by the benzoyldihydroMD **3c*** performed in the absence of *h*GR and NADPH. *** For **4c** (40 µM), T = 37.0 °C (to increase the solubility), [*h*GR]$_0$ = 133 nM; [NADPH]$_0$ = 53 µM; [metHb]$_{tot}$ = 7.96 µM. **e)** Cyclic voltammetry (CV) and square wave voltammetry (SWV), DMSO (0.1 M NBu$_4$PF$_6$), v = 200 mV s^{-1}. References: (1) (Bielitza et al, submitted, 2014.) (2) (Friebolin et al, 2008) (3) (Johann et al, 2012) (4) (Müller et al, 2011) (5) (Winterbourn et al, 1979). Abbreviations: AQ, amodiaquine; CQ, chloroquine; GR, glutathione reductase; metHb, methemoglobin; MD, menadione; nd = not determined

Table A3 *In vitro* susceptibility profiles of *Plasmodium falciparum* strains to antimalarial agents

P. falciparum strains and origin		Susceptibility to antimalarial agents										
		PPQ	CQ	QN	MFQ	MDAQ	LMF	DHA	AS	ATO	PY	DOX
3D7	Sierra Leone	S	S	S	R	S	S	S	S	S	S	S
W2	Indochina	S	R	I	I	R	S	S	S	S	R	S
D6	Africa	S	S	S	R	S	S	S	S	S	S	S
FCM29	Cameroon	S	R	I	I	R	S	S	S	S	R	S
FCR3	The Gambia	S	R	I	I	S	S	S	S	S	S	S
PA	Uganda	S	R	I	I	R	S	S	S	S	S	S
Bres [a]	Brazil	S	R	I	I	R	S	S	S	S	S	S
8425 [a]	Senegal	S	S	S	R	S	S	S	S	S	S	S
K14 [a]	Cambodia	S	R	RS	I	R	S	S	S	S	R	S
K2 [a]	Cambodia	S	R	I	I	R	S	S	S	S	R	S
L1 [a]	Niger	S	R	I	I	R	S	S	S	S	S	S
Vol [a]	Djibouti	S	R	S	I	R	S	S	S	S	S	S
Dd2 [b]	Indochina (W2)	-	R	-	R	-	-	-	-	-	R	-
Resistance cut-off values		R > 150 nM	> 100 nM	I: 500-800 nM, RS > 800 nM	I: 30-40 nM R > 40 nM	R > 80 nM	RS > 150 nM		RS > 10.5 nM	I: 30-390 nM R > 390 nM	I: 200-1000 nM R > 1000 nM	RS> 35 nM

Chemosusceptibility profiles were kindly provided by Dr. Bruno Pradines, Institut de Médecine Tropicale du Service de Santé des Armées, Marseille, France. a strains were isolated at the Institut de Médecine Tropicale du Service de Santé des Armées, b chemosusceptibility according to (Ding et al, 2012). Antimalarial agents: PPQ, piperaquine; CQ, chloroquine; QN, quinine; MFQ, mefloquine; MDAQ, monodesethylamodiaquine; LMF, lumefantrine; AS, artesunate; ATO, atovaquone; DHA, dihydroartemisinin; PY, pyrimethamine and DOX, doxycycline. Resistance cut-off values: I, intermediate; RS, reduced susceptibility; R, resistance.

Table A4 *In vitro* antimalarial activity of benzylMD 1c and antimalarial agents against twelve drug-sensitive and resistant *P. falciparum* strains originating from Asia, Africa or South America

P. falciparum strains	Agents:	benzylMD 1c	CQ	QN	MDAQ	MQ
3D7	IC$_{50}$	94.2	21.3	103.8	19.5	52.1
	[CI95%]	[80-111]	[17.9-25.3]	[73-148]	[14.1-26.9]	[47.0-57.8]
	IC$_{90}$	246.6	40.4	597.0	31.4	119.4
	[CI95%]	[216-281]	[33.2-49.0]	[512-696]	[23.4-42.1]	[103-138]
D6	IC$_{50}$	138.0	23.0	61.8	17.5	62.1
	[CI95%]	[101-189]	[18.8-28.0]	[44.5-85.9]	[11.2-27.3]	[52.5-73.4]
	IC$_{90}$	248.3	44.4	464.5	37.0	111.9
	[CI95%]	[172-358]	[37.2-52.9]	[337-640]	[24.3-56.3]	[97-129]
8425	IC$_{50}$	54.3	25.5	130.3	26.4	44.1
	[CI95%]	[46.2-63.9]	[19.6-33.1]	[87-195]	[20.9-33.2]	[38.7-50.2]
	IC$_{90}$	135.8	59.2	389.9	41.4	85.3
	[CI95%]	[135-137]	[45.5-76.9]	[272-560]	[29.9-57.3]	[74.2-98.1]
Voll	IC$_{50}$	68.6	262.4	421.7	77.5	32.5
	[CI95%]	[44-107]	[236-292]	[377-472]	[71.1-84.4]	[25.8-40.9]
	IC$_{90}$	143.6	316.2	843.3	113.0	53.7
	[CI95%]	[75-276]	[241-415]	[753-944]	[102-125]	[42.3-68.2]
L1	IC$_{50}$	104.0	273.5	530.9	86.1	38.0
	[CI95%]	[82-133]	[235-319]	[441-639]	[72-103]	[32.3-44.7]
	IC$_{90}$	201.4	417.8	995.4	125.0	78.5
	[CI95%]	[124-328]	[355-492]	[809-1225]	[96-162]	[68.0-90.7]
PA	IC$_{50}$	70.8	330.4	626.6	72.8	36.9
	[CI95%]	[59.1-84.8]	[275-398]	[505-778]	[56.5-93.7]	[31.5-43.2]
	IC$_{90}$	195.0	483.1	1106.6	106.4	63.2
	[CI95%]	[162-235]	[377-619]	[871-1406]	[82-138]	[53.3-75.1]
Bres	IC$_{50}$	191.4	442.6	604.9	100.2	30.2
	[CI95%]	[177-207]	[392-500]	[488-736]	[85-119]	[23.4-39.1]
	IC$_{90}$	328.1	613.8	1112.5	143.2	51.5
	[CI95%]	[297-362]	[561-672]	[957-1281]	[116-176]	[40.0-65.1]
FCR3	IC$_{50}$	73.5	477.5	665.3	79.1	35.9
	[CI95%]	[48-112]	[376-607]	[546-811]	[66.3-94.3]	[28.5-45.2]
	IC$_{90}$	160.7	685.5	1111.7	129.7	59.2
	[CI95%]	[91-284]	[555-848]	[928-1332]	[110-153]	[47.0-74.5]
W2	IC$_{50}$	215.3	485.3	683.9	146.2	32.0
	[CI95%]	[198-235]	[377-625]	[576-812]	[113-189]	[27.4-37.3]
	IC$_{90}$	368.1	693.4	1247.4	201.8	49.2
	[CI95%]	[349-389]	[598-805]	[1109-1403]	[170-240]	[41.5-58.4]
K2	IC$_{50}$	163.3	493.2	619.4	91.2	33.3
	[CI95%]	[134-199]	[388-626]	[558-687]	[81-103]	[28.2-39.3]
	IC$_{90}$	310.5	912.0	1510.1	143.6	97.3
	[CI95%]	[272-354]	[659-1262]	[1278-1785]	[102-202]	[82-116]
K14	IC$_{50}$	57.2	648.6	495.5	160.3	30.7
	[CI95%]	[41.5-78.7]	[529-795]	[421-583]	[134-192]	[26.6-35.5]
	IC$_{90}$	92.3	1129.8	1636.8	220.3	94.2
	[CI95%]	[82-104]	[1042-1225]	[1404-1908]	[180-270]	[83-107]
FCM29	IC$_{50}$	41.0	879.0	543.3	317.7	27.5
	[CI95%]	[36.2-46.6]	[771-1002]	[416-709]	[278-369]	[21.1-36.0]
	IC$_{90}$	107.4	1241.7	1199.5	407.4	49.1
	[CI95%]	[85-135]	[1129-1365]	[1024-1405]	[349-475]	[32.9-73.4]

Antimalarial activity (presented as IC$_{50}$ and IC$_{90}$ values) was determined on *P. falciparum* blood-stage parasites using the ^{3}H-hypoxanthine incorporation assay. The chemosusceptibility profiles and multi-drug resistance phenotypes of the strains are given in Table A3, Appendix. Results are presented as mean values ± 95% confidence interval from 3 - 5 independent growth-inhibition assays. Results were kindly provided by Dr. Bruno Pradines, Institut de Médecine Tropicale du Service de Santé des Armées, Marseille, France. CI95%, 95% confidence interval; CQ, chloroquine; MF, Mefloquine; MDAQ, monodesethyl-amodiaquine; QN, quinine.

Table A5 Susceptibility of *P. falciparum* Dd2 parasites to benzylMD 1c and chloroquine prior to selection and after 1st (Dd2^{MD1}) and 2nd selection cycles (Dd2^{MD2} parasites)

Selection step						
Pre-selection	**benzylMD 1c**		**chloroquine**			
Culture	**IC$_{50}$ (nM)**	**IC$_{90}$ (nM)**	**IC$_{50}$ (nM)**			
Dd2	51 ± 1 (2)	138 ± 13 (2)	105 ± 20 (2)			

1st selection cycle (125 nM)	**weeks 1-3 after drug removal**			**weeks 4-6 after drug removal**		
	benzylMD 1c		**chloroquine**	**benzylMD 1c**		**chloroquine**
Culture	**IC$_{50}$ (nM)**	**IC$_{90}$ (nM)**	**IC$_{50}$ (nM)**	**IC$_{50}$ (nM)**	**IC$_{90}$ (nM)**	**IC$_{50}$ (nM)**
Dd2^{MD1} F2	162 ± 15 (3)	703 ± 250 (3)	101 ± 23 (3)	52 ± 9 (2)	105 ± 21 (2)	105 ± 30 (2)
Dd2^{MD1} F3	208 ± 17 (3)	983 ± 125 (3)	97 ± 10 (3)	57 ± 0,4 (2)	110 ± 14 (2)	103 ± 20 (2)
Dd2	55 ± 20 (3)	180 ± 52 (3)	123 ± 13 (3)	-	-	-

2nd selection cycle (500 nM)	**weeks 1-6 after drug removal**			**weeks 7-10 after drug removal**		
	benzylMD 1c		**chloroquine**	**benzylMD 1c**		**chloroquine**
Culture	**IC$_{50}$ (nM)**	**IC$_{90}$ (nM)**	**IC$_{50}$ (nM)**	**IC$_{50}$ (nM)**	**IC$_{90}$ (nM)**	**IC$_{50}$ (nM)**
Dd2^{MD2} F1	178 ± 68 (4)	495 ± 306 (4)	73 ± 8 (4)	74 (1)	170 (1)	80 (1)
Dd2^{MD2} F2	250 ± 30 (3)	917 ± 76 (3)	81 ± 13 (2)	90 ± 22 (3)	213 ± 40 (3)	74 ± 3 (3)
Dd2^{MD2} F3	197 ± 58 (5)	586 ± 176 (5)	87 ± 14 (5)	67 ± 18 (3)	145 ± 40 (3)	96 ± 22 (3)
Dd2^{MD2} F4	259 ± 63 (5)	812 ± 250 (5)	96 ± 10 (4)	86 ± 9 (3)	183 ± 42 (3)	105 ± 30 (3)
Dd2	63 ± 17 (8)	176 ± 45 (8)	95 ± 20 (3)	-	-	-

Susceptibility to benzylMD 1c and chloroquine was assessed on drug-adapted parasites after removal of drug pressure. Susceptibility of progenitor Dd2 parasites was assessed in parallel. IC$_{50}$ and IC$_{90}$ values are presented as mean ± standard deviation (SD) determined from (n) independent experiments using the SYBR® green technique.

Table A6 Susceptibility of drug-adapted parasites to benzylMD 1c after the 1st selection cycle (independent repetition)

1st selection cycle	benzylMD 1c		chloroquine
Culture	IC$_{50}$ (nM)	IC$_{90}$ (nM)	IC$_{50}$ (nM)
Dd2^{MD1} F1	163 ± 70 (3)	475 ± 301 (3)	136 ± 46 (3)
Dd2^{MD1} F2	223 ± 169 (3)	783 ± 883 (3)	137 ± 39 (3)
Dd2^{MD1} F3	178 ± 125 (3)	630 ± 754 (3)	128 ± 37 (3)
Dd2^{MD1} F4	211 ± 115 (3)	947 ± 732 (3)	118 ± 34 (3)
Dd2^{MD1} F5	104 ± 35 (3)	227 ± 95 (5)	99 ± 13 (3)
Dd2^{MD1} F6	158 ± 85 (3)	425 ± 289 (3)	103 ± 6 (3)
Dd2	57 ± 11 (3)	173 ± 15 (3)	108 ± 19 (3)
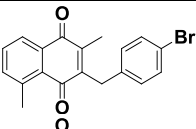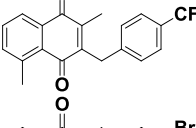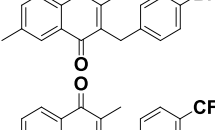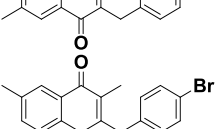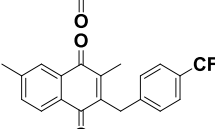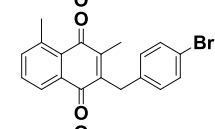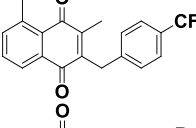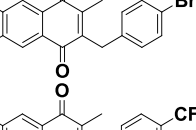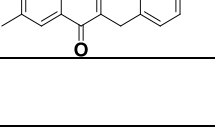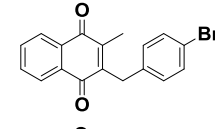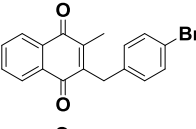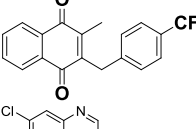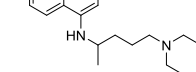
Susceptibility to benzylMD 1c was assessed on Dd2^{MD2} parasites after removal of drug pressure and over a total period of 10 weeks. Susceptibility of progenitor Dd2 parasites was assessed in parallel. IC$_{50}$ and IC$_{90}$ values are presented as mean ± standard deviation (SD) determined from (n) independent experiments using the SYBR® green technique.

Table A7 Compounds selected for *in vitro* drug interaction studies (Results, section 3.3.3)

Compound	Structure	IC$_{50}$ (mM) ± SD (n)
Acetaminophen		1.2 ± 0.4 (3)
Amodiaquine		0.01×10^{-3} (3)
Ascorbic acid		6.8 ± 2.1 (3)
BenzylMD 7a [a]		0.013 ± 0.004 (3)
BSO		0.21 ± 0.03 (3)
CB83 [a]		0.015 ± 0.0003 (2)
DFO [a]		0.012 ± 0.0008 (3)
Ferroquine		0.02×10^{-3}
ML276 [a]		0.002 ± 0.0004 (3)
N-acetyl-cysteine		16.9 ± 3.5 (3)

IC$_{50}$ values of single compounds were assessed in the frame of *in vitro* drug interactions studies on *P. falciparum* 3D7 strain according to the fixed-ratio isobologram method. Results are presented as mean IC$_{50}$ values ± standard deviation (SD) determined from (n) independent experiments. Results of according *in vitro* drug-drug interactions are presented in Table 12, section 3.3.3. [a] Results are presented in modified form in Bielitza et al. (Bielitza et al, submitted, 2014.). BSO, Buthionine sulfoximine; DFO, desferrioxamine B.

Table A8 *In vitro* antimalarial activity of methyl-substituted benzylMD derivatives

Compound name	Structure	*P. falciparum* Dd2 strain IC_{50} (nM) ± SD (n)
EC124		1820 ± 71 (3)
EC122		3638 ± 193 (2)
EC019		171 ± 66 (3)
EC021		215 ± 68 (3)
EC146		992 ± 107 (3)
EC145		439 ± 205 (5)
EC148		3761 ± 972 (3)
EC147		3004 ± 941 (2)
EC157		2706 ± 26 (2)
EC156		3243 ± 260 (3)
Controls compounds		
First hit benzylMD 1a		82 ± 20 (7)
Lead compound benzylMD 1c		58 ± 11 (9)
Chloroquine		99 ± 19 (6)
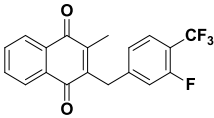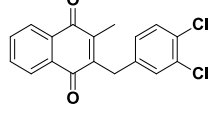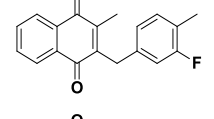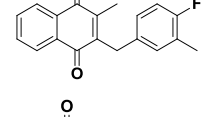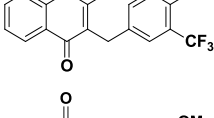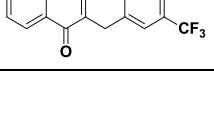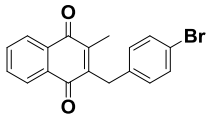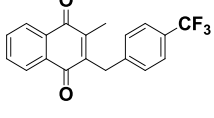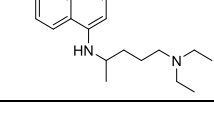
Activity against cultured parasites of *P. falciparum* Dd2 strain is presented as mean IC_{50} values ± standard deviation (SD) determined from (n) independent experiments using the SYBR® green technique. Results will be published in Cesar-Rodo et al. (in preparation).

Table A9 *In vitro* **antimalarial activity of fluorine- or diethylphosphate-substituted benzylMD derivatives**

Compound name	Structure	*P. falciparum* Dd2 strain IC$_{50}$ (nM) ± SD (n)
EC061		74 ± 32 (4)
EC060		83 ± 12 (4)
DAL53		83 ± 23 (3)
DAL54		59 ± 11 (3)
JB006		157 ± 49 (2)
JB008		518 ± 231 (3)
Control compounds		
First hit benzylMD 1a		82 ± 20 (7)
Lead compound benzylMD 1c		58 ± 11 (9)
Chloroquine		99 ± 19 (6)
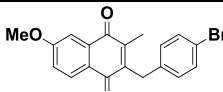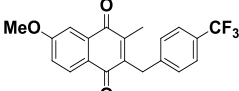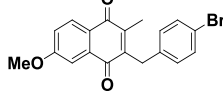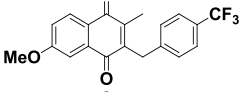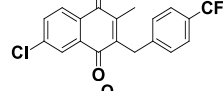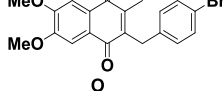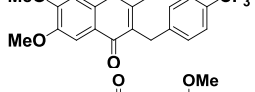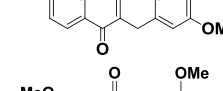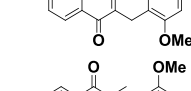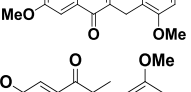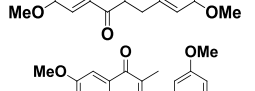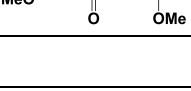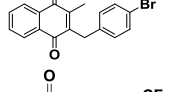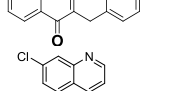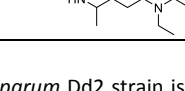
Activity against cultured parasites of *P. falciparum* Dd2 strain is presented as mean IC$_{50}$ values ± standard deviation (SD) determined from (n) independent experiments using the SYBR® green technique. Results will be published in Cesar-Rodo et al. (in preparation).

Table A10 In vitro antimalarial activity of halogen- or methoxy-substituted benzylMD derivatives

Compound name	Structure	P. falciparum Dd2 strain IC$_{50}$ (nM) ± SD (n)
KU036		64 ± 17 (3)
KU040		99 ± 17 (3)
KU060		168 ± 30 (3)
KU062		118 ± 36 (3)
KU065		132 ± 29 (3)
KU066		245 ± 80 (3)
Control compounds		
First hit benzylMD 1a		82 ± 20 (7)
Lead compound benzylMD 1c		58 ± 11 (9)
Chloroquine		99 ± 19 (6)
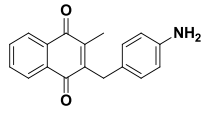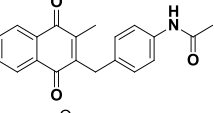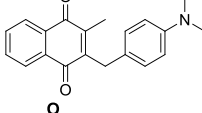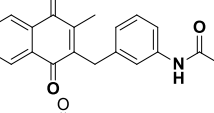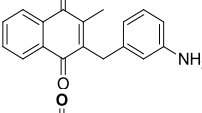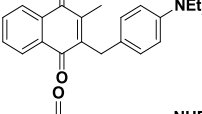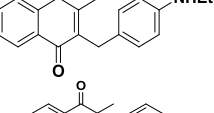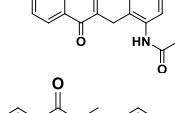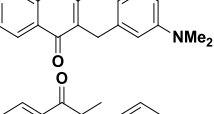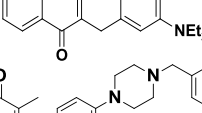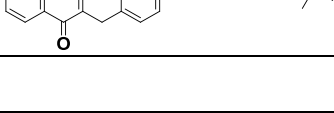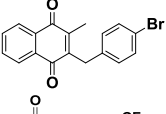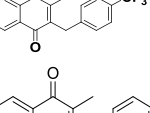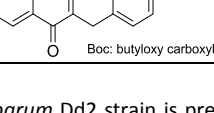
Activity against cultured parasites of *P. falciparum* Dd2 strain is presented as mean IC$_{50}$ values ± standard deviation (SD) determined from (n) independent experiments using the SYBR® green technique. Results will be published in Cesar-Rodo et al. (in preparation).

Table A11 *In vitro* antimalarial activity of methoxy-substituted benzylMD derivatives

Compound name	Structure	*P. falciparum* Dd2 strain IC$_{50}$ (nM) ± SD (n)
EC005		3230 (1)
EC006		3187 (1)
DAL48		171 ± 69 (3)
DAL50		186 ± 58 (3)
EC050		242 ± 60 (4)
EC055		881 ± 129 (4)
EC054		3685 (1)
EC067		778 ± 89 (4)
EC069		2187 (1)
EC125		104 ± 58 (4)
EC057		2704 (1)
EC058		1365 ± 521 (4)

Control compounds:		
First hit benzylMD 1a		82 ± 20 (7)
Lead compound benzylMD 1c		58 ± 11 (9)
Chloroquine		99 ± 19 (6)

Activity against cultured parasites of *P. falciparum* Dd2 strain is presented as mean IC$_{50}$ values ± standard deviation (SD) determined from (n) independent experiments using the SYBR® green technique. Results will be published in Cesar-Rodo et al. (in preparation).

Table A12 *In vitro* antimalarial activity of benzylMD derivatives with a N-dimethyl or N-diethyl group

Compound name	Structure	*P. falciparum* Dd2 strain IC_{50} (nM) ± SD (n)
KU097		303 ± 138 (3)
KU230		411± 220 (3)
KU234		567 ± 217 (3)
KU244		310 ± 134 (3)
KU249		1198 ± 1651 (3) Precipitates in DMSO
KU250 F1		418 ± 166 (3)
KU250 F2		2056 ± 1073 (3)
KU266		282 ± 86 (3)
KU271		386 ± 151 (3)
KU272		236 ± 97 (3)
P_TM87		777 ± 248 (3)
Control compounds		
First hit benzylMD 1a		82 ± 20 (7)
Lead compound benzylMD 1c		58 ± 11 (9)
P_TM45	Boc: butyloxy carboxyl	109 ± 46 (3)

Activity against cultured parasites of *P. falciparum* Dd2 strain is presented as mean IC_{50} values ± standard deviation (SD) determined from (n) independent experiments using the SYBR® green technique. Results will be published in Cesar-Rodo et al. (in preparation).

Acknowledgements